

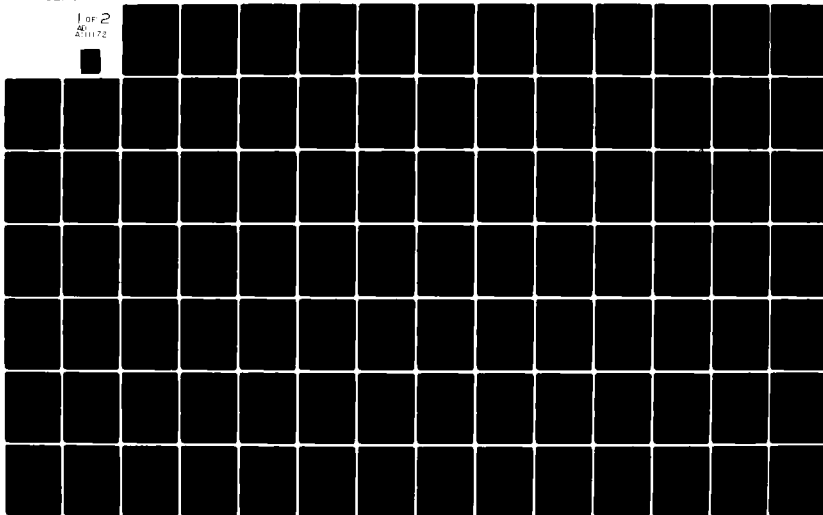
AD-A111 172

AIR FORCE INST OF TECH WRIGHT-PATTERSON AFB OH SCHOOL--ETC P/S 1/3  
USE OF THE PSEUDO-INVERSE FOR DESIGN OF A RECONFIGURABLE FLIGHT--ETC(U)  
DEC 81 S J RASA  
AFIT/GAE/AA/81D-23

UNCLASSIFIED

NL

1 of 2  
2511172



AD A111172

LEVEL II

①



ATC  
FEB 10 1982



copy 3 of 5

DEPARTMENT OF THE AIR FORCE  
AIR UNIVERSITY (ATC)  
**AIR FORCE INSTITUTE OF TECHNOLOGY**

Wright-Patterson Air Force Base, Ohio

This document has been approved  
for public release and sale; its  
distribution is unlimited.

82 02 18 033

AFIT/GAE/AA/81D-23

**LEVEL II**

①

USE OF THE PSEUDO-INVERSE FOR  
DESIGN OF A RECONFIGURABLE  
FLIGHT CONTROL SYSTEM  
THESIS

AFIT/GAE/AA/81D-23

Syed Javed Raza  
Sqn. Ldr. PAF

Approved for Public Release; Distribution Unlimited

E

AFIT/GAE/AA/81D-23

USE OF THE PSEUDO-INVERSE  
FOR DESIGN OF A RECONFIGURABLE FLIGHT CONTROL SYSTEM

THESIS

Presented to the Faculty of the School of Engineering  
of the Air Force Institute of Technology

Air University

In Partial Fulfillment of the  
Requirements for the Degree of

Master of Science

by

Syed Javed Raza

Sqn. Ldr. PAF

Graduate Aeronautical Engineering

December 1981

Approved for Public Release; Distribution Unlimited

Accession For	
NTIS GRA&I	<input checked="checked" type="checkbox"/>
DTIC TAB	<input type="checkbox"/>
Unannounced	<input type="checkbox"/>
Justification	<input type="checkbox"/>
By	
Date	
Dist	
A	

## Preface

I picked the area of controls for independent research based on two factors. First is simply the fascination that I hold for "automatic" control systems in general. The second has been the challenge I found in Wilbur Wright's address to the Western Society of Engineers in 1901 when he said

"....Men already know how to construct wings and aeroplanes which when driven through the air at sufficient speed will not only sustain the weight of the wings themselves, but also that of the engine, and of the engineer as well....Inability to steer still confronts students of the flying problem....when this one feature has been worked out, the age of flying machines will have arrived, for all other difficulties are of minor importance."

Fortunately, this area paralleled the major sequences of my graduate course at AFIT. The topic I chose was of current interest to the AF Flight Dynamics Laboratory as an alternative to redundancy for enhancing combat aircraft survivability.

I have attempted to design a reconfigurable flight control system that is practically feasible and is based on a novel approach. It is hoped that this concept will attract the attention of tomorrow's designers and will, therefore, be of some practical utility.

For the successful completion of this project, I wish to express my sincere gratitude to my thesis advisor, Captain James T. Silverthorn, whose depth of knowledge and unending will to work are impressive. His suggestions during the study were valuable and his help in compiling the draft invaluable. I also wish to thank Dr. Robert A. Calico, Jr. and Captain D. Audley for their useful guidelines. Thanks are also due to the AF Flight Dynamics Laboratory for sponsoring the project. The manuscript could not have been in its present form except for the conscious effort of Sharon A. Gabriel, which I appreciate. Last, but not the least, I acknowledge with pride the patience with which my wife took the late hours, the weekends, and all that went with it during my work.

Syed Javed Raza

## Table of Contents

	Page
Preface-----	ii
List of Figures-----	v
List of Tables-----	vii
List of Symbols-----	viii
Abstract-----	xiii
I. Introduction-----	1
Background-----	2
Previous Work-----	4
Problem Statement-----	5
Purpose-----	5
Scope-----	6
Approach-----	8
Assumptions-----	10
Sign Convention-----	11
Presentation-----	11
II. Development of Equations for the A-7D Aircraft---	12
Introduction-----	12
Physical Description-----	12
Aircraft Dynamics-----	13
State Variable Representation-----	27
A-7D Parameters-----	28
A and B Matrices-----	36
Eigenvalues of the Plant Matrix-----	37
Summary-----	37
III. Reconfigurable Flight Control System Design Using Pseudo-Inverse-----	39
Introduction-----	39
The Design Philosophy-----	40
Generic Inputs-----	41
Basic Flight Control System-----	42
Transformation Matrix Using Pseudo-Inverse---	44
Reconfiguration for Right Elevator Failure---	48
Reconfiguration for Other Surface Failures---	52
Summary-----	55
IV. Reconfigurable Flight Control System Design for the A-7D-----	56

	<u>Page</u>
Introduction-----	56
Basic Flight Control System-----	56
No Failure Transformation Matrix-----	70
Failure Transformation Matrix-----	75
Summary-----	77
 V. Flight Simulation-----	 79
Introduction-----	79
System Model for Six Degree-of-Freedom Simulation-----	80
Flight Simulation (Existing Flight Control System)-----	83
Flight Simulation (Reconfigurable Flight Control System)-----	84
Summary-----	86
 VI. Comparison of Results-----	 88
Introduction-----	88
No-Failure Flight Simulation-----	89
Simulation of "Failure" Flights-----	89
Determining Time Specifications for Failure Identification-----	104
Sensitivity to Parameter Variations-----	105
 VII. Conclusions and Recommendations-----	 108
 Bibliography-----	 113
 APPENDIX A: Basic Flight Control System Design Using Classical Techniques-----	 115
 APPENDIX B: Existing and Design Flight Control System Representation-----	 129
 Vita-----	 140

## List of Figures

<u>Figure</u>		<u>Page</u>
3.1	Block Diagram Representation of the Design Scheme for the "No-Failure" Case-----	43
3.2	Block Diagram Representation of the Design Scheme for the Right Elevator Failure Case-----	50
3.3	Block Diagram Representation of the Design Scheme for the Reconfigurable Flight Control System-----	54
4.1	Pitch Stability Augmentation System and Normal "g" Command System-----	61
4.2	Time Response of Longitudinal Flight Control System to $A_{N_c}$ -----	63
4.3	Time Response for $b_{long}$ -----	64
4.4	Yaw Stability Augmentation System with Washout Circuit-----	67
4.5	p-command System-----	67
5.1	General Simulation Scheme-----	85
6.1	Short Period Response of Existing Flight Control System-----	90
6.2	Dutch Roll Response of Existing Flight Control System-----	91
6.3	Short Period Response of Design Flight Control System-----	92
6.4	Dutch Roll Response of Design Flight Control System-----	93
6.5	Normal Acceleration Response for Right Elevator Failure at Zero Degrees-----	95
6.6	Roll Rate Response for Right Elevator Failure; No Reconfiguration-----	96
6.7	Roll Rate Response for Right Elevator Failure with Reconfiguration-----	97



<u>Figure</u>		<u>Page</u>
6.8	Roll Rate Response for Right Aileron Failure; No Reconfiguration-----	98
6.9	Roll Rate Response for Right Aileron Failure with Reconfiguration-----	99
6.10	Roll Rate Response for Right Elevator Failure at Maximum Deflection-----	102
6.11	Roll Rate Response for Right Aileron Failure at Maximum Deflection-----	103
A.1	Inner Loop Closure, Longitudinal Flight Control System-----	116
A.2	Initial Outer Loop Closure, Longitudinal Flight Control System-----	118
A.3	Frequency Response of a Pure Gain Controller--	120
A.4	Time Response of Proportional Plus Integral Controller-----	121
A.5	Frequency Response of Proportional Plus Integral Controller-----	122
A.6	Frequency Response of Longitudinal Flight Control System-----	123
B.1	A-7D Existing Pitch Axis Control (Simplified)-	130
B.2	A-7D Existing Roll Axis Control (Simplified)--	131
B.3	A-7D Existing Yaw Axis Control (Simplified)---	132
B.4	Design Pitch Axis Control System-----	137
B.5	Design Roll Axis Control System-----	138
B.6	Design Yaw Axis Control System-----	138

## List of Tables

<u>Table</u>		<u>Page</u>
I	A-7D Cruise Configuration Data-----	14
II	Definition of New Longitudinal Dimensional Control Derivatives-----	18
III	Definition of New Lateral-Directional Dimensional Control Derivatives-----	23
IV	Non-Dimensional Stability and Control Derivatives for the A-7D in Cruise Configuration-----	32
V	Dimensional Stability and Control Derivatives for the A-7D in Cruise Configuration-----	34
VI	Summary of Results for Delay Time Specifications-----	105
VII	Summary of Results for Sensitivity Analysis-----	106

# List of Symbols

$A_N$	Normal acceleration	g
$b$	(Wing) span	ft
$\bar{c}$	Mean aerodynamic (geometric) chord	ft
$C_L = \frac{L}{qS}$	Lift coefficient (airplane)	
$C_D = \frac{D}{qS}$	Drag coefficient (airplane)	
$C_m = \frac{M}{qS\bar{c}}$	Pitching moment coefficient (airplane, planform)	
$C_\ell = \frac{L}{qSb}$	Rolling moment coefficient	
$C_n = \frac{N}{qSb}$	Yawing moment coefficient	
$C_y = \frac{F_y}{qS}$	Side force coefficient	
$C_{D_\delta} = \frac{\partial C_D}{\partial \delta}$	Variation of drag coefficient with control surface angle	rad <sup>-1</sup>
$C_{L_\delta} = \frac{\partial C_L}{\partial \delta}$	Variation of lift coefficient with control surface angle	rad <sup>-1</sup>
$C_{m_\alpha} = \frac{\partial C_m}{\partial \alpha}$	Variation of Pitching moment coefficient with angle of attack (i.e., longitudinal stability)	rad <sup>-1</sup>
$C_{m_\delta} = \frac{\partial C_m}{\partial \delta}$	Variation of pitching moment coefficient with control surface angle	rad <sup>-1</sup>

$C_{\ell\delta} = \frac{\partial C_{\ell}}{\partial \delta}$	Variation of rolling moment coefficient with control surface angle	rad <sup>-1</sup>
$C_{y\delta} = \frac{\partial C_y}{\partial \delta}$	Variation of side force coefficient with control surface angle	rad <sup>-1</sup>
$C_{n\delta} = \frac{\partial C_n}{\partial \delta}$	Variation of yawing moment coefficient with control surface angle	rad <sup>-1</sup>
$g$	Acceleration of gravity	ft/sec <sup>2</sup>
$I_{xx}, I_{yy}, I_{zz}$	Moments of inertia about X, Y, Z axes, respectively	slug ft <sup>2</sup>
$I_{xz}$	Product of inertia in XYZ system	slug/ft <sup>2</sup>
$L_{\beta}$	Dimensional variation of rolling moment about $X_s$ with sideslip angle	sec <sup>-2</sup>
$L_p$	Dimensional variation of rolling moment about $X_s$ with roll rate	sec <sup>-1</sup>
$L_r$	Dimensional variation of rolling moment about $X_s$ with yaw rate	sec <sup>-1</sup>
$L_{\delta}$	Dimensional variation of rolling moment about $X_s$ with elevator, aileron and rudder angle	sec <sup>-2</sup>
$m$	Mass (airplane)	slugs
$M_u$	Dimensional variation of pitching moment with speed	ft <sup>-1</sup> sec <sup>-1</sup>
$M_{\alpha}$	Dimensional variation of pitching moment with angle of attack	sec <sup>-2</sup>

$M_{\dot{\alpha}}$	Dimensional variation of pitching moment with rate of change of angle of attack	$\text{sec}^{-1}$
$M_q$	Dimensional variation of pitching moment with pitch rate	$\text{sec}^{-1}$
$M_{\delta}$	Dimensional variation of pitching moment with elevator, aileron and rudder angle	$\text{sec}^{-2}$
$n$	Perturbed yawing moment	ft lbs
$N_{\beta}$	Dimensional variation of yawing moment about $Z_s$ with sideslip angle	$\text{sec}^{-2}$
$N_p$	Dimensional variation of yawing moment about $Z_s$ with roll rate	$\text{sec}^{-1}$
$N_r$	Dimensional variation of yawing moment about $Z_s$ with yaw rate	$\text{sec}^{-2}$
$N_{\delta}$	Dimensional variation of yawing moment about $Z_s$ with elevator, aileron and rudder angle	$\text{sec}^{-2}$
$p$	Perturbed roll rate (about x)	rad/sec
$\bar{q}$	Dynamic pressure	$\text{lb}_f/\text{ft}^2$
$r$	Perturbed yaw rate	rad/sec
$S$	Surface area, Reference (wing) area	$\text{ft}^2$
$U_1$	Forward velocity (along X) steady state	ft/sec
$u$	Perturbed forward velocity (along X)	ft/sec

$v$	Perturbed side velocity	ft/sec
$w$	Perturbed downward velocity	ft/sec
$X_u$	Dimensional variation of $X_s$ -force with speed	sec <sup>-1</sup>
$X_\alpha$	Dimensional variation of $X_s$ -force with angle of attack	ft/sec <sup>2</sup>
$X_{\dot{\alpha}}$	Dimensional variation of $X_s$ -force with rate of change of angle of attack	ft/sec
$X_\delta$	Dimensional variation of $X_s$ -force with elevator, aileron and rudder angle	ft/sec <sup>2</sup>
$Y_\beta$	Dimensional variation of $Y_s$ -force with sideslip angle	ft/sec <sup>2</sup>
$Y_p$	Dimensional variation of $Y_s$ -force with roll rate	ft/sec
$Y_r$	Dimensional variation of $Y_s$ -force with yaw rate	ft/sec
$Y_\delta$	Dimensional variation of $Y_s$ -force with elevator, aileron and rudder angle	ft/sec <sup>2</sup>
$Z_u$	Dimensional variation of $Z_s$ -force with speed	sec <sup>-1</sup>
$Z_\alpha$	Dimensional variation of $Z_s$ -force with angle of attack	ft/sec <sup>2</sup>
$Z_{\dot{\alpha}}$	Dimensional variation of $Z_s$ -force with rate of change of angle of attack	ft/sec

$Z_q$	Dimensional variation of $Z_S$ -force with pitch rate	ft/sec
$Z_\delta$	Dimensional variation of $Z_S$ -force with elevator, aileron and rudder angle	ft/sec <sup>2</sup>
$\theta, \theta_1, \theta$	Pitch attitude angle (total, steady state, perturbed)	rad
$\phi, \phi$	Bank angle (total, perturbed)	rad
$\alpha$	Angle of attack	rad
$\beta$	Sideslip angle	rad
$\lambda$	Closed-loop eigenvalue	

Abstract

A technique for the design of a reconfigurable flight control system using the pseudo-inverse is developed and applied. To study the problem, single primary control surface failure is considered and the A-7D aircraft is used as a model. Each individual control surface is treated independently, resulting in coupling of the longitudinal and lateral-directional response. Linearized aircraft equations of motion are developed, taking into account the effect of this coupling.

A basic flight control system is designed that is capable of generating generic longitudinal, lateral and directional commands. Using a transformation matrix, these generic inputs are defined as some linear combination of the available control surfaces. For each failure case considered, unique transformation matrices are developed using the pseudo-inverse. Reconfiguration is achieved not by redefining control laws of the basic flight control system for each failure case, but by implementing appropriate transformation matrices.

The design is tested against a six degree-of-freedom nonlinear simulation capable of simulating flights with and without failure of control surfaces. A time lag of 0.5 seconds was used for all the tests as the time delay between actual surface failure, its identification and finally, reconfiguration. Reconfiguration achieved by this design is shown to provide desirable flying qualities even in the event of one primary control surface failure. Surface was simulated to fail both at neutral (zero degree) position and maximum deflection. Response is also found to be good for parameter variation.



USE OF THE PSEUDO-INVERSE  
FOR DESIGN OF A RECONFIGURABLE FLIGHT CONTROL SYSTEM

I. Introduction

The short history of flight has seen extensive enhancements in the performance of aircraft. Naturally, as the performance has gone up, so has the requirement for better automated control. Existing aircraft are, therefore, equipped with flight control systems which provide the automated assistance and tend to have more moveable surfaces such as the ailerons, spoilers, flaps and elevators for redundant and adequate control. However, a serious limitation on these flight control systems has been their applicability only during normal operation of the various flight control system components like the control surfaces, actuators and linkages. In case of an emergency when one of the primary control surfaces becomes inoperative due to in-flight damage, mechanical failure, etc., of one of these components, the needed assistance of the flight control system is withdrawn and the pilot is confronted with the task of controlling the aircraft against the unwanted forces and moments generated by the failed surface.

Such a situation highlights the requirement of a reconfigurable flight control system that could be implemented during those rare circumstances to assist the pilot in controlling the aircraft. Its purpose would be to produce normal flight characteristics in the event of any control surface failure by utilizing the remaining control surfaces. Although degraded performance may be expected, the flying quality parameters after reconfiguration must remain in the acceptable range. This thesis is an effort to design such a reconfigurable flight control system.

#### Background

The Air Force Flight Dynamics Laboratory (AFFDL) has been exploring the feasibility of employing reconfiguration technique to restore stability and controllability in the event of a primary control surface failure. As briefly outlined above, the motivation for such a study evolves from the stringent control requirements that are placed on modern and future aircraft. The existing flight control systems are valid only if each element of the control loop is operative. Primary control surfaces like the elevators, ailerons, flaps, spoilers, etc., are the major functional elements of the control loop. These can become inoperative/ineffective during flight for several reasons such as hardware failure, mechanical failure, or battle damage. Under such circumstances, the control laws of the flight

control system become invalid. This situation is further aggravated in the case of modern aircraft which are primarily statically unstable and therefore depend on the operation of the flight control system for flight. In an emergency, therefore, when the pilot himself might not perform his best, he is required to mentally analyze the failure and manually generate the commands necessary to control the damaged aircraft. For example, if the right elevator were to become ineffective during flight, any elevator commands, either by the pilot or the flight control system, would produce one-half the desired effect on the longitudinal motion. More significantly, deflections of the operating surface would produce undesired rolling moments. In this situation, the pilot would have to continuously remember to apply opposing lateral control when he applied longitudinal inputs.

Reconfiguration of control laws appears to be a promising solution to this problem. It implies compensation of a surface failure by using the remaining surfaces to control the aircraft. It has the great advantage of not only providing at least a "get home" capability after failure of any primary flight control surface, but it offers in addition the greatest potential for improvement of flight control survivability. In a study of control surface reconfiguration, Reference 1 indicates that vulnerability of the aircraft may be reduced by as much as a factor of two in case of reconfigurable control surfaces.

### Previous Work

Such desirable advantages as described above have been reason enough for further study and investigation in this field. In fact, two major works have already been published on the subject, with various conclusions. In one of the studies (Ref 1), the set of moveable surfaces on the baseline aircraft were examined to establish feasible alternate control surface combinations for each of the control axes. Digital control laws were then formulated for the alternate control surfaces, and simulation runs were performed to evaluate the control performance. The results of this study indicated that the use of a single horizontal tail panel for alternate pitch control was impractical. It concludes by remarking that "...The key to mechanizing this is to find the best way to combine the available surfaces..... to get the best compromise for both pitch and roll control."

Reference 2, which was an effort to use entire eigenstructure assignment (EEA) for designing the multivariable reconfigurable control law points out that, in the absence of some criteria for picking the eigenvectors of the closed loop plant matrix, the technique remains doubtful inasmuch as the initial control inputs are concerned which could well exceed the physical limits of the actuator. Both of these works were based on a digital flight control system which provides the capability of processing information and data within short times.

### Problem Statement

The A-7D primarily uses the horizontal stabilator for pitch control, the ailerons for lateral or roll control and the rudder for directional control. If, during a straight and level flight, one of the primary flight control systems, e.g., the right elevator or the right aileron, becomes ineffective or inoperative and, for instance, gets stuck at the trim position, then in response to any command given by either the pilot or the flight control system, it will generate unwanted forces and moments that would tend to render the aircraft unstable. A worst case could be when it gets stuck at a position other than zero or trim value, more precisely at some max deflection. In the latter case, the aircraft would go unstable more rapidly. To recover the aircraft from such a situation, an obvious method is to use the remaining control surfaces in order to counter the unwanted forces and moments and to restore stability and control of the aircraft.

### Purpose

The purpose of this research is, therefore, to design a reconfigurable flight control system for the A-7D Digitac II aircraft that will produce flight characteristics similar to the existing flight control system even in the event of failure of any one of the primary flight control surfaces, i.e., the right or left elevator or the right or

left aileron. Specifically, the reconfigurable flight control system should enable three-axis control with one of the following inoperable:

one horizontal stabilator

one aileron.

This flight control system would be tested by simulating failure flights of one primary flight control surface and then evaluating the flight control system in terms of closed loop eigenvalues, step response, transient response and effect of parameter variations.

The A-7D Digitac II aircraft was chosen since an earlier work (Ref 2) has already been done on that aircraft and some data would be used from that work.

### Scope

Obviously, the reconfiguration technique would require two major steps:

(a) The failure or loss of a surface function must be detected and isolated to a specific surface panel and reconfigured control laws must be implemented depending on the specific failure.

(b) The control laws must be reconfigured to provide suitable commands to the remaining surfaces to permit correct aircraft response.

The scope of this work is strictly limited to paragraph (b) above. It does not address the first problem

at all except for allowing a delay time between the occurrence of failure and implementation of the reconfigured control laws. The delay time is the time elapsed in performing the detection and identification of the failure and the reconfiguration of the control laws.

A reasonable estimate of this delay time has been taken from Reference 1, where it is concluded in the control surface failure tests that the failures were detected and isolated within a maximum of 1.2 seconds for all maneuvers and for all flight conditions with and without turbulence. For this study, therefore, delay times between 0.5 seconds and 2.0 seconds were examined.

The design is further limited to the case where only one primary flight control surface fails. Although, as will be shown later, the same technique could also be successfully applied to two or more surface failures. Due to this limitation, the independent controls needed to provide stability and control were also limited to four of the five remaining primary flight control surfaces; namely, right and left elevator, right and left aileron, and the rudder. It was felt, for example, that for a right elevator failure, the left elevator, the two ailerons and the rudder would suffice for the necessary three-axis control.

## Approach

In contrast to the previous work (Refs 1 and 2), which dealt with the design of reconfigurable control laws in the digital domain, this research deals with design of reconfigurable control laws for the analog flight control system; the reason primarily being that the digital flight control system is itself a relatively new idea. Design of reconfigurable control laws for the digital flight control system, therefore, would mean attacking two new problems at the same time. On the other hand, design of reconfigurable control laws for the existing analog flight control system, which are generally well understood and successfully employed in the current aircraft, would allow concentration of effort on the reconfiguration technique. The theory used in this study for reconfiguration, while applied to an analog flight control system, is directly transferrable to a digital flight control system.

The general approach to the problem is completely different from the previous works and is found to provide some very encouraging results. The reason for employing this different approach is because the earlier approaches employed complex design techniques, e.g., multi-input, multi-output control, and produced designs that would be difficult to implement. To illustrate this point better, the method of Reference 2 is described here before the approach of the present work is outlined.



Reference 2 uses state variable feedback for compensation of a surface failure. The reconfigured control laws are designed for one surface failure and one flight condition using entire eigenstructure assignment for the multi-input/multi-output case. As the author has mentioned in his conclusions, this process of designing multivariable control laws, while being feasible, is tedious and wanting of certain decision making criteria in respect to the eigenvectors of the closed loop plant matrix. In the absence of such criteria, the designed control law is not insured to be practically realizable. However, given that a set of realizable control laws is obtained for that surface failure and that flight condition, the process is to be started from ground zero for any other flight condition. It follows, therefore, that for each surface failure and each flight condition, the complete design process is to be repeated from the same starting point. Subsequently, when it comes to applying this set of control laws, the gain scheduling might become unmanageably complicated. These difficulties established the need for an approach where such problems are either not encountered or at least minimized to manageable levels.

The approach followed here is to consider each individual primary flight control surface as an independent control input. Thus, the right elevator may be commanded independently of the left elevator, or vice versa. Similarly, the right aileron may be commanded independently of the left

aileron, etc. Then, instead of considering each one of these as an independent input, three generic inputs are defined for the three-axis control. These generic inputs are basically expressed as some linear combination of the available control inputs. Based on these inputs, a set of control laws is developed for a no-failure case that meets the flying qualities criteria. Next, a failure case is considered; for instance, the right elevator becoming inoperative. In order to achieve the same performance level, the generic inputs now have to be defined as a different linear combination of the available control inputs. This is achieved by using a pseudo inverse matrix. For each surface failure, therefore, there is a different transformation matrix relating generic inputs to available control surfaces, but the same elementary control law. Hence, this approach is simpler to use for design as well as promising insofar as practical application is concerned. Details of the methodology are given in Chapter III.

#### Assumptions

Consistent with literature in the area of controls, certain assumptions were made. For the design of the control laws, the assumption of small perturbations about trimmed flight generates linear, constant coefficient differential equations. These control laws were, however, evaluated against a non-linear six degree of freedom simulation of the aircraft. For the flight condition

picked, Mach 0.6 at an altitude of 15,000 feet, the thrust was assumed independent of aircraft speed.

### Sign Convention

The following (standard) sign convention is used throughout the work.

1. Right and left elevator  $\delta_{e_r}$ ,  $\delta_{e_l}$  and left aileron  $\delta_{a_l}$  taken positive for trailing edge down.
2. Right aileron  $\delta_{a_r}$  taken positive for trailing edge up.
3. Rudder  $\delta_r$  taken positive for trailing edge left in top view.
4. All other aerodynamic forces and moments follow the sign conventions of Reference 3, which are fairly well accepted as standard.

### Presentation

This thesis is composed of seven chapters. Chapter II deals with the development of aircraft equations for the A-7D aircraft. Chapter III covers the design theory for the reconfigurable control laws, while Chapter IV applies this theory to the A-7D linearized equations. Chapter V details the development of flight simulation for evaluating the design flight control system. Chapter VI is mainly comparison of results for the existing and design flight control systems, while Chapter VII gives conclusions and recommendations based on the entire work.

## II. Development of Equations for the A-7D Aircraft

### Introduction

A set of differential equations that represents aircraft dynamics is usually the starting point in design works of this nature. The accuracy of the final design obviously depends upon the accuracy of these equations. A special consideration in this study is that each individual control surface is treated independent, as opposed to considering the right and left surface as a set. Since this results in input coupling between the longitudinal and lateral directional modes of motion, this set of equations will be different from that which is generally available in other references. This chapter deals with development of these equations in light of the above mentioned considerations. It presents a physical description of the aircraft, the effect of input coupling on certain aircraft parameters, and finally, the development of the aircraft model in the state variable form.

### Physical Description

The A-7D is a subsonic, single-seat tactical fighter with moderately swept wing and tail surfaces. It is powered by one Allison TF41-A-1 turbofan engine rated at 14,250 lb

without afterburning. The wing control surfaces include plain sealed inset ailerons activated by the hydraulic system, leading edge flaps, single slotted trailing edge flaps and spoilers. The tail unit embodies a swept vertical fin and rudder and one-piece horizontal "slab" tailplane, all operated by the hydraulic system. Its automatic flight control system provides control-stick steering, altitude hold, heading hold, heading pre-select and attitude hold (Ref 4).

A cruise configuration with medium dynamic pressure has been selected as a representative flight condition for this study. Aircraft data under this configuration as obtained from Reference 5 is tabulated in Table I.

#### Aircraft Dynamics

Experience has shown that in many cases aircraft dynamics may be satisfactorily represented by assuming small perturbations away from steady state or trimmed flight. Since this assumption is widely used in other control works, it is adopted in this study as well. Furthermore, the following assumptions also apply:

- The X and Z axes are in the plane of symmetry and the origin of the axes is at the center of gravity of the aircraft
- The mass of the aircraft is constant
- The aircraft is a rigid body

- The earth is an inertial reference frame, and
- The flow is quasi-steady.

TABLE I  
A-7D Cruise Configuration Data

Altitude	$h$	15,000 feet
Mach No.	$M$	0.6
Weight	$W$	25,338 lbs
Center of Gravity	$C_g$	28.7% of $mgc$
Dynamic Pressure	$\bar{q}$	300.88 slugs/ft <sup>2</sup>
Wing Area	$S$	375 ft <sup>2</sup>
Wing Span	$b$	38.73 ft
Mean Aero Chord	$\bar{c}$	10.84 ft
Moment of Inertia	$I_{xx}$	15,365 slugs ft <sup>2</sup>
Moment of Inertia	$I_{yy}$	69,528 slugs ft <sup>2</sup>
Moment of Inertia	$I_{zz}$	79,005 slugs ft <sup>2</sup>
Moment of Inertia	$I_{xz}$	-1,664 slugs ft <sup>2</sup>

Based on these assumptions, the longitudinal and lateral-directional equations are developed as follows:

Longitudinal Motion. The linearized longitudinal equations of motion in stability axes assuming small

perturbations about a straight and level trim condition, as obtained from Reference 3 are

$$\begin{aligned} m\dot{u} = & -mg\theta\cos\theta + \bar{q}S \{ -(C_{D_u} + 2C_D) \frac{u}{U} + (C_{T_u}) \frac{u}{U} \\ & - (C_{D_\alpha} - C_L)\alpha - C_{D_{\delta_e}} \delta_e \} \end{aligned} \quad (1)$$

$$\begin{aligned} m(\dot{w} - Uq) = & -mg\theta\sin\theta + \bar{q}S \{ -(C_{L_u} + 2C_L) \frac{u}{U} - (C_{L_\alpha} + C_D)\alpha \\ & - C_{L_\alpha} \frac{\dot{\alpha}}{2U} - C_{L_q} \frac{q}{2U} - C_{L_{\delta_e}} \delta_e \} \end{aligned} \quad (2)$$

$$\begin{aligned} I_{yy}\dot{q} = & \bar{q}S\bar{c} \{ (C_{m_u} + 2C_m) \frac{u}{U} + (C_{m_{T_u}} + 2C_{m_T}) \frac{u}{U} \\ & + C_{m_\alpha} \alpha + C_{m_{T_\alpha}} + C_{m_\alpha} \frac{\dot{\alpha}}{2U} + C_{m_q} \frac{q}{2U} + C_{m_{\delta_e}} \delta_e \} \end{aligned} \quad (3)$$

The variables  $\bar{q}$ ,  $U$ ,  $\theta$  and all other aerodynamic coefficients are evaluated at their trim or equilibrium value. For the stability axes and assuming horizontal flight  $q_1 = 0$ , and for the small perturbations case  $w = U\alpha$ . Furthermore, since all the primary flight control surfaces are independently controllable, instead of assuming  $\delta_e$  as the only longitudinal control input, all the primary flight control surface inputs are assumed effective for both longitudinal and lateral directional motions. Hence, the single input  $\delta_e$  is replaced by the five independent inputs, the right and left elevator, the

right and left aileron and the rudder; symbolically, inputs  $\delta_{e_r}$ ,  $\delta_{e_\ell}$ ,  $\delta_{a_r}$ ,  $\delta_{a_\ell}$  and  $\delta_r$ . Along with these new inputs, the appropriate non-dimensional control derivatives like  $C_{L_{\delta_{a_r}}}$ ,  $C_{D_{\delta_r}}$  and  $C_{m_{\delta_{e_\ell}}}$ , which are not required in the conventional equations, are also introduced. With these substitutions, and assuming thrust is independent of speed, Eqs (1), (2) and (3) may be rewritten as:

$$\begin{aligned} m\dot{u} = & -mg\theta + \bar{q}S \{ -(C_{D_u} + 2C_D) \frac{u}{U} - (C_{D_\alpha} - C_L)\alpha \\ & - (C_{D_{\delta_{e_r}}} \delta_{e_r}) - (C_{D_{\delta_{e_\ell}}} \delta_{e_\ell}) - (C_{D_{\delta_{a_r}}} \delta_{a_r}) \\ & - (C_{D_{\delta_{a_\ell}}} \delta_{a_\ell}) - (C_{D_{\delta_r}} \delta_r) \} \end{aligned} \quad (4)$$

$$\begin{aligned} mU\dot{\alpha} = & mUq + \bar{q}S \{ -(C_{L_u} + 2C_L) \frac{u}{U} - (C_{L_\alpha} + C_D)\alpha - (C_{L_\alpha} \frac{\dot{\alpha}}{2U}) \\ & - C_{L_q} \frac{q}{2U} - C_{L_{\delta_{e_r}}} \delta_{e_r} - C_{L_{\delta_{e_\ell}}} \delta_{e_\ell} - C_{L_{\delta_{a_r}}} \delta_{a_r} - C_{L_{\delta_{a_\ell}}} \delta_{a_\ell} - C_{L_{\delta_r}} \delta_r \} \end{aligned} \quad (5)$$

$$\begin{aligned} I_{yy}\dot{q} = & \bar{q}S\bar{c} \{ (C_{m_u} + 2C_m) \frac{u}{U} + C_{m_\alpha} \alpha + C_{m_\alpha} \frac{\dot{\alpha}}{2U} + C_{m_q} \frac{q}{2U} \\ & + C_{m_{\delta_{e_r}}} \delta_{e_r} + C_{m_{\delta_{e_\ell}}} \delta_{e_\ell} + C_{m_{\delta_{a_r}}} \delta_{a_r} + C_{m_{\delta_{a_\ell}}} \delta_{a_\ell} + C_{m_{\delta_r}} \delta_r \} \end{aligned} \quad (6)$$



Dividing both sides by  $U$  or  $I_{yy}$  as applicable, and following the definition of dimensional derivatives as in Reference 3, certain new dimensional control derivatives are defined as detailed in Table II. Substituting these dimensional stability and control derivatives of Table II as well as those defined in Reference 3, Eqns (4), (5) and (6) become:

$$\begin{aligned} \dot{u} = & -g\theta + X_u u + X_\alpha \alpha + X_{\delta_{e_r}} \delta_{e_r} + X_{\delta_{e_l}} \delta_{e_l} \\ & + X_{\delta_{a_r}} \delta_{a_r} + X_{\delta_{a_l}} \delta_{a_l} + X_{\delta_r} \delta_r \end{aligned} \quad (7)$$

$$\begin{aligned} \dot{\alpha} = & q + \frac{1}{U} [Z_u u + Z_\alpha \alpha + Z_{\dot{\alpha}} \dot{\alpha} + Z_q q + Z_{\delta_{e_r}} \delta_{e_r} \\ & + Z_{\delta_{e_l}} \delta_{e_l} + Z_{\delta_{a_r}} \delta_{a_r} + Z_{\delta_{a_l}} \delta_{a_l} + Z_{\delta_r} \delta_r] \end{aligned} \quad (8)$$

$$\begin{aligned} \dot{q} = & M_u u + M_\alpha \alpha + M_{\dot{\alpha}} \dot{\alpha} + M_q q + M_{\delta_{e_r}} \delta_{e_r} + M_{\delta_{e_l}} \delta_{e_l} \\ & + M_{\delta_{a_r}} \delta_{a_r} + M_{\delta_{a_l}} \delta_{a_l} + M_{\delta_r} \delta_r \end{aligned} \quad (9)$$

Eliminating  $\dot{\alpha}$  from Eq (9), substituting  $Z_{\dot{\alpha}} = 0$  for the A-7D aircraft (Ref 5), and rearranging:

TABLE II			
DEFINITION OF NEW LONGITUDINAL DIMENSIONAL CONTROL DERIVATIVES			
	Derivative	Definition	Units
X force	$X_{\delta e_r}$	$-\frac{\bar{q}S}{m} C_{D\delta e_r}$	ft-sec <sup>-2</sup> rad <sup>-1</sup>
	$X_{\delta e_\ell}$	$-\frac{\bar{q}S}{m} C_{D\delta e_\ell}$	ft-sec <sup>-2</sup> rad <sup>-1</sup>
	$X_{\delta a_r}$	$-\frac{\bar{q}S}{m} C_{D\delta a_r}$	ft-sec <sup>-2</sup> rad <sup>-1</sup>
	$X_{\delta a_\ell}$	$-\frac{\bar{q}S}{m} C_{D\delta a_\ell}$	ft-sec <sup>-2</sup> rad <sup>-1</sup>
	$X_{\delta r}$	$-\frac{\bar{q}S}{m} C_{D\delta r}$	ft-sec <sup>-2</sup> rad <sup>-1</sup>
Z force	$Z_{\delta e_r}$	$-\frac{\bar{q}S}{m} C_{L\delta e_r}$	ft-sec <sup>-2</sup> rad <sup>-1</sup>
	$Z_{\delta e_\ell}$	$-\frac{\bar{q}S}{m} C_{L\delta e_\ell}$	ft-sec <sup>-2</sup> rad <sup>-1</sup>
	$Z_{\delta a_r}$	$-\frac{\bar{q}S}{m} C_{L\delta a_r}$	ft-sec <sup>-2</sup> rad <sup>-1</sup>
	$Z_{\delta a_\ell}$	$-\frac{\bar{q}S}{m} C_{L\delta a_\ell}$	ft-sec <sup>-2</sup> rad <sup>-1</sup>
	$Z_{\delta r}$	$-\frac{\bar{q}S}{m} C_{L\delta r}$	ft-sec <sup>-2</sup> rad <sup>-1</sup>

(Table II continued on next page)

(Table II Cont'd)

	Derivative	Definition	Units
pitching moment	$M_{\delta e_r}$	$\frac{\bar{q}S\bar{c}}{I_{yy}} C_{m_{\delta e_r}}$	$\text{sec}^{-2} \text{ rad}^{-1}$
	$M_{\delta e_\ell}$	$\frac{\bar{q}S\bar{c}}{I_{yy}} C_{m_{\delta e_\ell}}$	$\text{sec}^{-2} \text{ rad}^{-1}$
	$M_{\delta a_r}$	$\frac{\bar{q}S\bar{c}}{I_{yy}} C_{m_{\delta a_r}}$	$\text{sec}^{-2} \text{ rad}^{-1}$
	$M_{\delta a_\ell}$	$\frac{\bar{q}S\bar{c}}{I_{yy}} C_{m_{\delta a_\ell}}$	$\text{sec}^{-2} \text{ rad}^{-1}$
	$M_{\delta r}$	$\frac{\bar{q}S\bar{c}}{I_{yy}} C_{m_{\delta r}}$	$\text{sec}^{-2} \text{ rad}^{-1}$

$$\begin{aligned}
\dot{q} = & (M_u + \frac{M_{\dot{\alpha}}}{U} Z_u)u + (M_{\alpha} + \frac{M_{\dot{\alpha}}}{U} Z_{\alpha})\alpha + (M_{\dot{\alpha}} + Z_q + M_q)q \\
& + (\frac{M_{\dot{\alpha}}}{U} Z_{\delta_{e_r}} + M_{\delta_{e_r}})\delta_{e_r} + (\frac{M_{\dot{\alpha}}}{U} Z_{\delta_{e_l}} + M_{\delta_{e_l}})\delta_{e_l} \\
& + (\frac{M_{\dot{\alpha}}}{U} Z_{\delta_{a_r}} + M_{\delta_{a_r}})\delta_{a_r} + (\frac{M_{\dot{\alpha}}}{U} Z_{\delta_{a_l}} + M_{\delta_{a_l}})\delta_{a_l} \\
& + (\frac{M_{\dot{\alpha}}}{U} Z_{\delta_r} + M_{\delta_r})\delta_r
\end{aligned} \tag{10}$$

Equations (7), (8) and (10) form a set of three first order coupled ordinary differential equations which are linear in the four variables  $u$ ,  $\alpha$ ,  $q$  and  $\theta$ . To complete the set of longitudinal equations, therefore, the fourth kinematic equation is introduced.

$$\dot{\theta} = q \tag{11}$$

Lateral Directional Motion. The linearized lateral-directional equations of motion assuming small perturbations about straight and level flight, as obtained from Reference 3, are:

$$\begin{aligned}
m(\dot{v} + Ur) = & mg\phi\cos\theta_1 + \bar{q}S(C_{y_{\beta}}\beta + C_{y_p}\frac{pb}{2U} + C_{y_r}\frac{rb}{2U} \\
& + C_{y_{\delta_a}}\delta_a + C_{y_{\delta_r}}\delta_r)
\end{aligned} \tag{12}$$

$$\begin{aligned}
I_{xx}\dot{p} - I_{xz}\dot{r} &= \bar{q}Sb(C_{l_\beta}\beta + C_{l_p}\frac{pb}{2U} \\
&+ C_{l_r}\frac{rb}{2U} + C_{l_{\delta_a}}\delta_a + C_{l_{\delta_r}}\delta_r)
\end{aligned} \tag{13}$$

$$\begin{aligned}
I_{zz}\dot{r} - I_{xz}\dot{p} &= \bar{q}Sb(C_{n_\beta}\beta + C_{n_T}\frac{pb}{2U} \\
&+ C_{n_r}\frac{rb}{2U} + C_{n_{\delta_a}}\delta_a + C_{n_{\delta_r}}\delta_r)
\end{aligned} \tag{14}$$

Rewriting these equations for the stability axes ( $\Theta_1 = 0$ ), assuming thrust independent of speed, replacing control inputs  $\delta_a$  and  $\delta_r$  by the same five independent control inputs as for the longitudinal case, introducing new non-dimensional control derivatives like  $C_{y_{\delta_{e_r}}}$ ,  $C_{n_{\delta_{e_\ell}}}$  and  $C_{l_{\delta_{e_\ell}}}$  and rearranging:

$$\begin{aligned}
\dot{v} &= -Ur + g\phi + \frac{\bar{q}S}{m} [C_{y_\beta}\beta + C_{y_p}\frac{pb}{2U} + C_{y_r}\frac{rb}{2U} \\
&+ C_{y_{\delta_{e_r}}}\delta_{e_r} + C_{y_{\delta_{e_\ell}}}\delta_{e_\ell} + C_{y_{\delta_{a_r}}}\delta_{a_r} + C_{y_{\delta_{a_\ell}}}\delta_{a_\ell} + C_{y_{\delta_r}}\delta_r]
\end{aligned} \tag{15}$$

$$\begin{aligned} \dot{p} = & \frac{I_{xz}}{I_{xx}} \dot{r} + \frac{\bar{q}Sb}{I_{xx}} [C_{l_{\beta}} \beta + C_{l_p} \frac{pb}{2U} + C_{l_r} \frac{rb}{2U} \\ & + C_{l_{\delta e_r}} \delta e_r + C_{l_{\delta e_l}} \delta e_l + C_{l_{\delta a_r}} \delta a_r + C_{l_{\delta a_l}} \delta a_l + C_{l_{\delta r}} \delta_r] \end{aligned} \quad (16)$$

$$\begin{aligned} \dot{r} = & \frac{I_{xz}}{I_{zz}} \dot{p} + \frac{\bar{q}Sb}{I_{zz}} [C_{n_{\beta}} \beta + C_{n_p} \frac{pb}{2U} + C_{n_r} \frac{rb}{2U} \\ & + C_{n_{\delta e_r}} \delta e_r + C_{n_{\delta e_l}} \delta e_l + C_{n_{\delta a_r}} \delta a_r + C_{n_{\delta a_l}} \delta a_l + C_{n_{\delta r}} \delta_r] \end{aligned} \quad (17)$$

These equations can be simplified by using the definition of dimensional control derivatives as in Reference 3, and by defining new dimensional control derivatives as before. These are detailed in Table III. Substituting these dimensional derivatives of Table III as well as those defined in Reference 3, noting that for the small perturbations case  $\dot{v} = U\dot{\beta}$ , and eliminating  $\dot{r}$  and  $\dot{p}$  from Eqns (16) and (17), respectively, Eqns (15), (16) and (17) are rewritten as:

TABLE III

DEFINITION OF NEW LATERAL-DIRECTIONAL  
DIMENSIONAL CONTROL DERIVATIVES

	Derivative	Definition	Units
Y force	$Y_{\delta_{e_r}}$	$\frac{\bar{q}S}{m} C_{y_{\delta_{e_r}}}$	ft-sec <sup>-2</sup> rad <sup>-1</sup>
	$Y_{\delta_{e_l}}$	$\frac{\bar{q}S}{m} C_{y_{\delta_{e_l}}}$	ft-sec <sup>-2</sup> rad <sup>-1</sup>
	$Y_{\delta_{a_r}}$	$\frac{\bar{q}S}{m} C_{y_{\delta_{a_r}}}$	ft-sec <sup>-2</sup> rad <sup>-1</sup>
	$Y_{\delta_{a_l}}$	$\frac{\bar{q}S}{m} C_{y_{\delta_{a_l}}}$	ft-sec <sup>-2</sup> rad <sup>-1</sup>
	$Y_{\delta_r}$	$\frac{\bar{q}S}{m} C_{y_{\delta_r}}$	ft-sec <sup>-2</sup> rad <sup>-1</sup>
rolling moment	$L_{\delta_{e_r}}$	$\frac{\bar{q}Sb}{I_{xx}} C_{l_{\delta_{e_r}}}$	sec <sup>-2</sup> rad <sup>-1</sup>
	$L_{\delta_{e_l}}$	$\frac{\bar{q}Sb}{I_{xx}} C_{l_{\delta_{e_l}}}$	sec <sup>-2</sup> rad <sup>-1</sup>
	$L_{\delta_{a_r}}$	$\frac{\bar{q}Sb}{I_{xx}} C_{l_{\delta_{a_r}}}$	sec <sup>-2</sup> rad <sup>-1</sup>
	$L_{\delta_{a_l}}$	$\frac{\bar{q}Sb}{I_{xx}} C_{l_{\delta_{a_l}}}$	sec <sup>-2</sup> rad <sup>-1</sup>
	$L_{\delta_r}$	$\frac{\bar{q}Sb}{I_{xx}} C_{l_{\delta_r}}$	sec <sup>-2</sup> rad <sup>-1</sup>

(Table III continued on next page)

(Table III cont'd)

	Derivative	Definition	Units
yawing moment	$N_{\delta_{e_r}}$	$\frac{\bar{q}Sb}{I_{zz}} C_{n_{\delta_{e_r}}}$	$\text{sec}^{-2} \text{ rad}^{-1}$
	$N_{\delta_{e_\ell}}$	$\frac{\bar{q}Sb}{I_{zz}} C_{n_{\delta_{e_\ell}}}$	$\text{sec}^{-2} \text{ rad}^{-1}$
	$N_{\delta_{a_r}}$	$\frac{\bar{q}Sb}{I_{zz}} C_{n_{\delta_{a_r}}}$	$\text{sec}^{-2} \text{ rad}^{-1}$
	$N_{\delta_{a_\ell}}$	$\frac{\bar{q}Sb}{I_{zz}} C_{n_{\delta_{a_\ell}}}$	$\text{sec}^{-2} \text{ rad}^{-1}$
	$N_{\delta_r}$	$\frac{\bar{q}Sb}{I_{zz}} C_{n_{\delta_r}}$	$\text{sec}^{-2} \text{ rad}^{-1}$



$$\begin{aligned}
\dot{\beta} = & \frac{1}{U} [Y_{\beta}\beta + g\phi + Y_p p] + \left[\frac{Y_r}{U} - 1\right]r \\
& + \frac{1}{U} [Y_{\delta_{e_r}}\delta_{e_r} + Y_{\delta_{e_{\ell}}}\delta_{e_{\ell}} + Y_{\delta_{a_r}}\delta_{a_r} + Y_{\delta_{a_{\ell}}}\delta_{a_{\ell}} + Y_{\delta_r}\delta_r]
\end{aligned}
\tag{18}$$

$$\begin{aligned}
\dot{p}\left(1 - \frac{I_{xz}^2}{I_{xx}I_{zz}}\right) = & \left(\frac{I_{xz}}{I_{xx}}N_{\beta} + L_{\beta}\right)\beta + \left(\frac{I_{xz}}{I_{zz}}N_p + L_p\right)p \\
& + \left(\frac{I_{xz}}{I_{xx}}N_r + L_r\right)r + \left(\frac{I_{xz}}{I_{xx}}N_{\delta_{e_r}} + L_{\delta_{e_r}}\right)\delta_{e_r} \\
& + \left(\frac{I_{xz}}{I_{xx}}N_{\delta_{e_{\ell}}} + L_{\delta_{e_{\ell}}}\right)\delta_{e_{\ell}} + \left(\frac{I_{xz}}{I_{xx}}N_{\delta_{a_r}} + L_{\delta_{a_r}}\right)\delta_{a_r} \\
& + \left(\frac{I_{xz}}{I_{xx}}N_{\delta_{a_{\ell}}} + L_{\delta_{a_{\ell}}}\right)\delta_{a_{\ell}} + \left(\frac{I_{xz}}{I_{xx}}N_{\delta_r} + L_{\delta_r}\right)\delta_r
\end{aligned}
\tag{19}$$

$$\begin{aligned}
\dot{r}\left(1 - \frac{I_{xz}^2}{I_{xx}I_{zz}}\right) = & \left(\frac{I_{xz}}{I_{zz}}L_{\beta} + N_{\beta}\right)\beta + \left(\frac{I_{xz}}{I_{zz}}L_p + N_p\right)p \\
& + \left(\frac{I_{xz}}{I_{zz}}L_r + N_r\right)r + \left(\frac{I_{xz}}{I_{zz}}L_{\delta_{e_r}} + N_{\delta_{e_r}}\right)\delta_{e_r} + \left(\frac{I_{xz}}{I_{zz}}L_{\delta_{e_{\ell}}} + N_{\delta_{e_{\ell}}}\right)\delta_{e_{\ell}} \\
& + \left(\frac{I_{xz}}{I_{zz}}L_{\delta_{a_r}} + N_{\delta_{a_r}}\right)\delta_{a_r} + \left(\frac{I_{xz}}{I_{zz}}L_{\delta_{a_{\ell}}} + N_{\delta_{a_{\ell}}}\right)\delta_{a_{\ell}} \\
& + \left(\frac{I_{xz}}{I_{zz}}L_{\delta_r} + N_{\delta_r}\right)\delta_r
\end{aligned}
\tag{20}$$

To simplify these expressions, define

$$L_i' = \frac{L_i + \left(\frac{I_{xz}}{I_{xx}}\right) N_i}{1 - \frac{I_{xz}^2}{I_{xx} I_{zz}}} \quad (21)$$

and

$$N_i' = \frac{N_i + \left(\frac{I_{xz}}{I_{zz}}\right) L_i}{1 - \frac{I_{xz}^2}{I_{xx} I_{zz}}} \quad (22)$$

where  $i$  represents  $\beta$ ,  $p$ ,  $r$ ,  $\delta_{e_r}$ ,  $\delta_{e_\ell}$ ,  $\delta_{a_r}$ ,  $\delta_{a_\ell}$  and  $\delta_r$ , successively.

Substituting these definitions in Eqns (19) and (20):

$$\begin{aligned} \dot{p} = & L_\beta' \beta + L_p' p + L_r' r + L_{\delta_{e_r}}' \delta_{e_r} \\ & + L_{\delta_{e_\ell}}' \delta_{e_\ell} + L_{\delta_{a_r}}' \delta_{a_r} + L_{\delta_{a_\ell}}' \delta_{a_\ell} + L_{\delta_r}' \delta_r \end{aligned} \quad (23)$$

$$\begin{aligned} \dot{r} = & N_\beta' \beta + N_p' p + N_r' r + N_{\delta_{e_r}}' \delta_{e_r} \\ & + N_{\delta_{e_\ell}}' \delta_{e_\ell} + N_{\delta_{a_r}}' \delta_{a_r} + N_{\delta_{a_\ell}}' \delta_{a_\ell} + N_{\delta_r}' \delta_r \end{aligned} \quad (24)$$

Equations (18), (23) and (24) are a set of three coupled first order ordinary differential equations which are linear in the four variables  $\beta$ ,  $p$ ,  $r$ , and  $\phi$ . To complete the set of lateral-directional equations, the fourth kinematic equation is introduced.

$$\dot{\phi} = p \quad (25)$$

#### State Variable Representation

The longitudinal and the lateral-directional set of equations, Eqns (7), (8), (10), (11), (18), (23), (24) and (25), form the comprehensive set of eight first order coupled ordinary differential equations with constant coefficients that represent the aircraft model. These are linear in the eight variables  $u$ ,  $\alpha$ ,  $q$ ,  $\theta$ ,  $\beta$ ,  $p$ ,  $r$  and  $\phi$ . Based on this set of equations, the state vector  $\underline{x}$  and the input vector  $\underline{u}$  are defined as

$$\underline{x} = \begin{bmatrix} u \\ \alpha \\ q \\ \theta \\ \beta \\ p \\ r \\ \phi \end{bmatrix} \quad \underline{u} = \begin{Bmatrix} \delta e_r \\ \delta e_\ell \\ \delta a_r \\ \delta a_\ell \\ \delta r \end{Bmatrix}$$

Finally, the set of linearized equations is rewritten in the state variable format

$$\dot{\underline{x}} = A\underline{x} + B\underline{u}$$

where A and B are, respectively, the plant matrix of dimension 8 x 8 and the control matrix of dimension 8 x 5.

(See Eq (26) on the next page.)

#### A-7D Parameters

To finally insert numerical values in Eq (26) and obtain system model in the state variable form requires A-7D parameters under cruise configuration. These parameter values have been gathered in the following groups:

- (a) Cruise configuration airplane data such as wing area, aircraft weight and moments of inertia
- (b) Cruise configuration stability derivatives such as  $C_{L_{trim}}$ ,  $C_{m_{\alpha}}$ ,  $C_{y_{\beta}}$  and  $C_{n_p}$ .
- (c) Traditional cruise configuration control derivatives such as  $C_{L_{\delta_{e_r}}}$ ,  $C_{m_{\delta_{e_l}}}$ ,  $C_{y_{\delta_r}}$  and  $C_{l_{\delta_{a_r}}}$ .
- (d) Newly defined cruise configuration control derivatives such as  $C_{L_{\delta_{a_r}}}$ ,  $C_{m_{\delta_r}}$ ,  $C_{y_{\delta_{e_l}}}$  and  $C_{n_{\delta_{e_l}}}$ .
- (e) Dimensional stability derivatives in cruise configuration such as  $X_u$ ,  $Z_{\alpha}$ ,  $Y_{\beta}$  and  $N_r$ .

$$\begin{bmatrix} \dot{u} \\ \dot{\alpha} \\ \dot{q} \\ \dot{\theta} \\ \dot{\beta} \\ \dot{p} \\ \dot{r} \\ \dot{\phi} \end{bmatrix} = \begin{bmatrix} X_u & X_\alpha & 0 & -g & 0 & 0 & 0 & 0 \\ Z_u/U & Z_\alpha/U & 1 & 0 & 0 & 0 & 0 & 0 \\ \frac{M_\alpha^*}{(M_u + \frac{1}{U}Z_u)} & \frac{M_\alpha^*}{(M_\alpha + \frac{1}{U}Z_\alpha)} & (M_q + M_\alpha^*) & 0 & 0 & 0 & 0 & 0 \\ 0 & 0 & 1 & 0 & 0 & 0 & 0 & 0 \\ 0 & 0 & 0 & 0 & \frac{Y_\beta}{U} & \frac{Y_p}{U} & (\frac{Y_r}{U} - 1) & \frac{g}{U} \\ 0 & 0 & 0 & 0 & L_\beta' & L_p' & L_r' & 0 \\ 0 & 0 & 0 & 0 & N_\beta' & N_p' & N_r' & 0 \\ 0 & 0 & 0 & 0 & 0 & 1 & 0 & 0 \end{bmatrix} \begin{bmatrix} u \\ \alpha \\ q \\ \theta \\ \beta \\ p \\ r \\ \phi \end{bmatrix}$$

$$+ \begin{bmatrix} X_{\delta e_r} & X_{\delta e_\ell} & X_{\delta a_r} & X_{\delta a_\ell} & X_{\delta r} \\ Z_{\delta e_r}/U & Z_{\delta e_\ell}/U & Z_{\delta a_r}/U & Z_{\delta a_\ell}/U & Z_{\delta r}/U \\ \frac{M_\alpha^*}{(\frac{1}{U}Z_{\delta e_r} + M_{\delta e_r})} & \frac{M_\alpha^*}{(\frac{1}{U}Z_{\delta e_\ell} + M_{\delta e_\ell})} & \frac{M_\alpha^*}{(\frac{1}{U}Z_{\delta a_r} + M_{\delta a_r})} & \frac{M_\alpha^*}{(\frac{1}{U}Z_{\delta a_\ell} + M_{\delta a_\ell})} & \frac{M_\alpha^*}{(\frac{1}{U}Z_{\delta r} + M_{\delta r})} \\ 0 & 0 & 0 & 0 & 0 \\ Y_{\delta e_r}/U & Y_{\delta e_\ell}/U & Y_{\delta a_r}/U & Y_{\delta a_\ell}/U & Y_{\delta r}/U \\ L_{\delta e_r}' & L_{\delta e_\ell}' & L_{\delta a_r}' & L_{\delta a_\ell}' & L_{\delta r}' \\ N_{\delta e_r}' & N_{\delta e_\ell}' & N_{\delta a_r}' & N_{\delta a_\ell}' & N_{\delta r}' \\ 0 & 0 & 0 & 0 & 0 \end{bmatrix} \begin{bmatrix} \delta e_r \\ \delta e_\ell \\ \delta a_r \\ \delta a_\ell \\ \delta r \end{bmatrix}$$

(26)

(f) Dimensional control derivatives in cruise

configuration such as  $X_{\delta_{e_r}}$ ,  $M_{\delta_{e_l}}$ ,  $L_{\delta_{a_r}}$  and  $N_{\delta_r}$ .

Of these, (a) has already been presented in Table I; (b) has been obtained from Reference 5 and is presented in Table IV. Parameters of paragraph (c) require some discussion.

Parameter values for these control derivatives have been obtained from Reference 5, where they are tabulated in the conventional fashion viz  $C_{L_{\delta_e}}$ ,  $C_{m_{\delta_e}}$ ,  $C_{l_{\delta_a}}$ , etc. This implies that the values listed there are applicable to the pair of control surfaces as a set. For instance,  $C_{L_{\delta_e}}$  gives the change of lift coefficient with changes in elevator angle when both left and right elevator move simultaneously. Likewise,  $C_{l_{\delta_a}}$  gives the change of rolling moment coefficient for varying aileron positions when the ailerons move simultaneously. However, this study requires control derivative values for each control surface independently; i.e.,  $C_{L_{\delta_{e_r}}}$  and  $C_{L_{\delta_{e_l}}}$  as opposed to  $C_{L_{\delta_e}}$ . To get these values, it has been assumed that, since the left and right elevators are geometrically similar and located symmetrically with respect to aircraft axes, their effect on various coefficients will also be equal. That is, the individual surface effect would

be one half that of the pair. More precisely

$$C_{L\delta_{e_r}} = C_{L\delta_{e_l}} = \frac{1}{2} C_{L\delta_e} \rightarrow C_{L\delta_e} = C_{L\delta_{e_r}} + C_{L\delta_{e_l}}$$

Likewise for  $C_{D\delta_e}$  and  $C_{m\delta_e}$ .

For the ailerons, again due to their similarity, symmetry and sign convention, it follows that:

$$C_{l\delta_{a_r}} = C_{l\delta_{a_l}} = \frac{1}{2} C_{l\delta_a} \rightarrow C_{l\delta_a} = C_{l\delta_{a_r}} + C_{l\delta_{a_l}}$$

Likewise for  $C_{y\delta_a}$  and  $C_{n\delta_a}$ . Values of the traditional control derivatives obtained from Reference 5 have, therefore, been adopted for this study for individual surfaces as discussed above, and are also tabulated in Table IV.

The parameters of paragraph (d) have been obtained from Reference 2 and listed in Table IV, insuring their consistency with the sign convention defined in Chapter I. Reference 2 used Digital Datcom (Ref 6) to obtain these coefficients.

The dimensional stability derivatives as grouped in paragraph (e) above have been obtained from Reference 5 and are listed in Table V. Finally, the dimensional control derivatives of paragraph (f) have been calculated on the basis of their definition as given in Tables II and III, and by utilizing parameter values of Tables I and IV. These are also tabulated in Table V.

TABLE IV			
Non-Dimensional Stability and Control Derivatives for the A-7D in Cruise Configuration (Stability Axes) All Values per Radian Except $C_{L_o}$ and $C_{D_o}$			
Longitudinal		Lateral-Directional	
Derivative	Value	Derivative	Value
$C_{L_o}$	.225 (trim $C_L$ )	$C_{y_\beta}$	-.7162
$C_{D_o}$	.0219 (trim $C_D$ )	$C_{y_p}$	+.129
$C_{L_\alpha}$	4.412	$C_{y_r}$	+.0501
$C_{L_q}$	1.0	$C_{\ell_\beta}$	-.0905
$C_{m_\alpha}$	-.4636	$C_{\ell_p}$	-.346
$C_{m_q}$	-3.95	$C_{\ell_r}$	-.104
$C_{m_{\dot{\alpha}}}$	.77	$C_{n_\beta}$	.0722
		$C_{n_p}$	-.00397
		$C_{n_r}$	-.302

(Table IV continued on next page)



(Table IV Cont'd)

Longitudinal		Lateral-Directional	
Derivative	Value	Derivative	Value
$C_{D\delta_{er}}$	+0.1146	$C_{y\delta_{er}}$	0
$C_{D\delta_{el}}$	+0.1146	$C_{y\delta_{el}}$	0
$C_{L\delta_{er}}$	0.2980	$C_{l\delta_{er}}$	-0.0283
$C_{L\delta_{el}}$	0.2980	$C_{l\delta_{el}}$	+0.0283
$C_{m\delta_{er}}$	-0.4528	$C_{n\delta_{er}}$	-0.0109
$C_{m\delta_{el}}$	-0.4528	$C_{n\delta_{el}}$	+0.0109
$C_{D\delta_{ar}}$	0.0	$C_{y\delta_{ar}}$	-0.0251
$C_{D\delta_{al}}$	0.0	$C_{y\delta_{al}}$	-0.0251
$C_{L\delta_{ar}}$	-0.2120	$C_{l\delta_{ar}}$	+0.0605
$C_{L\delta_{al}}$	+0.2120	$C_{l\delta_{al}}$	+0.0605
$C_{m\delta_{ar}}$	+0.0229	$C_{n\delta_{ar}}$	+0.0071
$C_{m\delta_{al}}$	-0.0229	$C_{n\delta_{al}}$	+0.0071
$C_{D\delta_r}$	0.0	$C_{y\delta_r}$	+0.2006
$C_{L\delta_r}$	0.0	$C_{l\delta_r}$	+0.0190
$C_{m\delta_r}$	0.0	$C_{n\delta_r}$	-0.0917

TABLE V

DIMENSIONAL STABILITY AND CONTROL DERIVATIVES FOR THE A-7D IN CRUISE CONFIGURATION					
Longitudinal					
$X_u$ (sec <sup>-1</sup> )	-.00829	$Z_u$ (sec <sup>-1</sup> )	-0.1132	$M_u$ (ft <sup>-1</sup> sec <sup>-1</sup> )	0.00036
$X_\alpha$ (ft-sec <sup>-2</sup> )	5.4775	$Z_\alpha$ (ft-sec <sup>-2</sup> )	-632.64	$M_\alpha$ (sec <sup>-2</sup> )	-8.1555
		$Z_{\dot{\alpha}}$ (ft-sec <sup>-2</sup> )	0	$M_{\dot{\alpha}}$ (sec <sup>-1</sup> )	-0.1157
		$Z_q$ (ft-sec <sup>-1</sup> )	0	$M_q$ (sec <sup>-1</sup> )	-0.5933
$X_{\delta_{e_r}}$ (ft-sec <sup>-2</sup> /rad-1)	-16.432	$Z_{\delta_{e_r}}$ (ft-sec <sup>-2</sup> /rad-1)	-42.7234	$M_{\delta_{e_r}}$ (sec <sup>-2</sup> /rad-1)	-7.9646
$X_{\delta_{e_\ell}}$ "	-16.432	$Z_{\delta_{e_\ell}}$ "	-42.7234	$M_{\delta_{e_\ell}}$ "	-7.9646
$X_{\delta_{a_r}}$ "	0	$Z_{\delta_{a_r}}$ "	+30.3979	$M_{\delta_{a_r}}$ "	+4028
$X_{\delta_{a_\ell}}$ "	0	$Z_{\delta_{a_\ell}}$ "	-30.3979	$M_{\delta_{a_\ell}}$ "	-4028
$X_{\delta_r}$ "	0	$Z_{\delta_r}$ "	0	$M_{\delta_r}$ "	0

(Table V continued on next page)

(Table V Cont'd)

Lateral - Directional					
$Y_{\beta}$ (ft-sec <sup>-2</sup> )	-102.6961	$L_{\beta}$ (sec <sup>-2</sup> )	-25.7350	$N_{\beta}$ (sec <sup>-2</sup> )	3.9938
$Y_p$ (ft-sec <sup>-1</sup> )	+0.5643	$L_p$ (sec <sup>-1</sup> )	-3.00146	$N_p$ (sec <sup>-1</sup> )	-0.0067
$Y_r$ (ft-sec <sup>-1</sup> )	+1.3516	$L_r$ (sec <sup>-1</sup> )	0.9022	$N_r$ (sec <sup>-1</sup> )	-0.5096
$Y_{\delta e_r}$ (ft-sec <sup>-2</sup> /rad-1)	0	$L_{\delta e_r}$ (sec <sup>-2</sup> /rad-1)	-8.0402	$N_{\delta e_r}$ (sec <sup>-2</sup> /rad-1)	-6.0124
$Y_{\delta e_{\lambda}}$ "	0	$L_{\delta e_{\lambda}}$ "	+8.0402	$N_{\delta e_{\lambda}}$ "	+6.0124
$Y_{\delta a_r}$ "	-3.5918	$L_{\delta a_r}$ "	+17.1924	$N_{\delta a_r}$ "	+3.927
$Y_{\delta a_{\lambda}}$ "	-3.5918	$L_{\delta a_{\lambda}}$ "	+17.1924	$N_{\delta a_{\lambda}}$ "	+3.927
$Y_{\delta r}$ "	28.7562	$L_{\delta r}$ "	+5.4094	$N_{\delta r}$ "	-5.0721

## A and B Matrices

Equation (26) represents the state variable form of the system model. Using numerical values from Tables I, IV and V, the A and B matrices have been evaluated and are shown in Eq (27) below.

$$\begin{bmatrix} \dot{u} \\ \dot{\alpha} \\ \dot{q} \\ \dot{\theta} \\ \dot{\beta} \\ \dot{p} \\ \dot{r} \\ \dot{\phi} \end{bmatrix} = \begin{bmatrix} -.00829 & 5.478 & & -32.174 & 0 & 0 & 0 & 0 \\ -.0001784 & -.9966 & 1.0 & 0 & 0 & 0 & 0 & 0 \\ 0.0003806 & -8.2707 & -.7089 & 0 & 0 & 0 & 0 & 0 \\ 0 & 0 & 1 & 0 & 0 & 0 & 0 & 0 \\ 0 & 0 & 0 & 0 & -.1618 & .0008889 & -.9979 & .0507 \\ 0 & 0 & 0 & 0 & -26.2273 & -3.0076 & 0.9595 & 0 \\ 0 & 0 & 0 & 0 & 4.5462 & 0.05665 & -.5298 & 0 \\ 0 & 0 & 0 & 0 & 0 & 1 & 0 & 0 \end{bmatrix} \begin{bmatrix} u \\ \alpha \\ q \\ \theta \\ \beta \\ p \\ r \\ \phi \end{bmatrix}$$

$$+ \begin{bmatrix} -16.432 & -16.432 & 0 & 0 & 0 \\ -.0673 & -.0673 & .0479 & -.0479 & 0 \\ -7.9568 & -7.9568 & +.3973 & -.3973 & 0 \\ 0 & 0 & 0 & 0 & 0 \\ 0 & 0 & -.00566 & -.00566 & .0453 \\ -7.9933 & +7.9933 & +17.2743 & +17.2743 & 5.9723 \\ -.4329 & +.4329 & .0307 & .0307 & -5.3071 \\ 0 & 0 & 0 & 0 & 0 \end{bmatrix} \begin{bmatrix} \delta_{e_r} \\ \delta_{e_\ell} \\ \delta_{a_r} \\ \delta_{a_\ell} \\ \delta_r \end{bmatrix} \quad (27)$$

### Eigenvalues of the Plant Matrix

Having obtained the plant matrix, its eigenvalues are obtained and analyzed for both longitudinal and lateral directional modes. These are summarized below.

EIGENVALUES OF THE "A" MATRIX				
Mode	Eigenvalues $\lambda$	Natural Frequency $\omega_n$ (rad/sec)	Damping Ratio $\zeta$	Time* Constant $T$ (sec)
Short Period	$-.8528 \pm j2.871$	2.995	0.285	1.1726
Phugoid	$-.00412 \pm j.08145$	.0815	.0174	704.23
Spiral	$-.03578$	--	--	27.95
Roll	$-2.988$	--	--	0.3347
Dutch Roll	$-.3376 \pm j2.1$	2.127	0.159	2.96

\*For complex eigenvalues, time constant defined as  $T = \left| \frac{1}{\zeta \omega_n} \right|$

### Summary

In this chapter, the aircraft dynamics are developed, taking into account coupling of the longitudinal and lateral directional axes. This is done by defining a new set of non-dimensional and dimensional control derivatives. Finally,

a comprehensive state space model is developed and numerical values inserted for the A-7D in the cruise configuration under study.

### III. Reconfigurable Flight Control System Design Using Pseudo Inverse

#### Introduction

The basic purpose of any flight control system is twofold:

- (a) To establish and maintain certain specified equilibrium states of vehicle motion.
- (b) To remedy aircraft handling quality deficiencies.

These end results are accomplished by feedback control or crossfeed control of appropriate variables. For instance, in the longitudinal motion an increase in short period damping may be achieved by feedback of the pitch rate to the elevator input. Likewise, the dutch roll damping may be enhanced by feeding back yaw rate to the rudder input for the lateral-directional mode.

These flight control systems add to the normal flight characteristics and assist the pilot in controlling the aircraft against gust inputs, turbulence and other disturbances. The major functional elements of all these multiloop controls are the primary control surfaces such as the elevator or the rudder in the instances quoted above. For satisfactory operation, these control surfaces depend, among other flight control loop hardware, on mechanical devices such as the actuators and hinges. These devices are obviously

susceptible to inflight malfunction as a result of mechanical failure or enemy action, which renders the control surface inoperative. This, in turn, not only invalidates the flight control system, but causes severe control problems. In the past, redundancy has been the major approach to this problem. But the impracticality caused by increasing weight and dispersal of hardware in this approach has dictated the need for a more viable alternate solution.

A reconfigurable flight control system, that is, a flight control system that makes use of only the operating control surfaces to maintain satisfactory handling qualities, seems to be a promising alternative. This chapter presents in detail a new method for designing such a reconfigurable flight control system.

### The Design Philosophy

Before going into the actual design process, the broader scheme on which the design has been based is presented. This simplifies comprehension of the design process. Briefly, the approach may be described in two steps:

- (a) Subsequent to a pilot's command input, the flight control system generates certain "generic" commands necessary to execute the command, irrespective of the control surfaces available.
- (b) Depending on the operational control surfaces, these generic commands are transformed into actual



surface commands via a transformation matrix.

This transformation depends on which specific control surface has failed, if any.

What follows is an elaboration of this idea into a working reconfigurable flight control system.

In the previous chapter, it was assumed that the five primary control surfaces, namely the left elevator, the right elevator, the left aileron, the right aileron and the rudder, may be commanded independently. Thus, as opposed to the traditional control surface movements, the ailerons or the elevators may be deflected independently either individually or simultaneously, in similar or opposite directions by equal or unequal amounts. Based on this assumption, the control matrix (B matrix of Eq (27)) was developed considering input vector  $\underline{u}$  to consist of the five inputs  $\delta_{e_r}$ ,  $\delta_{e_\ell}$ ,  $\delta_{a_r}$ ,  $\delta_{a_\ell}$ ,  $\delta_r$ .

#### Generic Inputs

Now three new generic inputs are defined for the complete three axis control of the aircraft. They are denoted by the symbols

$\delta_{long}$  = a generic longitudinal input

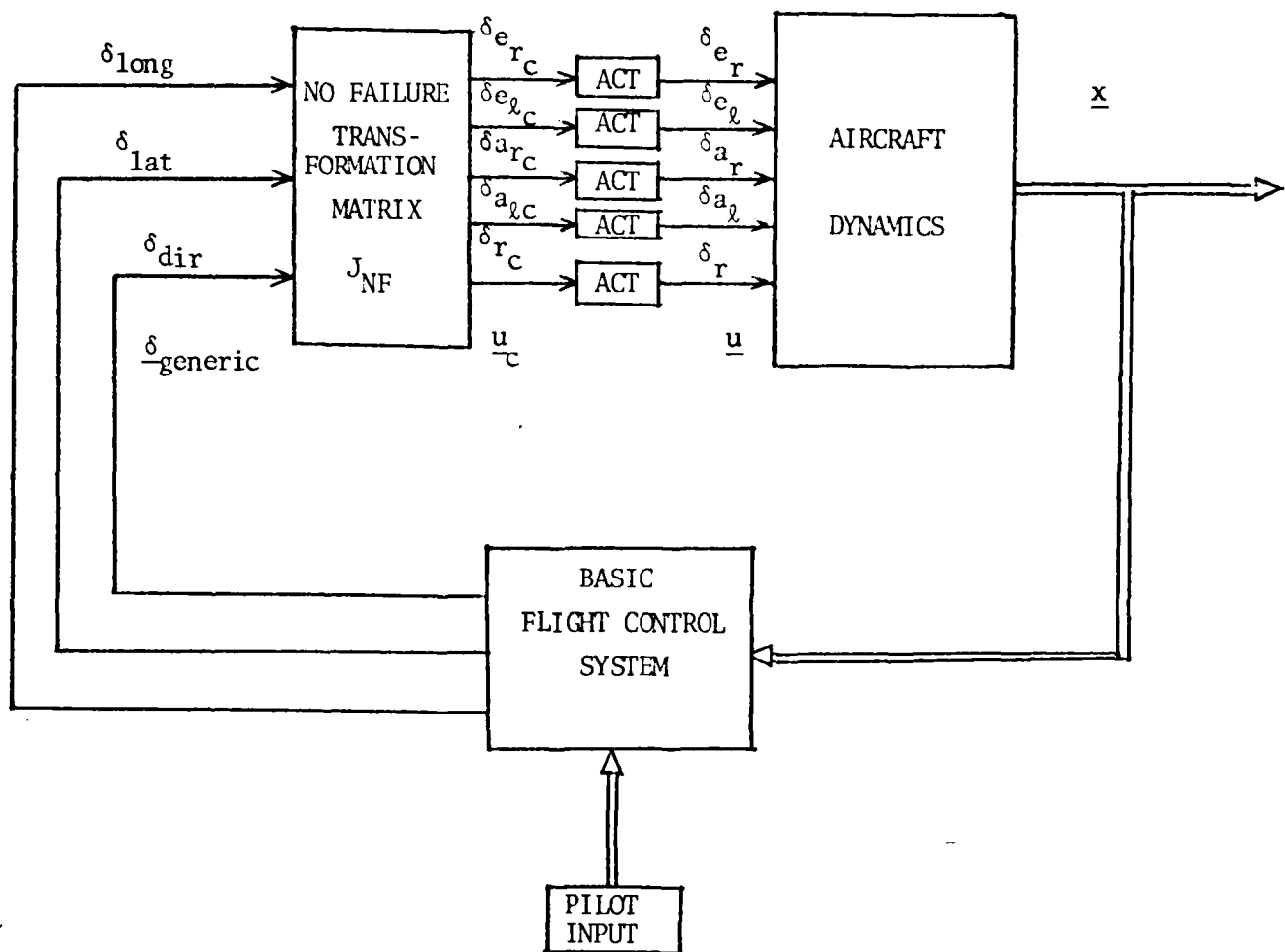
$\delta_{lat}$  = a generic lateral input

$\delta_{dir}$  = a generic directional input.

Instead of the elevator,  $\delta_{\text{long}}$  is now considered as the primary longitudinal control. Likewise,  $\delta_{\text{lat}}$  and  $\delta_{\text{dir}}$  are considered as the primary lateral and directional controls, respectively. As the term generic implies belonging to a general class, similarly these generic inputs are also the essential commands necessary to execute a commanded maneuver such as a pull-up. These generic commands are fulfilled by physical movement of the actual control surfaces. How much of each control surface is deflected depends on how many operational surfaces are available. Precisely, each one of the generic inputs is defined as a specific linear combination of the available control surfaces. To illustrate this, a block diagram representation of this scheme is presented in Figure 3.1.

#### Basic Flight Control System

To further the idea, it is assumed that there exists a flight control system consisting of such usual systems as the pitch stability augmentation, normal g's command and yaw and roll augmentation. This flight control system, referred to as the basic flight control system, is capable of generating the generic input commands  $\delta_{\text{long}}$ ,  $\delta_{\text{lat}}$  and  $\delta_{\text{dir}}$  based on pilot inputs and appropriate feedback. It is assumed that the control laws of this basic flight control system have been established so as to produce desirable flight characteristics that meet the flying qualities criteria.



ACT  $\equiv$  Actuator Dynamics

Figure 3.1. Block Diagram Representation of the Design Scheme for the "No-Failure" Case

### Transformation Matrix Using Pseudo Inverse

Referring to Figure 3.1, it may be observed that in response to a pilot's input, the basic flight control system generates appropriate generic commands which are then transformed into actual surface commands. This is achieved by the transformation matrix  $[J]$  which directly depends on the number of operational surfaces available. For the no-failure case, that is, normal flight with all five primary flight control surfaces operational, which is the case depicted in Figure 3.1, this transformation matrix  $J_{NF}$  establishes for each individual generic input a specific linear combination of the five control surfaces necessary to execute that generic command. For instance, an uncoupled purely longitudinal command of 1-g pull-up results in a certain  $\delta_{long}$ . This is transformed via the transformation matrix  $J_{NF}$  to a simultaneous movement of the left and right elevator by a certain equal amount. In this case, therefore,  $\delta_{long}$  has been established by the transformation matrix as a linear combination of  $\delta_{e_r}$  and  $\delta_{e_l}$  alone. Likewise,  $\delta_{lat}$  and  $\delta_{dir}$  may be established as some other specific linear combinations of the  $\delta_{a_r}$ ,  $\delta_{a_l}$ , and  $\delta_r$ .

In order to derive an expression for the transformation matrix, it is further assumed that, using conventional design techniques, an  $8 \times 3$  control matrix has also been determined whose control coefficients produce desirable

flight characteristics when used with the 3 x 1 generic control vector. This desired control matrix  $B_d$  of dimension 8 x 3 has the form

$$B_d = \begin{bmatrix} \underline{b}_{\text{long}} & | & \underline{b}_{\text{lat}} & | & \underline{b}_{\text{dir}} \end{bmatrix}$$

where  $\underline{b}_{\text{long}}$ ,  $\underline{b}_{\text{lat}}$  and  $\underline{b}_{\text{dir}}$  are each an 8 x 1 vector.

Now, by definition the transformation for the no-failure case takes the form

$$\underline{u}_{\text{NF}} = [J_{\text{NF}}] \begin{bmatrix} \delta_{\text{long}} \\ \delta_{\text{lat}} \\ \delta_{\text{dir}} \end{bmatrix} \quad (28)$$

where  $\underline{u}_{\text{NF}}$  is the (5 x 1) control vector

$$\underline{u}_{\text{NF}} = \begin{bmatrix} \delta e_r \\ \delta e_\ell \\ \delta a_r \\ \delta a_\ell \\ \delta r \end{bmatrix}$$

and  $[J_{\text{NF}}]$  is the (5 x 3) transformation matrix that is to be determined such that

$$[B_{NF}] \quad \underline{u}_{NF} = \begin{bmatrix} \underline{b}_{long} & | & \underline{b}_{lat} & | & \underline{b}_{dir} \end{bmatrix} \begin{bmatrix} \delta_{long} \\ \delta_{lat} \\ \delta_{dir} \end{bmatrix} \quad (29)$$

Substituting Eq (28) for  $\underline{u}$  into Eq (29) and simplifying:

$$[B_{NF}] \quad [J_{NF}] = [B_d] \quad (30)$$

Equation (30) then defines a transformation matrix that is required to establish specific linear relationships between the generic inputs and the actual inputs which produce the desired control coefficient matrix  $B_d$ .

The Pseudo-Inverse. Since  $B_{NF}$  is a 5 x 8 non-square matrix, its inverse is not defined. Hence, to evaluate  $J_{NF}$  in terms of  $B_{NF}$  and  $B_d$ , the concept of generalized or pseudo-inverse is utilized as follows. Premultiplying both sides of Eq (30) by  $[B_{NF}]^T$ :

$$[B_{NF}]^T [B_{NF}] [J_{NF}] = [B_{NF}]^T [B_d] \quad (31)$$

where  $[B_{NF}]^T [B_{NF}]$  is a 5 x 5 square matrix whose inverse exists provided  $B_{NF}$  has full rank. In this case, the rank of  $B_{NF}$  is equal to the control surfaces since the control surfaces are linearly independent. Hence,  $[B_{NF}]^T [B_{NF}]^{-1}$  exists and therefore

$$J_{NF} = [B_{NF}^T B_{NF}]^{-1} [B_{NF}]^T [B_d] = B_{NF}^T B_d \quad (32)$$

Equation (32) defines the transformation matrix  $J_{NF}$  in terms of the  $B$  matrix which is known and the  $B_d$  matrix which has been specified. In the same equation,  $B_{NF}^T = [B_{NF}^T B_{NF}]^{-1} [B_{NF}]^T$  is defined as the pseudo-inverse of the  $8 \times 5$  non square  $B_{NF}$  matrix. Since the pseudo-inverse only minimizes the sum of squares of the residuals, a substitution of  $J$  as found in Eq (32) into Eq (30) does not reproduce  $B_d$  exactly (Ref 7). Rather, it produces the "best"  $b_d$  in the least square sense. But, as weill be shown in the following chapters, the difference between the two is negligibly small and the flight characteristics produced by this  $B_d$  are within the flying qualities specifications. Hence, the method of pseudo (or generalized) inverse is feasible in this case.

Having gone through the detailed discussion on the generic inputs, the basic flight control system and the transformation matrix, the block diagram representation of the design scheme given in Figure 3.1 may now be followed in its essence. Its working may once again be exemplified by assuming that the system is in trim condition when the pilot commands a one-g pull-up. The flight control system generates the necessary generic input commands to effect

the commanded pull-up. These generic inputs are translated into commanded inputs of the primary flight control surfaces, i.e.,  $\delta_{e_r}$ ,  $\delta_{e_l}$ ,  $\delta_{a_r}$ ,  $\delta_{a_l}$  and  $\delta_r$ , through the  $J_{NF}$  matrix. Movement of the primary control surfaces as governed by the generic inputs then executes the desired pull-up. A feedback of the normal acceleration stabilizes the system soon after.

#### Reconfiguration for Right Elevator Failure

Next, the case of one primary flight control surface, namely the right elevator, becoming inoperative is examined. It is pertinent to point out here that, in this approach, reconfiguration of the flight control system for a failure case is effected not by redesigning elementary control laws of the basic flight control system, but by redefining a new transformation matrix  $J$ , depending on the number of available control surfaces. Using the same basic flight control system of the previous (no-failure) case and duplicating a 1-g pull-up command prompts the same generic input  $\delta_{long}$ . However, excluding the right elevator which may not be commanded any more, only four control surfaces are available. Therefore, to achieve the same flight characteristics as before, the four available control surfaces must be deflected by different degrees. In other words, the generic commands must be interpreted as some other linear combination of the available control surfaces. For instance, to



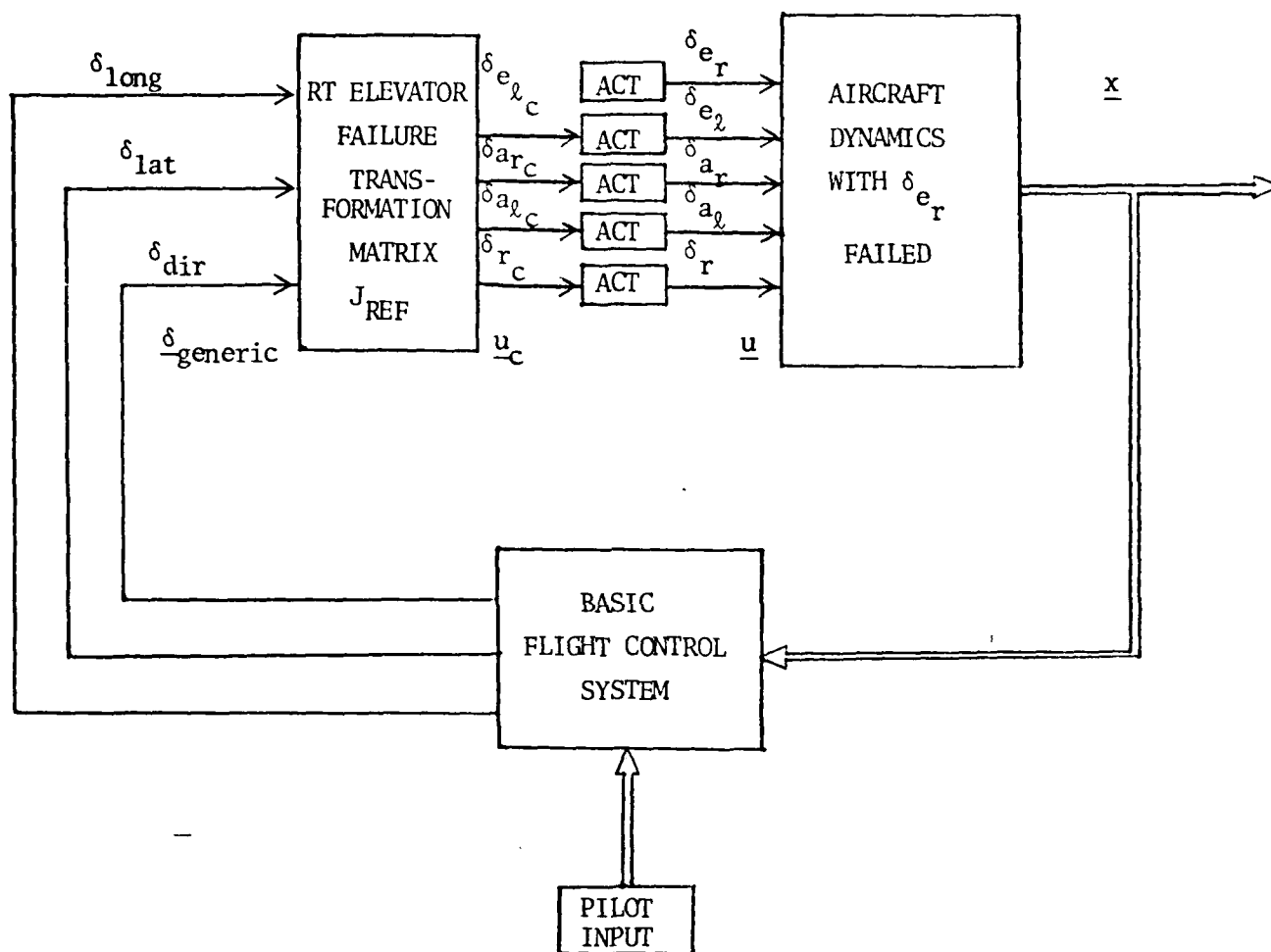
achieve the same horizontal tail effectiveness, deflection of the available left elevator should be approximately doubled. Likewise, in order to counter the unwanted rolling moment generated by the failed right elevator, the left and right ailerons must also be deflected even though the original command was purely longitudinal.

This fresh linear combination of the available control surfaces that interprets the generic inputs for the right elevator failure case in terms of the remaining four flight control systems is obtained by the new transformation matrix  $J_{REF}$ . Figure 3.2 presents a schematic diagram for this case.

Before attempting to derive an expression for  $J_{REF}$ , it may be observed from Eq (27) that due to the right elevator failure,  $\underline{u}$  is reduced to a (4 x 1) vector  $\underline{u}_{REF}$  consisting of  $\delta_{e_l}$ ,  $\delta_{a_r}$ ,  $\delta_{a_l}$  and  $\delta_r$  as the inputs. Similarly, B is reduced to an 8 x 4 control matrix  $B_{REF}$ , its first column being deleted owing to  $\delta_{e_r}$  failure.

Now, to find this new transformation, Eq (28) may be rewritten for this case as

$$\underline{u}_{REF} = [J_{REF}] \begin{bmatrix} \delta_{long} \\ \delta_{lat} \\ \delta_{dir} \end{bmatrix} \quad (33)$$



ACT  $\equiv$  Actuator

Figure 3.2. Block Diagram Representation  
of the Design Scheme for the Right Elevator Failure Case

where

$$\underline{u}_{REF} = \begin{bmatrix} \delta e_l \\ \delta a_r \\ \delta a_l \\ \delta r \end{bmatrix}$$

and  $[J_{REF}]$  is to be determined such that

$$[B_{REF}]\underline{u}_{REF} = \begin{bmatrix} b_{long} & | & b_{lat} & | & b_{dir} \end{bmatrix} \begin{bmatrix} \delta_{long} \\ \delta_{lat} \\ \delta_{dir} \end{bmatrix}$$

Substituting Eq (32) for  $\underline{u}_{REF}$  in the above equation and simplifying

$$[B_{REF}][J_{REF}] = [B_d] \quad (34)$$

and again using the pseudo-inverse technique,  $[J_{REF}]$  is found by premultiplying both sides of Eq (34) by  $[B]^T$ :

$$[B_{REF}]^T[B_{REF}][J_{REF}] = [B_{REF}]^T[B_d] \quad (35)$$

where  $B_{REF}^T B_{REF}$  is a 4 x 4 square matrix whose inverse exists.

Then

$$[J_{REF}] = [B^T B]^{-1} [B]^T [B_d] \quad (36)$$

$$\text{or } J_{REF} = B_{REF}^T B_d$$

which will be used to relate  $\underline{u}_{REF}$  to the generic inputs as given by Eq (32).

This new transformation matrix defined by Eq (36), when substituted in Eq (34), also produces a "best"  $B_d$  in the least square sense. The rest of the implications of using the pseudo-inverse remain the same as in the no-failure case.

#### Reconfiguration for Other Surface Failures

There are three other failure cases which could be examined in this study; namely the left elevator failure, the right aileron failure and the left aileron failure. It follows from the discussion of the right elevator failure, case that each one of the other failures only requires determining a distinct transformation matrix ( $J$ ) depending on the specific failure. Even though normal flight characteristics are insured, the basic flight control system and its elementary control laws remain unaffected.

To summarize, therefore, this reconfigurable flight control system consists of five transformation matrices; namely

- $J_{NF}$  , transformation matrix for no failure.
- $J_{REF}$ , transformation matrix for right elevator failure.
- $J_{LEF}$ , transformation matrix for left elevator failure.
- $J_{RAF}$ , transformation matrix for right aileron failure.
- $J_{LAF}$ , transformation matrix for left aileron failure.

It is the job of the failure detection system to identify the failure to a single surface and implement the appropriate

transformation. This situation is represented in the block diagram of Figure 3.3.

From the definition of  $J_{NF}$  and  $J_{REF}$  of Eq (32) and (36), it follows that

$$\begin{aligned} J_{LEF} &= [B_{LEF}^T B_{LEF}]^{-1} B_{LEF}^T B_d = B_{LEF}^+ B_d \\ J_{RAF} &= [B_{RAF}^T B_{RAF}]^{-1} B_{RAF}^T B_d = B_{RAF}^+ B_d \\ J_{LAF} &= [B_{LAF}^T B_{LAF}]^{-1} B_{LAF}^T B_d = B_{LAF}^+ B_d \end{aligned} \quad (37)$$

To summarize the discussion, it may be pointed out that this new approach for designing reconfigurable flight control systems provides a technique in which reconfiguration is achieved not by redesigning the elementary control laws of the flight control system as has been done previously (Refs 1 and 2), but by merely implementing an appropriate transformation matrix. The design process itself is simple and results in a system that may be implemented without confronting unrealizable gain scheduling problems.

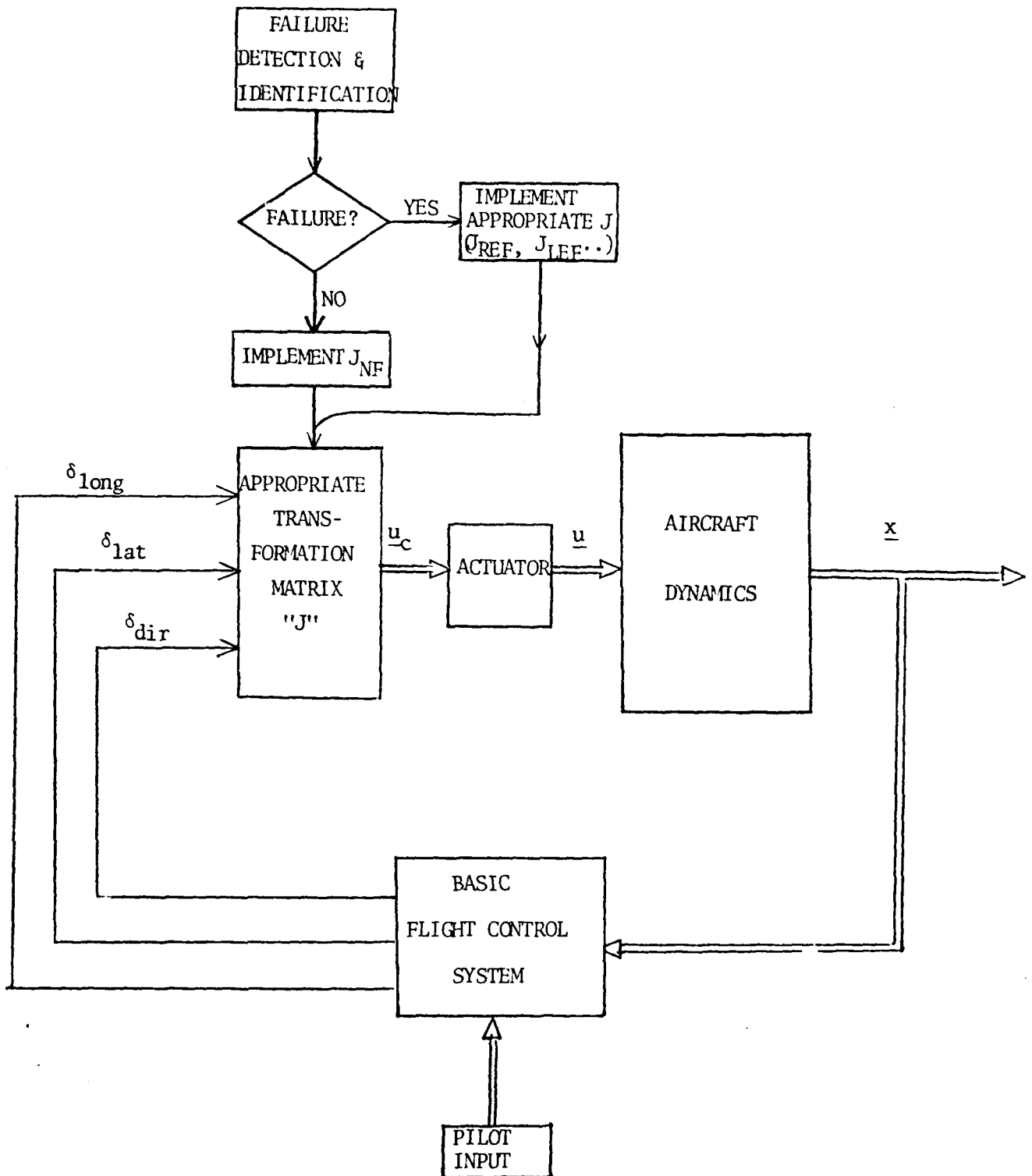


Figure 3.3. Block Diagram Representation  
of the Design Scheme for the Reconfigurable Flight Control System

### Summary

In this chapter, the essence of the new approach being followed in this thesis is presented with the help of schematic representations. The idea of using generic inputs and appropriate transformation matrices is developed into the reconfigurable flight control systems. Use of the pseudo inverse in evolving an expression for the transformation matrix is also elaborated. Finally, the entire design scheme is summarized and its major advantages pointed out.

#### IV. Reconfigurable Flight Control System

##### Design for the A-7D

##### Introduction

The overall scheme of reconfiguration involves, first, the design of a basic flight control system that generates generic input commands  $\delta_{\text{long}}$ ,  $\delta_{\text{lat}}$  and  $\delta_{\text{dir}}$ , based upon pilot input, irrespective of any control surface failures. This basic flight control system must be designed to produce desirable flight characteristics such as those specified in Reference 8. Since it need not take into consideration surface failures, if any, this basic flight control system is valid not only for the no failure case, but also for any failure cases. It, therefore, needs to be designed only once. The second step in the overall design is the determination of transformation matrices that are unique for each failure/no surface failure case. This process of designing the basic flight control system and determining various transformation matrices is carried out for the A-7D in this chapter to obtain a reconfigurable flight control system for the following failures:

- right or left elevator
- right or left aileron.

##### Basic Flight Control System Design

Essentially, a flight control system consists of closed loop systems formed by feedback of aircraft motion quantities



to the controls. Whether the system is a simple single-loop flight controller or a multi-loop closure depends on the purpose of the flight control system. As outlined above, the purpose of the basic flight control system here is twofold; namely, generating generic commands irrespective of surface failures and providing desirable flight characteristics. The implications of these two purposes on the design of the basic flight control system are discussed below.

Generic Commands. The basic flight control system simply generates "essential" commands necessary for a commanded maneuver. Therefore, for the purpose of this design, the control inputs considered are the generic inputs  $\delta_{\text{long}}$ ,  $\delta_{\text{lat}}$ , and  $\delta_{\text{dir}}$  rather than the five actual inputs  $\delta_{e_r}$ ,  $\delta_{e_l}$ ,  $\delta_{a_r}$ ,  $\delta_{a_l}$ , and  $\delta_r$ . Furthermore, these generic inputs should produce response only in their primary axes. Specifically,  $\delta_{\text{long}}$  should generate no lateral-directional forces or moments, while  $\delta_{\text{lat}}$  and  $\delta_{\text{dir}}$  should produce no longitudinal effects. Obviously, this can be achieved if  $\delta_{\text{long}}$  is simply the sum of the right and left elevator deflection. As shown in later paragraphs, permitting  $\delta_{\text{long}}$  to also produce symmetric aileron deflections results in improved performance while still not exciting the lateral-directional motion of the aircraft. As a consequence of this assumption, the 8 x 5 control matrix B of Eq (27) is not used directly in the design of the basic flight control system. Rather, three 8 x 1 column vectors,  $\underline{b}_{\text{long}}$ ,  $\underline{b}_{\text{lat}}$  and  $\underline{b}_{\text{dir}}$ , each corresponding to the three inputs

$\delta_{\text{long}}$ ,  $\delta_{\text{lat}}$  and  $\delta_{\text{dir}}$  are used. As a result of the assumption that  $\delta_{\text{long}}$  produces forces and moments only along the longitudinal axis, the last four coefficients of the column vector  $\underline{b}_{\text{long}}$  are identically zero. Similarly, due to the assumption that  $\delta_{\text{lat}}$  and  $\delta_{\text{dir}}$  produce only lateral-directional effects, the first four coefficients of the column vectors  $\underline{b}_{\text{lat}}$  and  $\underline{b}_{\text{dir}}$  are also identically equal to zero. Consequently, since the eight state variables of Eq (27) were already decoupled into two sets of equations, this input decoupling allows the entire system to be decoupled into separate longitudinal and lateral directional sets of equations.

This is a significant advantage of this approach over the method used by References 1 and 2. In their approach, all available inputs were used to control the entire system using multi-input multi-output control technique, which proved to be a complicated task. As opposed to this, the present approach deals with longitudinal and lateral-directional control separately using decoupled inputs  $\delta_{\text{long}}$ ,  $\delta_{\text{lat}}$  and  $\delta_{\text{dir}}$ . This single input system is simpler in design as well as application.

"Desirable" Characteristics. Consistent with current trends, it was decided that the basic flight control system should include pitch stability augmentation, normal "g" command, yaw stability augmentation with washout and roll damping systems. This would also make it comparable to the existing flight control system of the A-7D. This basic

flight control system must be designed to produce desirable flight characteristics. Specification of these "desirable" characteristics can be a complicated task. A reasonable approximation is to assume that the existing aircraft has desirable characteristics. Therefore, using as a starting point  $\underline{b}$  vectors  $\underline{b}_{long}$ ,  $\underline{b}_{lat}$  and  $\underline{b}_{dir}$  that mimic those of the existing A-7D aircraft should produce desirable characteristics.

Longitudinal Flight Control System. The design of a longitudinal flight control system with pitch stability augmentation system and normal g command system implies closed loop feedback with double-loop closure (Ref 9). Feedback of pitch rate to the input control,  $\delta_{long}$  in this case, forms the inner loop that adds to short period damping while feedback of normal acceleration to the longitudinal control forms the outer loop that provides the normal g command system and alleviates vertical gust response. Furthermore, to improve steady state response, a proportional plus integral controller is used which has a transfer function of the form

$$G_c = K_A \left( \frac{s + z}{s} \right)$$

where  $K_A$  and  $z$  are two parameters to be determined in the design process.

Proportional plus integral control effectively eliminates the "droop" in the closed loop frequency response curves near the closed loop natural frequency. Appendix A demonstrates

this result. In the design, actuator dynamics are represented by the transfer function  $(\frac{20}{s+20})$ . A block diagram of this longitudinal feedback system is shown in Figure 4.1. For analysis, the uncoupled longitudinal equations are extracted from Eq (27) which is the state variable representation of the entire system model. In doing so, it is noted that the input here is the single generic input  $\delta_{long}$  with a corresponding  $b_{long}$ . Initially,  $\delta_{long}$  was assumed to be the combined effect of  $\delta_{e_r}$  and  $\delta_{e_l}$ . Therefore, the longitudinal control matrix  $b_{long}$  is obtained by adding the control coefficients corresponding to right and left elevator inputs in the B matrix of Eq (27). This yields the following set of equations:

$$\begin{bmatrix} \dot{u} \\ \dot{\alpha} \\ \dot{q} \\ \dot{\theta} \end{bmatrix} = \begin{bmatrix} -0.00083 & 5.48 & 0 & -32.17 \\ -0.00018 & -.997 & 1.0 & 0 \\ 0.00038 & -8.27 & -0.709 & 0 \\ 0 & 0 & 1.0 & 0 \end{bmatrix} \begin{bmatrix} u \\ \alpha \\ q \\ \theta \end{bmatrix} + \begin{bmatrix} -32.86 \\ -0.135 \\ -15.91 \\ 0 \end{bmatrix} \delta_{long} \quad (38)$$

At the same time, based on its definition in Ref 3, an expression for normal acceleration is derived as

$$A_N = .113 u + 632.6 \alpha + 85.4 \delta_{long} \quad (39)$$

Root locus and Bode plot techniques were used to analyze the above system. Details of this process are given in Appendix A. The design resulted in values of the inner and

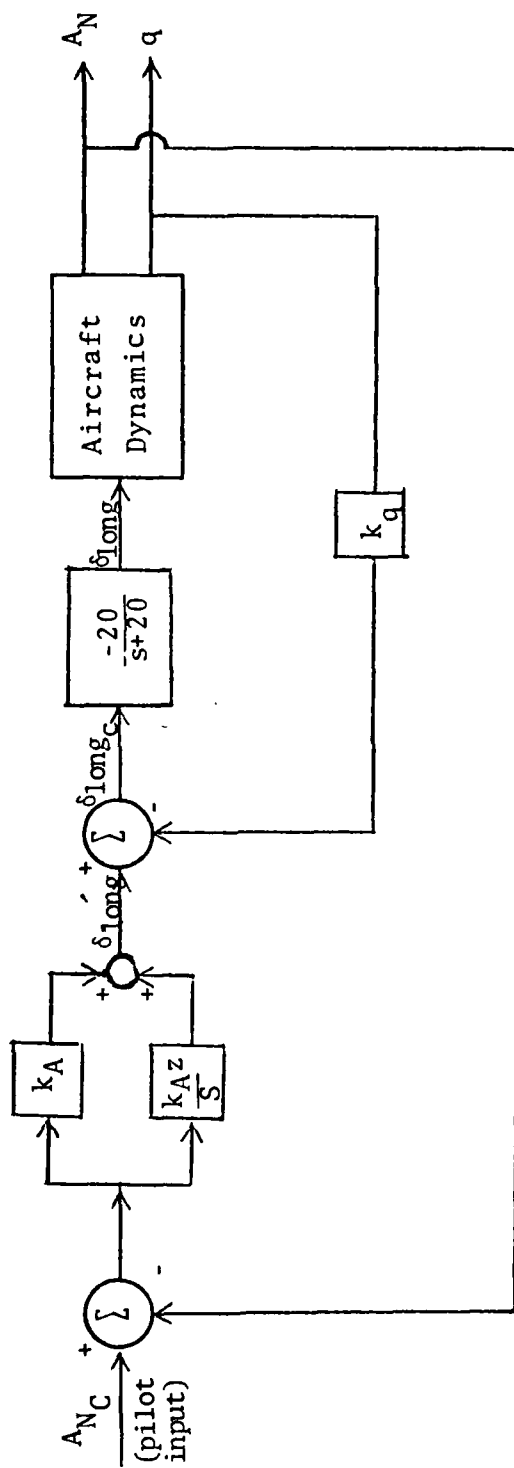


Figure 4.1. Pitch Stability Augmentation System and Normal "G"  
Command System (Basic Flight Control System)

outer loop gains  $K_q = 0.261$ ,  $K_A = 0.0016$  and the compensator zero location to be at  $z = 2.0$ . These values give a normal acceleration response to a unit step normal acceleration command characterized by

$$\omega_{sp} = 5.7 \text{ rad/sec}$$

$$\zeta_{sp} = 0.42$$

$$T_s = (\text{settling time based on a 2\% criteria}) = 2.8 \text{ sec}$$

as defined in Ref 10.

$$\text{Peak time} = 0.8 \text{ sec}$$

which fall within the level 1 flying qualities criteria as specified in Ref 8. The time response is given in Figure 4.2. This time response indicates desirable flight characteristics that meet the specifications of Reference 8. However, it also shows an opposite initial trend for a commanded maneuver. This occurs due to the right hand plane zero in the closed loop ( $A_N/A_{N_C}$ ) transfer function, which is inherent in such systems. Whereas the initial trend prevails for a very brief time period and causes no control problems, it is desirable to eliminate this "initial sinking" when the pilot actually commands a pull-up. This could be achieved if the longitudinal control were to produce upward forces in conjunction with pitching up moments. Mathematically, this would result if the (2,1) element of  $b_{long}$  (i.e., the term corresponding to the lift equations) was positive.

A significant advantage of designing flight control systems using generic controls instead of actual control

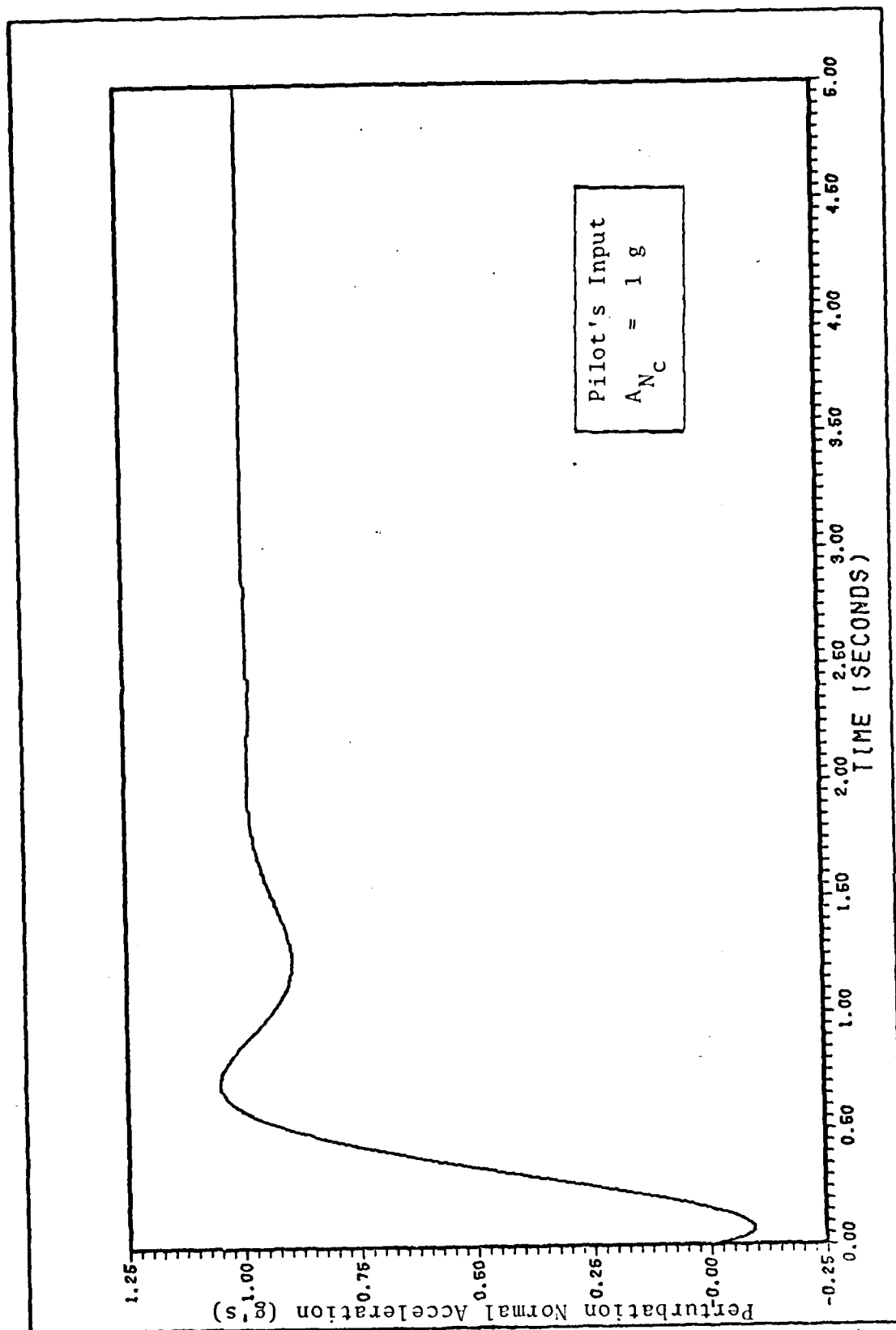


Figure 4.2. Time Response of Longitudinal Flight Control System

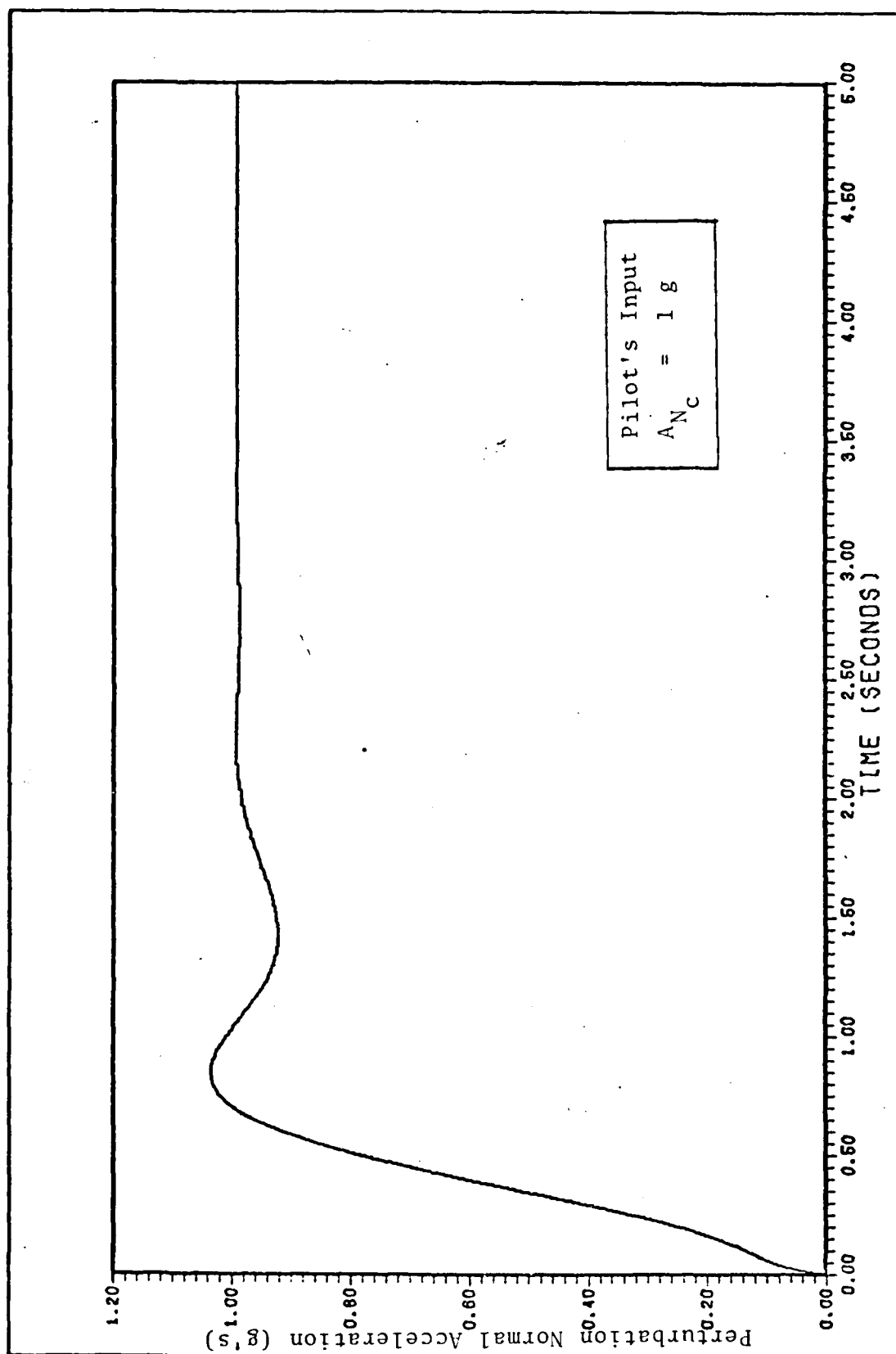


Figure 4.3. Time Response for  $b_{longd}$



surfaces is that the designer is free, within reason, to specify the  $\underline{b}_{\text{long}}$  he desires. The transformation matrix, relating actual control surface deflections to generic control surface commands, then determines the appropriate combination to achieve this desired  $\underline{b}_{\text{long}}$ . Therefore, repeating the longitudinal design using

$$\underline{b}_{\text{long}_d} = \begin{bmatrix} 32.86 \\ 0.135 \\ -15.91 \\ 0 \end{bmatrix} \quad (40)$$

produces the following results:

$$\begin{aligned} \omega_{\text{sp}} &= 4.97 \text{ rad/sec} \\ \zeta_{\text{sp}} &= 0.43 \end{aligned}$$

A-time response for the same unit normal acceleration input is shown in Figure 4.3. Complete absence of the initial opposite trend in Figure 4.3 indicates the effectiveness of this  $\underline{b}_{\text{long}_d}$ .

Lateral-Directional Flight Control System. Automatic control of the aircraft's lateral directional motions requires feedback to both the rudder and the ailerons. As previously stipulated, the lateral-direction flight control system for this study is to consist of a yaw stability augmentation system

and a roll damping system. The "directional" controller, designed to achieve enhanced dutch roll damping, is essentially a yaw stability augmentation which is accomplished by feedback of yaw rate to the directional input. A washout circuit is also included to avoid "fighting" intentional turns.

Yaw Stability Augmentation System. Figure 4.4 shows the closed loop feedback system. The actuator dynamics are represented by the equivalent transfer function  $(\frac{20}{s + 20})$ . The washout included in the loop has the form  $(\frac{s}{s + a})$ . The feedback loop gain  $K_r$  and the washout pole location "a" are the two parameters to be determined in the design process. The lateral-directional equations can be extracted from Eq (27) by noting that the states  $\beta$ ,  $p$ ,  $r$ , and  $\phi$  are uncoupled from the longitudinal equations, except for the input terms. Input decoupling is, however, achieved by definition of the generic inputs. As in the longitudinal case, a desirable  $\underline{b}_{dir}$  corresponding to the generic directional control, can be chosen by the designer. As a baseline, the author chose  $\underline{b}_{dir}$  to match the  $\underline{b}$  vector associated with the rudder input since historically a yaw stability augmentation system involved feedback of washed out yaw rate to the rudder. It is likely, however, that a different  $\underline{b}_{dir}$  vector might be even more effective in augmenting dutch roll damping. This different  $\underline{b}_{dir}$  would then mean that  $\delta_{dir}$  would produce not only rudder deflections, but also aileron deflections.

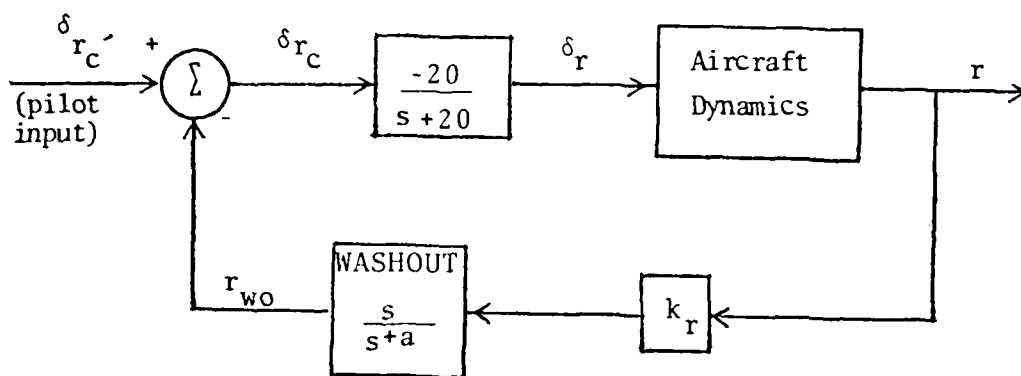


Figure 4.4. Yaw Stability Augmentation System  
with Washout Circuit (Basic Flight Control System)

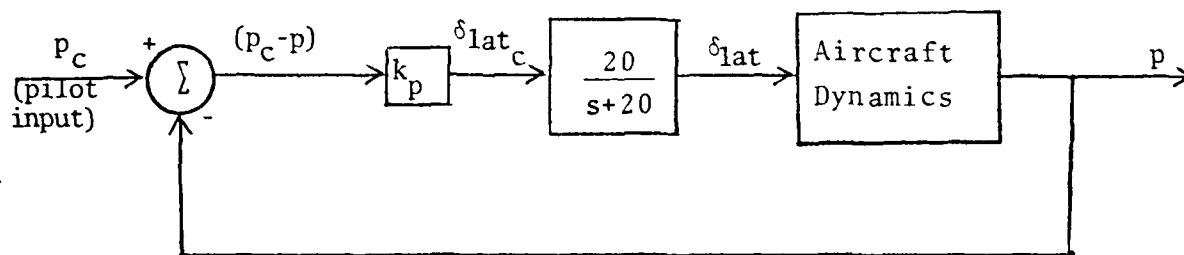


Figure 4.5. p-command System  
(Basic Flight Control System)

Using the  $\underline{b}$  vector corresponding to the rudder input of Eq (27), the lateral-directional set is

$$\begin{bmatrix} \dot{\beta} \\ \dot{p} \\ \dot{r} \\ \dot{\phi} \end{bmatrix} = \begin{bmatrix} -0.162 & 0.00089 & -0.998 & 0.051 \\ -26.23 & -3.010 & 0.959 & 0 \\ 4.55 & 0.057 & -0.530 & 0 \\ 0 & 1 & 0 & 0 \end{bmatrix} \begin{bmatrix} \beta \\ p \\ r \\ \phi \end{bmatrix} + \begin{bmatrix} 0.045 \\ 5.972 \\ -5.307 \\ 0 \end{bmatrix} \delta_{dir} \quad (41)$$

Using these equations for analysis, classical techniques were employed to design the two parameters  $K_r$  and  $a$ . Details of this process are given in Appendix A. The values obtained for the two parameters are feedback loop gain  $K_r = 0.386$  and the washout pole location  $a = 1.0$ . These values give a dutch roll mode characterized by

$$\begin{aligned} \omega_{dr} &= 1.41 \text{ rad/sec} \\ \zeta_{dr} &= 0.454 \end{aligned}$$

which fall within level 1 flying qualities criterion of Ref 8.

Since this is acceptable, no attempt was made to modify the  $\underline{b}_{dir}$  of Eq (41). Therefore, the desired  $\underline{b}_{dir}$ , to be used in later sections, is:

$$\underline{b}_{dir} = \begin{bmatrix} 0.045 \\ 5.972 \\ -5.307 \\ 0 \end{bmatrix} \quad (42)$$

Roll Damping System. To improve roll response and reduce roll sensitivity to gusts and other inputs, roll rate  $p$  is fed back to the aileron input using a p-command system. This feedback loop is shown in Figure 4.5 where actuator dynamics are once again represented by  $(\frac{20}{s+20})$ . The feedback loop gain,  $K_p$ , is the only parameter to be determined in the design process.

The uncoupled lateral-directional equations are derived from the state variable system model, Eq (27), by noting that the lateral input here is the single generic input " $\delta_{lat}$ ." Initially, this was chosen to correspond to the combined effect of the individual aileron inputs  $\delta_{a_r}$  and  $\delta_{a_l}$ . The control vector  $\underline{b}_{lat}$  was therefore obtained by adding the individual aileron inputs corresponding to each lateral equation. This process yields the following set of equations using  $\delta_{lat}$  as the single input.

$$\begin{bmatrix} \dot{\beta} \\ \dot{p} \\ \dot{r} \\ \dot{\phi} \end{bmatrix} = \begin{bmatrix} -0.162 & 0.00089 & -0.998 & 0.051 \\ -26.23 & -3.010 & 0.959 & 0 \\ 4.55 & 0.057 & -0.530 & 0 \\ 0 & 1 & 0 & 0 \end{bmatrix} \begin{bmatrix} \beta \\ p \\ r \\ \phi \end{bmatrix} + \begin{bmatrix} -0.011 \\ 34.55 \\ 0.061 \\ 0 \end{bmatrix} \delta_{lat} \quad (43)$$

These equations, when analyzed using classical techniques, gave a design value of the feedback loop gain of  $K_p = 0.014$ . Details of this process are also given in Appendix A. The above  $K_p$  results in a roll rate response characterized by:

$$\begin{aligned}
\omega_{dr} &= 1.44 \text{ rad/sec} \\
\zeta_{dr} &= 0.539 \\
\text{spiral time constant } T_s &= 37.4 \text{ sec} \\
\text{roll time constant} &= 0.29 \text{ sec}
\end{aligned}$$

which fall within level 1 flying qualities criterion as specified in Reference 8.

The time response, indicated desirable flight characteristics in terms of transient response, steady state error, etc. Since this response was acceptable, no other  $\underline{b}_{lat}$  was tried. Therefore, the lateral control vector of Eq (43) is selected as the desired lateral control vector for use in the reconfigurable flight control system.

$$\underline{b}_{lat_d} = \begin{bmatrix} -0.011 \\ 34.55 \\ 0.061 \\ 0 \end{bmatrix} \quad (44)$$

#### No-Failure Transformation Matrix $J_{NF}$

Having designed the basic flight control system, the next step is to compute the transformation matrices relating actual control surfaces to the generic controls, to effectively produce these desired  $\underline{b}$  vectors. First, the no-failure case

is examined. From Eq (32) of the previous chapter, it follows that:

$$J_{NF} = (B_{NF}^T B_{NF})^{-1} B_{NF}^T B_d$$

or

$$J_{NF} = B_{NF}^+ B_d \quad (45)$$

where  $B_{NF}$  is the control matrix of dimension  $8 \times 5$  and  $B_d$  is the desired control matrix of dimensions  $8 \times 3$ . As discussed in Chapter III,  $B_{NF}^+ = [B_{NF}^T B_{NF}]^{-1} B_{NF}^T$  is the pseudo-inverse that produces a best approximation to  $B_d$  in a least square sense. This is to say that the original problem is over-specified, requiring five unknowns (control coefficients of each dynamic equation) to satisfy eight equations. Since this is, in general, impossible, the intention is to keep the number of equations as close to five as possible. Of these eight equations,  $\dot{\phi}$  and  $\dot{\theta}$  equations are always satisfied, effectively reducing the number of equations to six. Furthermore, it is observed that the drag equation ( $\dot{u}$  equation) does not play any significant role in the control of the aircraft. This implies that the control coefficients corresponding to the control surface deflections in the drag equation are not critical. It is, therefore, appropriate to neglect the  $\dot{u}$  equation in order to achieve better accuracy for the other coefficients. The B matrix for the no failure case, therefore, reduces to

a matrix of dimension 7 x 5 as follows:

$$B_{NF} = \begin{bmatrix} -0.067 & -0.067 & 0.048 & -0.048 & 0 \\ -7.96 & -7.96 & 0.397 & -0.397 & 0 \\ 0 & 0 & 0 & 0 & 0 \\ 0 & 0 & -0.006 & -0.006 & 0.045 \\ -7.99 & 7.99 & 17.27 & 17.27 & 5.97 \\ -0.433 & 0.433 & 0.031 & 0.031 & -5.31 \\ 0 & 0 & 0 & 0 & 0 \end{bmatrix} \quad (46)$$

Desired Control Matrix  $B_d$ . According to the scheme of reconfiguration, the transformation matrix "J" is to be so selected that it produces the same desired control matrix  $B_d$  when multiplied with the appropriate control matrix  $B_{NF}$ ,  $B_{REF}$ , etc., depending on the respective case under consideration. This desired control matrix  $B_d$  is made up of three 8 x 1 column vectors, each corresponding to the three generic inputs  $\delta_{long}$ ,  $\delta_{lat}$  and  $\delta_{dir}$ . These desired column vectors have already been selected in the flight control system design as given in Eqs (40), (42) and (44). Therefore,  $B_d$  may be directly written as:



$$B_d = \begin{bmatrix} -32.86 & 0 & 0 \\ 0.135 & 0 & 0 \\ -15.91 & 0 & 0 \\ 0 & 0 & 0 \\ 0 & -0.011 & 0.045 \\ 0 & 34.55 & 5.972 \\ 0 & 0.061 & -5.307 \\ 0 & 0 & 0 \end{bmatrix} \quad (47)$$

To make row dimensions of  $B_d$  compatible with the row dimension of  $B_{NF}$ ,  $B_{REF}$ , etc., its first row (control coefficients of the  $\dot{u}$  equation) is also neglected. The same justification applies to this reduction as for  $B_{NF}$  given earlier. The (7 x 3) desired control matrix, therefore, becomes

$$B_d = \begin{bmatrix} 0.135 & 0 & 0 \\ -15.91 & 0 & 0 \\ 0 & 0 & 0 \\ 0 & -0.011 & 0.045 \\ 0 & 34.55 & 5.972 \\ 0 & 0.061 & -5.307 \\ 0 & 0 & 0 \end{bmatrix} \quad (48)$$

$J_{NF}$ . Use of singular value decomposition as suggested in Reference 11 simplifies the task of evaluating pseudo-inverse. This method was used to evaluate  $B_{NF}^+$ . Substituting values of  $B_{NF}^+$  so obtained and  $B_d$  as given in Eq (48) into Eq (45),  $J_{NF}$  is found as

$$J_{NF} = \begin{bmatrix} 1.151 & 0 & 0 \\ 1.151 & 0 & 0 \\ 3.022 & 1.0 & 0 \\ -3.022 & 1.0 & 0 \\ 0 & 0 & 1.0 \end{bmatrix} \quad (49)$$

This transformation matrix, when premultiplied by  $B_{NF}$ , reproduces the  $B_d$  exactly except for the first row corresponding to the  $\dot{u}$  equation. As is shown in the next chapter, this difference causes negligible effect on the aircraft response.

Recalling Eq (28)

$$\underline{u}_{NF} = \begin{bmatrix} J_{NF} \end{bmatrix} \begin{bmatrix} \delta_{long} \\ \delta_{lat} \\ \delta_{dir} \end{bmatrix}$$

it is seen that  $\delta_{long}$  produces not only elevator deflections, but also right and left aileron deflections.

### Evaluation of Failure Transformation Matrices

J<sub>REF</sub>. For the right elevator failure case, the transformation matrix J<sub>REF</sub> has been defined in Chapter III as

$$J_{REF} = [B_{REF}^T B_{REF}]^{-1} B_{REF}^T B_d$$

or

$$J_{REF} = B_{REF}^+ B_d \quad (50)$$

where  $B_{REF}^+$  is the pseudo-inverse of  $B_{REF}$ , and  $B_d$  is the desired control matrix. As discussed for the no-failure case, with a view toward keeping the number of equations as close to four as possible, the drag equation is neglected from the control matrix of Eq (27) to get the 7 x 5  $B_{NF}$  matrix of Eq (46). The matrix  $B_{REF}$ , since it corresponds to a right elevator failure, is then deduced from this  $B_{NF}$  by eliminating the first column corresponding to the right elevator input  $\delta_{e_r}$ .  $B_{REF}$ , therefore, is a matrix of dimensions 7 x 4 corresponding to a 4 x 1 input vector

$$\underline{u}_{REF} = [\delta_{e_l}, \delta_{a_r}, \delta_{a_l}, \delta_r]^T$$

Evaluating the pseudo-inverse of  $B_{REF}$  and then using Eq (50) yields

$$J_{REF} = \begin{bmatrix} 2.302 & 0 & 0 \\ 2.457 & 1.0 & 0 \\ -3.585 & 1.0 & 0 \\ 0.1812 & 0 & 1.0 \end{bmatrix} \quad (51)$$

This transformation matrix, when premultiplied by  $B_{REF}$  reproduces the  $B_d$  exactly except for the first row corresponding to the  $\dot{u}$  equation and the (4,1) element corresponding to the side force equation where a small input is introduced. As will be shown later, these differences cause negligible effect on the aircraft response.

Again recalling Eq (33), it is seen that a  $\delta_{long}$  command produces unequal deflections of the left elevator, right and left aileron and the rudder.

Other Failure Matrices. The three other failure transformation matrices  $J_{LEF}$ ,  $J_{RAF}$  and  $J_{LAF}$  are evaluated using their basic definitions from Chapter III.

$$\begin{aligned} J_{LEF} &= B_{LEF}^+ B_d \\ J_{RAF} &= B_{RAF}^+ B_d \\ J_{LAF} &= B_{LAF}^+ B_d \end{aligned} \quad (52)$$

In each case, the desired control matrix remains the same as defined in Eq (48). The control matrices  $B_{LEF}$ ,  $B_{RAF}$  and

$B_{LAF}$  are obtained by eliminating appropriate columns corresponding to the failed input from the no-failure matrix  $B_{NF}$  of Eq (46). Then using Eq (52) gives the respective failure transformation matrices:

$$J_{LEF} = \begin{bmatrix} 2.302 & 0 & 0 \\ 3.585 & 1 & 0 \\ -2.457 & 1 & 0 \\ - .1812 & 0 & 1 \end{bmatrix} \quad (53)$$

$$J_{RAF} = \begin{bmatrix} -4.546 & -1.885 & 0 \\ 6.824 & 1.887 & 0 \\ -5.571 & .1566 & 0 \\ .8952 & .2962 & 1 \end{bmatrix} \quad (54)$$

$$J_{LAF} = \begin{bmatrix} 6.824 & -1.877 & 0 \\ -4.546 & 1.885 & 0 \\ 5.571 & .1566 & 0 \\ - .8952 & .2962 & 1 \end{bmatrix} \quad (55)$$

### Summary

Design of a reconfigurable flight control system for the A-7D requires design of a basic flight control system and evaluation of certain transformation matrices. In this chapter, specifications of the basic flight control system

are established and their design values are developed using conventional techniques. Using this design, a desired B matrix is evolved which permits direct evaluation of the various transformation matrices. Use of singular value decomposition in the process of evaluating the pseudo-inverse has been found to simplify the process.

## V. Flight Simulation

### Introduction

Flight simulation using digital hardware is a powerful technique for verification of design concepts in aeronautical systems. Although laboratory environments prevent real time testing, it demonstrates the technical feasibility of the design and establishes confidence in the approach. This method has, therefore, been adopted for testing the design concept presented in this thesis.

In order to appreciate the effectiveness of reconfiguration, it is appropriate to carry out a simulation testing program that covers the following:

- (a) Flight simulation using existing A-7D flight control systems without failures.
- (b) Flight simulation using the reconfigurable flight control systems without failure.
- (c) Flight simulation using the reconfigurable flight control system with specific surface failures.

Comparison of the results of tests (b) and (c) proves the effectiveness of the reconfigurable flight control system, while tests (a) and (b) demonstrate that the flight control system designed in Chapter IV is comparable to the existing A-7D flight control system. In this chapter,

therefore, a complete nonlinear flight simulation, combined with failure analysis, is developed for the flight condition under study.

### System Model for Six Degree-of-Freedom Simulation

A realistic simulation requires that the airplane be considered as a three dimensional body capable of six degrees of freedom of motion; namely, the three translational and three angular displacements. This is achieved by using an aircraft model described by non-linear coupled ordinary differential equations rather than the linearized equations as presented in Chapter II. Such a set of nonlinear equations is obtained from Reference 3 for the flight simulation and is rearranged below:

$$\dot{U} = VR - WQ - g \sin \theta + \frac{\bar{q}S}{m} C_x + T$$

$$\dot{V} = -UR + WP + g \cos \theta \sin \phi + \bar{q}S C_y$$

$$\dot{W} = UQ - VP + g \cos \theta \cos \phi + \bar{q}S C_z$$

$$\begin{aligned} \dot{P} = & \left[ \frac{I_{zz}}{I_{xx}I_{zz} - I_{xz}^2} \right] \left[ L_A + \frac{I_{xz}}{I_{zz}} N_A - (I_{zz} - I_{yy} + \frac{I_{xz}^2}{I_{zz}}) QR \right. \\ & \left. + \frac{I_{xz}}{I_{zz}} (I_{xx} - I_{yy} + I_{zz}) PQ \right] \end{aligned}$$



$$\begin{aligned}
\dot{Q} &= \left[ \frac{1}{I_{yy}} \right] [M_A - I_{xz} (P^2 - R^2) - (I_{xx} - I_{zz}) PR] \\
\dot{R} &= \left[ \frac{I_{xx}}{I_{xx} I_{zz} - I_{xz}^2} \right] [N_A + \frac{I_{xz}}{I_{xx}} L_A - (I_{yy} - I_{xx} - \frac{I_{xz}^2}{I_{xx}}) PQ \\
&\quad + \frac{I_{xz}}{I_{xx}} (-I_{xx} + I_{yy} - I_{zz}) QR] \\
\dot{\phi} &= P + \tan \theta (Q \sin \phi + R \cos \phi) \\
\dot{\theta} &= Q \cos \phi - R \sin \phi \\
\dot{\psi} &= (Q \sin \phi + R \cos \phi) / \cos \theta \\
\dot{h} &= -[ -U \sin \theta + V \sin \phi \cos \theta + W \cos \phi \cos \theta ] \quad (56)
\end{aligned}$$

The above set of equations is to be read with the following supporting relationships:

$$\begin{aligned}
\bar{q} &= \frac{1}{2} \rho (U^2 + V^2 + W^2) \\
C_x &= -C_D \cos \alpha + C_L \sin \alpha \\
C_y &= C_{y_\beta} \beta + C_{y_p} \left( \frac{Pb}{2U} \right) + C_{y_r} \left( \frac{Rb}{2U} \right) + C_{y_{\delta_a}} \delta_a + C_{y_{\delta_r}} \delta_r \\
C_z &= -C_D \sin \alpha - C_L \cos \alpha
\end{aligned}$$

AD-A111 172

AIR FORCE INST OF TECH WRIGHT-PATTERSON AFB OH SCHOOL-ETC P/S 1/3  
USE OF THE PSEUDO-INVERSE FOR DESIGN OF A RECONFIGURABLE FLIGHT-ETC(U)  
DEC 81 S J RAZA

UNCLASSIFIED

AFIT/6AE/AA/61D-23

NL

2 of 2  
AD-A111 172

END  
DATE  
FILMED  
19-82  
DTIC

$$L_A = \bar{q} s b C_{l_{\alpha}}$$

$$M_A = \bar{q} s \bar{c} C_m$$

$$N_A = q S b C_n$$

$$C_D = C_{D_0} + k C_L^2, \text{ where } C_{D_0} \text{ is the zero lift drag.}$$

$$C_L = C_{L_0} + C_{L_{\alpha}} \alpha + C_{L_{\dot{\alpha}}} \left( \frac{\dot{\alpha} c}{2U} \right) + C_{L_q} \left( \frac{Q \bar{c}}{2U} \right) + C_{L_{\delta_e}} \delta_e$$

$$C_m = C_{m_0} + C_{m_{\alpha}} \alpha + C_{m_{\dot{\alpha}}} \left( \frac{\dot{\alpha} c}{2U} \right) + C_{m_q} \left( \frac{Q \bar{c}}{2U} \right) + C_{m_{\delta_r}} \delta_r$$

$$C_n = C_{n_{\beta}} \beta + C_{n_p} \left( \frac{P b}{2U} \right) + C_{n_r} \left( \frac{R b}{2U} \right) + C_{n_{\delta_a}} \delta_a + C_{n_{\delta_r}} \delta_r$$

$$\alpha = \tan^{-1} (W/U)$$

$$\beta = \tan^{-1} (V/U) \quad (57)$$

Parameter values for the sets of equations (56) and (57) are used from Tables I and IV of the linear model, except for the following two parameters not tabulated earlier.

k: In the equation  $C_D = C_{D_0} + k C_L^2$ , k is defined as:

$$k = \frac{1}{\pi A R e}$$

for an Oswalds efficiency factor e of 80%.

This may be calculated as

$$k = \frac{S}{\pi b^2 (.8)} = 0.0194$$

T: Thrust is evaluated by noting that in trimmed straight and level flight it balances the total drag, thus

$$\begin{aligned} T_{\text{trim}} &= D_{\text{trim}} \\ &= C_{D_{\text{trim}}} \bar{q} S \\ &= (.0219)(300.88)(375.0) \\ &= 2741 \text{ lbf} \end{aligned}$$

These equations were integrated forward in time using a Runge Kutta-Verner fifth and sixth order method available in the IMSL library package (Ref 12). A sample time of 0.05 sec was used.

#### Flight Simulation (Existing Flight Control System)

To execute this scheme, the existing A-7D flight control system is modelled as another set of differential equations which, when coupled to Eq (56) provides the input as a function of time. Details of this flight control system model are

placed at Appendix B for reference. Appropriate software is then developed that incorporates these flight control system equations into the aircraft simulation.

#### Flight Simulation (Reconfigurable Flight Control System)

Equations (56) are adapted to the reconfigurable flight control system by implementing individual control surface deflections unlike their deflection as a set in the previous case. These equations, including those representing the reconfigurable flight control system designed in Chapter IV, are then integrated in forward time using the method previously described. The general scheme of simulation for the reconfigurable flight control system is shown in the flow chart of Figure 5.1. Details of the equations representing the reconfigurable flight control system are given in Appendix B. As the flow chart indicates, the transformation matrices (of Eqs (49), (51), (53), (54), and (55)) are incorporated within aircraft dynamics through the flight control system. Reconfiguration is achieved by implementing the appropriate transformation matrix depending on surface failure, if any.

Salient features of the software developed for this scheme are:

- (a) User selection of the initial flight condition.
- (b) Specification of pilot inputs ( $A_{N_c}$ ,  $p_c$  and  $\delta_{r_c}$ )
- (c) Option of simulating normal/failure flight.
- (d) User selection of time at which failure occurs  $T_F$ .

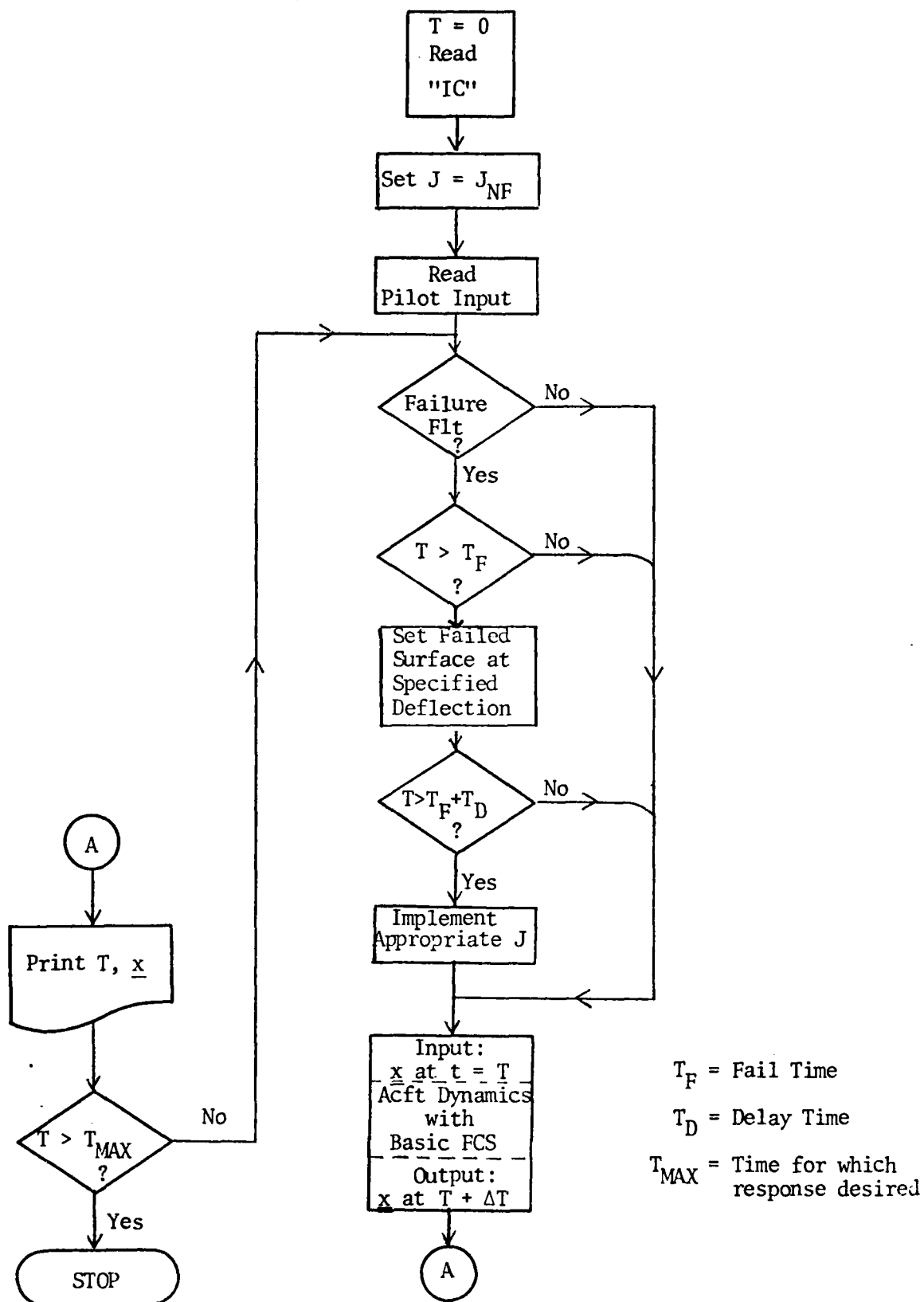


Figure 5.1. General Simulation Scheme  
(Reconfigurable Flight Control System)

- (e) Option of varying delay time ( $T_D$ ) between surface failure and reconfigurable flight control system takeover. This time is meant to represent the time it would take for a failure to be detected and identified.
- (f) Option of various control surface failures.
- (g) Option of specifying failed surface position as neutral or any other position up to maximum deflection.

Based on the above scheme, a failure flight using the reconfigurable flight control system may be exemplified as follows. At time  $T = 0$ , the aircraft is flying with some specified initial flight condition (Mach No., Altitude, etc.). After a previously set time, a specific failure occurs. This failure causes the failed surface to immediately deflect to some user specified angle.  $T_D$  seconds later, the reconfigurable flight control system takes over. After this time, the simulation gives the system response with the reconfigurable flight control system in effect.

Results of the several simulation tests conducted using this routine are discussed in the next chapter.

### Summary

In this chapter, a six degree of freedom aircraft model is developed that is used for flight simulation. The general scheme of the test simulation is presented first for the

existing flight control system, and then for the reconfigurable flight control system. Salient features of the software developed for implementing the reconfigurable flight control system simulation are also given. Detailed models for the existing and reconfigurable flight control system inputs are placed at Appendix B.



## VI. Comparison of Results

### Introduction

In this thesis, a reconfigurable flight control system has been designed based on the concept of generic commands and appropriate transformation matrices. Furthermore, a scheme has been developed to simulate flight under specified flight conditions with and without failures. What remains now is a test of the reconfigurable flight control system to prove its effectiveness and superiority over the existing non-reconfigurable one. This chapter, therefore, presents selected results with a view to

- (a) establishing confidence in the simulation scheme and comparing the design flight control system to the existing one,
- (b) proving effectiveness of the reconfigurable flight control system,
- (c) determining time specifications for identification of failure, and
- (d) studying sensitivity to parameter variations.

Of these objectives, (a) is demonstrated by simulating no-failure flights whereas (b), (c) and (d) are accomplished by simulating flights with certain control surface failures.

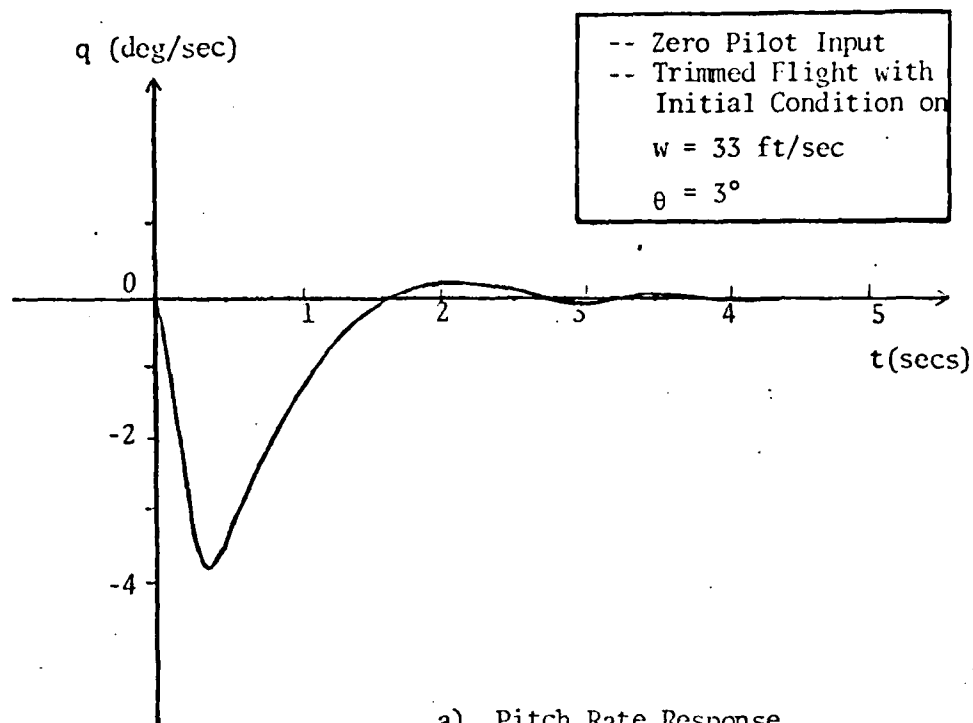
### No-Failure Flight Simulation

In order to show correctness of the simulation scheme and to form a basis for comparison with the design flight control system, flight simulation was carried out with the existing flight control system under the flight condition defined in Chapter II. Several simulation runs were carried out to study aircraft response to pilot input in the three axes. However, to limit the discussion and yet cover both the longitudinal and lateral-direction motion, time responses of only the short period and dutch roll modes are shown in Figure 6.1 and 6.2, respectively. These results compare well with the eigenvalues of the plant matrix as shown earlier in Chapter II. This shows correctness of simulation.

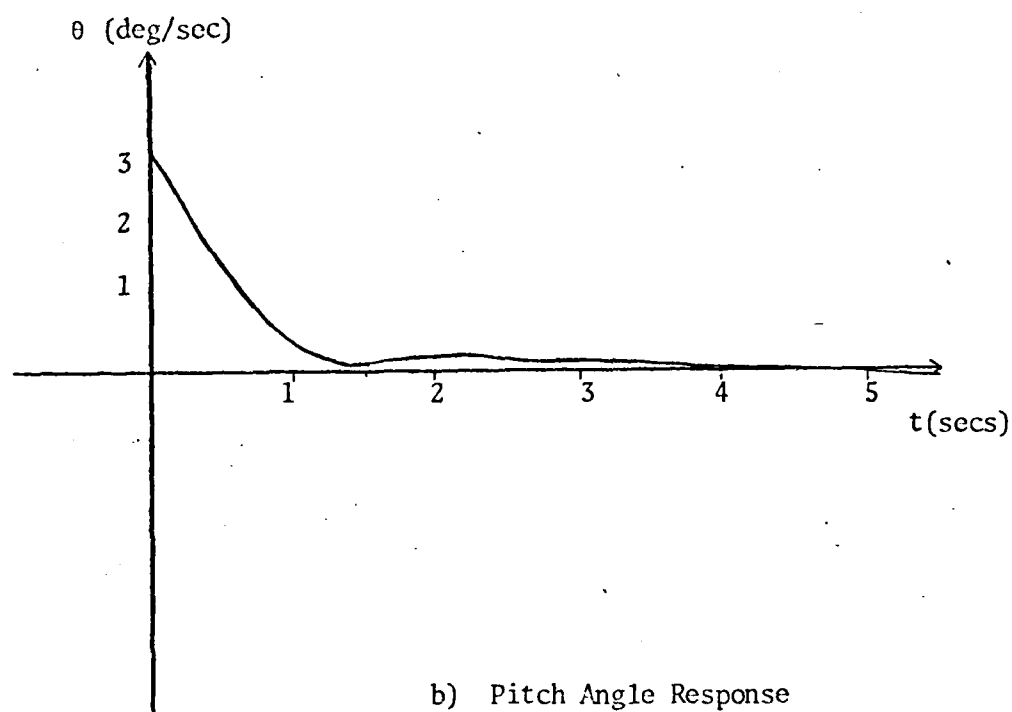
Next, flight simulation was carried out for the same flight condition and pilot input using the reconfigurable flight control system. Of the several simulations, time responses for short period and dutch roll modes are given in Figures 6.3 and 6.4, respectively.

### Simulation of "Failure Flights"

From the results of the previous paragraph, it may be observed that the design flight control system compares well to the existing flight control system of the A-7D. Therefore, to prove the effectiveness of reconfiguration, only the design flight control system is used. Flight simulation is carried out using the design flight control system for a surface



a) Pitch Rate Response



b) Pitch Angle Response

Figure 6 .1 Short Period Response of Existing Flight Control System

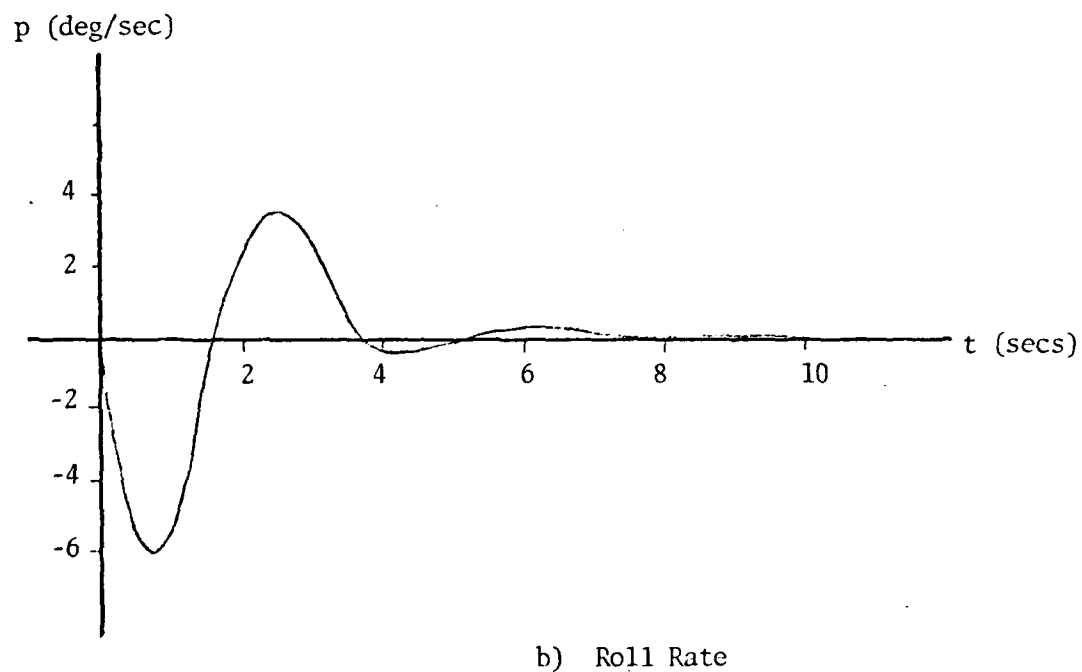
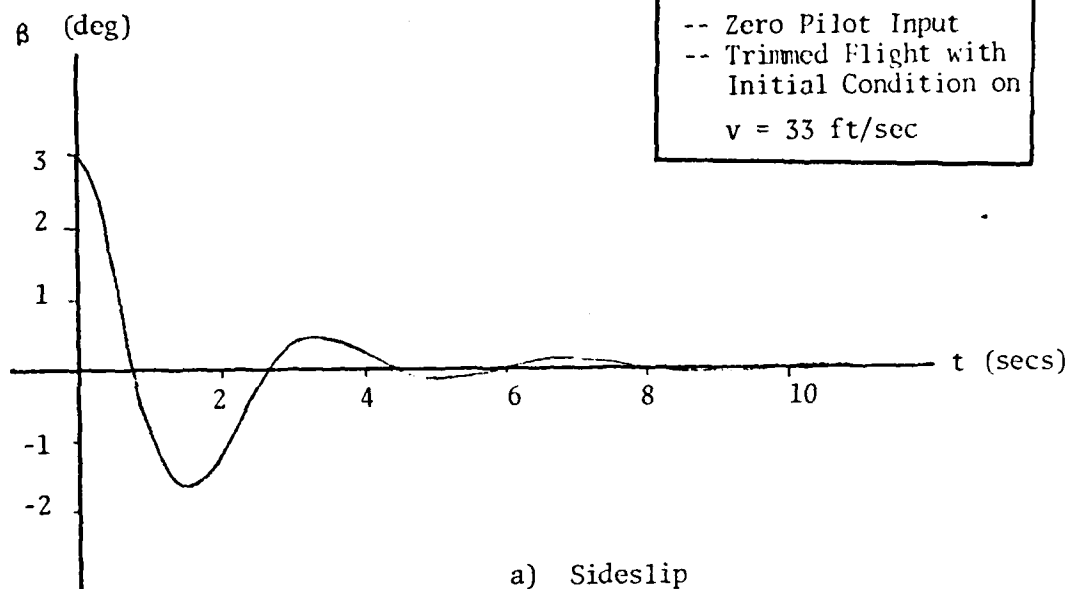


Figure 6.2 Dutch Roll Response for Existing Flight Control System

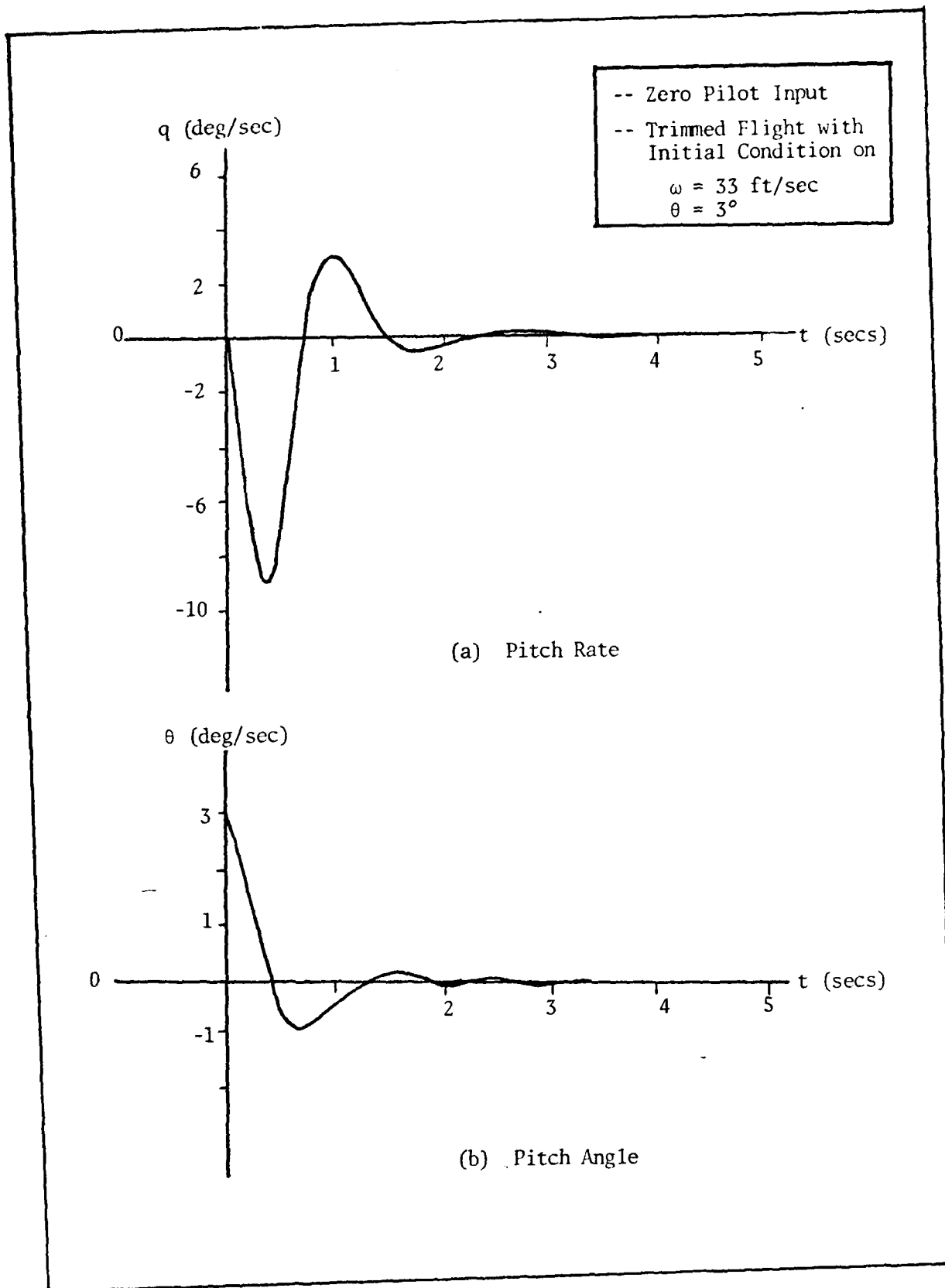
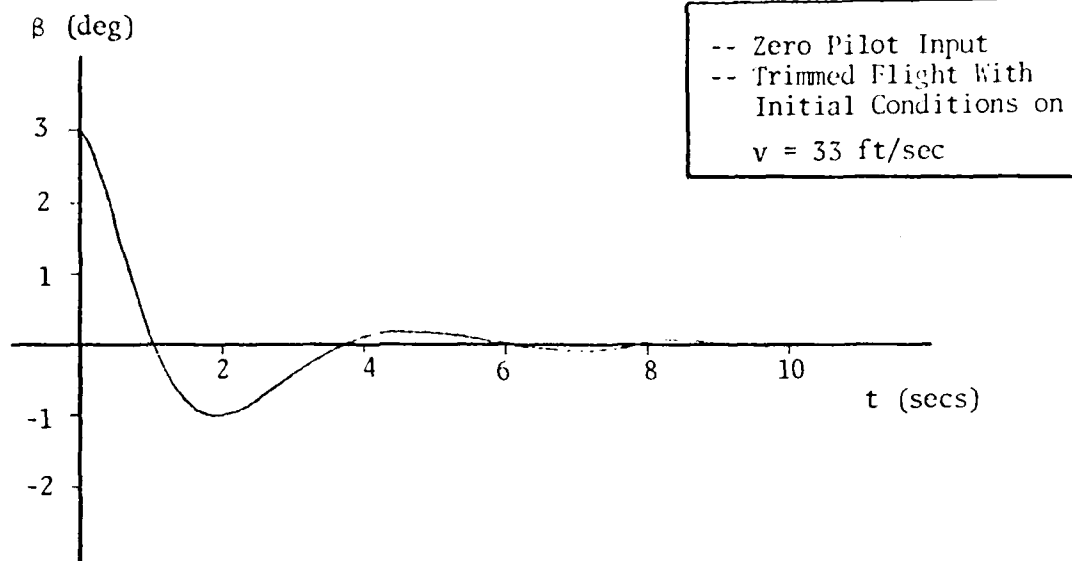
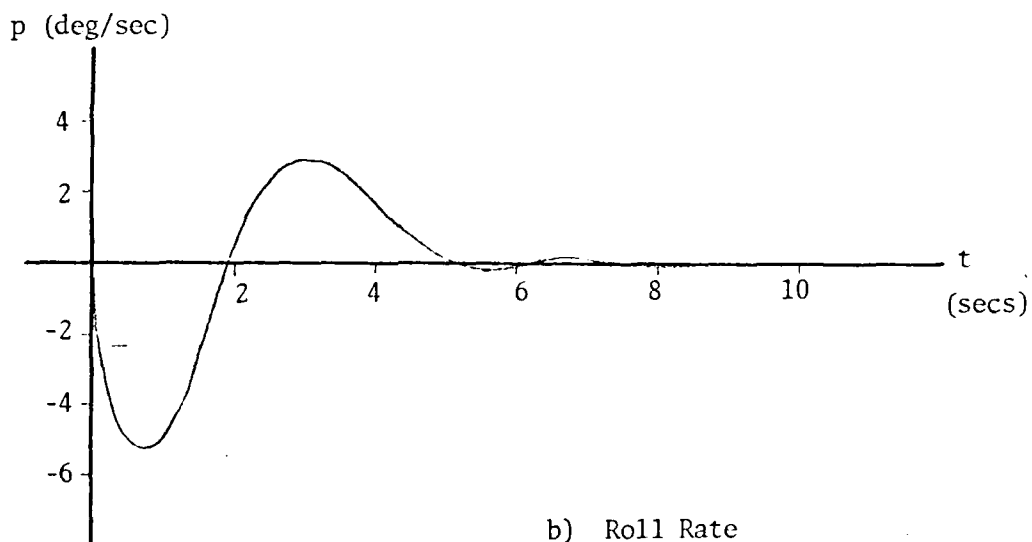


Figure 6.3. Short Period Response of Design Flight Control System



a) Sideslip



b) Roll Rate

Figure 6.4 Dutch Roll Response for Design Flight Control System

failure with and without reconfiguration. A comparison of aircraft response in either case proves the effectiveness of reconfiguration.

Surface Failures Considered. Since a left control surface failure produces an aircraft response symmetrically opposite to the corresponding right control surface failure, therefore, only right surface failure flights are simulated here. As a result, the two failures that fall within the scope of this study are the right elevator failure and the right aileron failure. Two extreme cases are studied for each one; namely, control surface failing at neutral or zero degree deflection and control surface failing at maximum deflection point. Of these two, the latter poses a more severe control problem. Results of these simulations are discussed below.

Right Elevator Failure at Zero Degrees. First, flight simulation was carried out for this failure without reconfiguration. The aircraft was simulated in trimmed flight with a commanded 1-g pull-up. At a specified time, the right elevator was simulated to fail and then response of the various quantities was studied. It was found that, while  $A_N$  response itself was reasonable (Figure 6.5), both roll and yaw rates were increasing with time. Roll rate was much faster and hence causing greater control difficulty. Roll rate response for this case is shown in Figure 6.6.

In the first five seconds,  $p$  reached a value of  $-7.9$  deg/sec, while the bank angle was greater than  $-25^\circ$ . In the same time, maximum excursions on the aileron were about  $10^\circ$ .

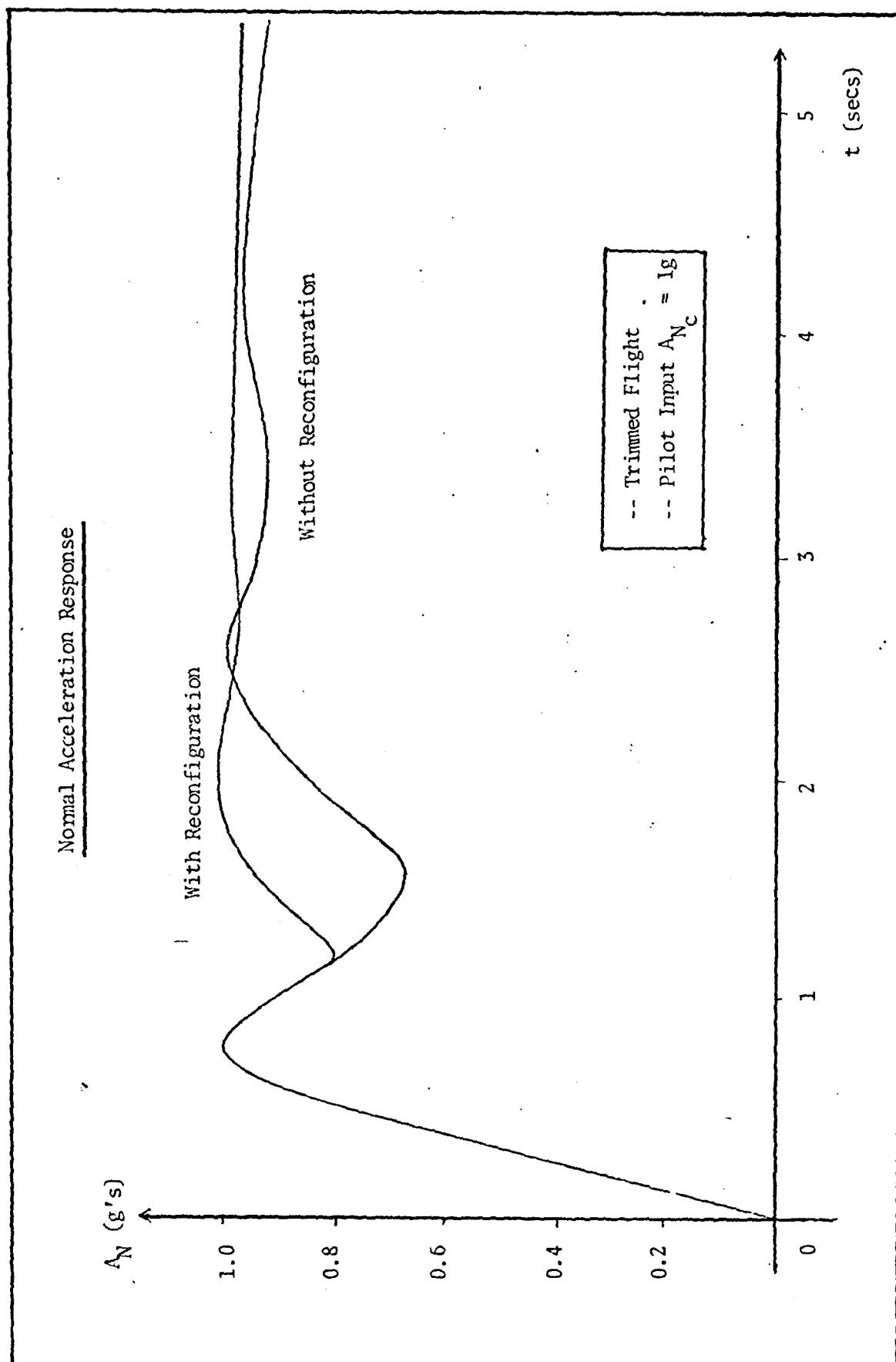


Figure 6 . 5 Right Elevator Failure at Zero Degrees



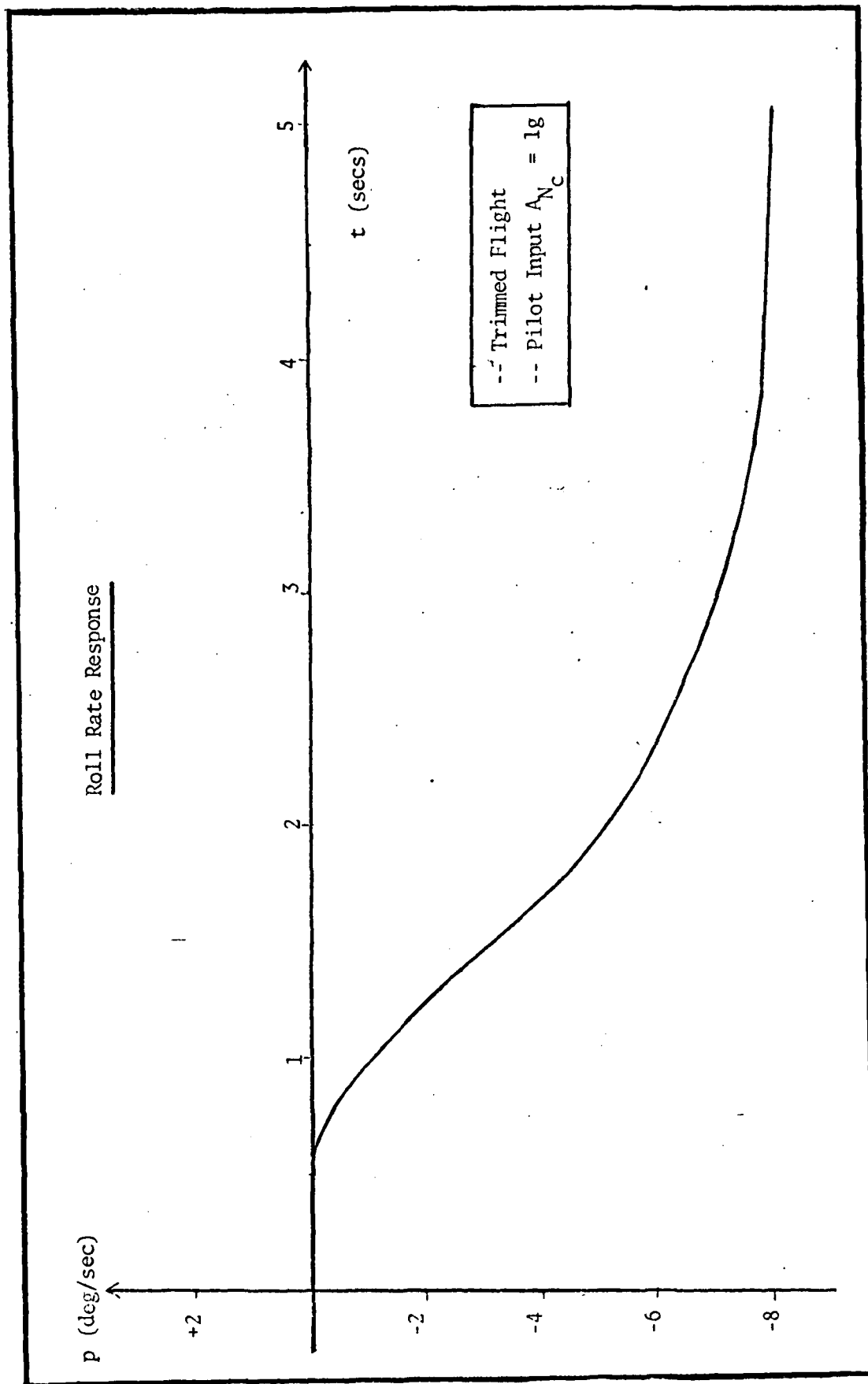


Figure 6.6 Right Elevator Failure at Zero Degrees; No Reconfiguration

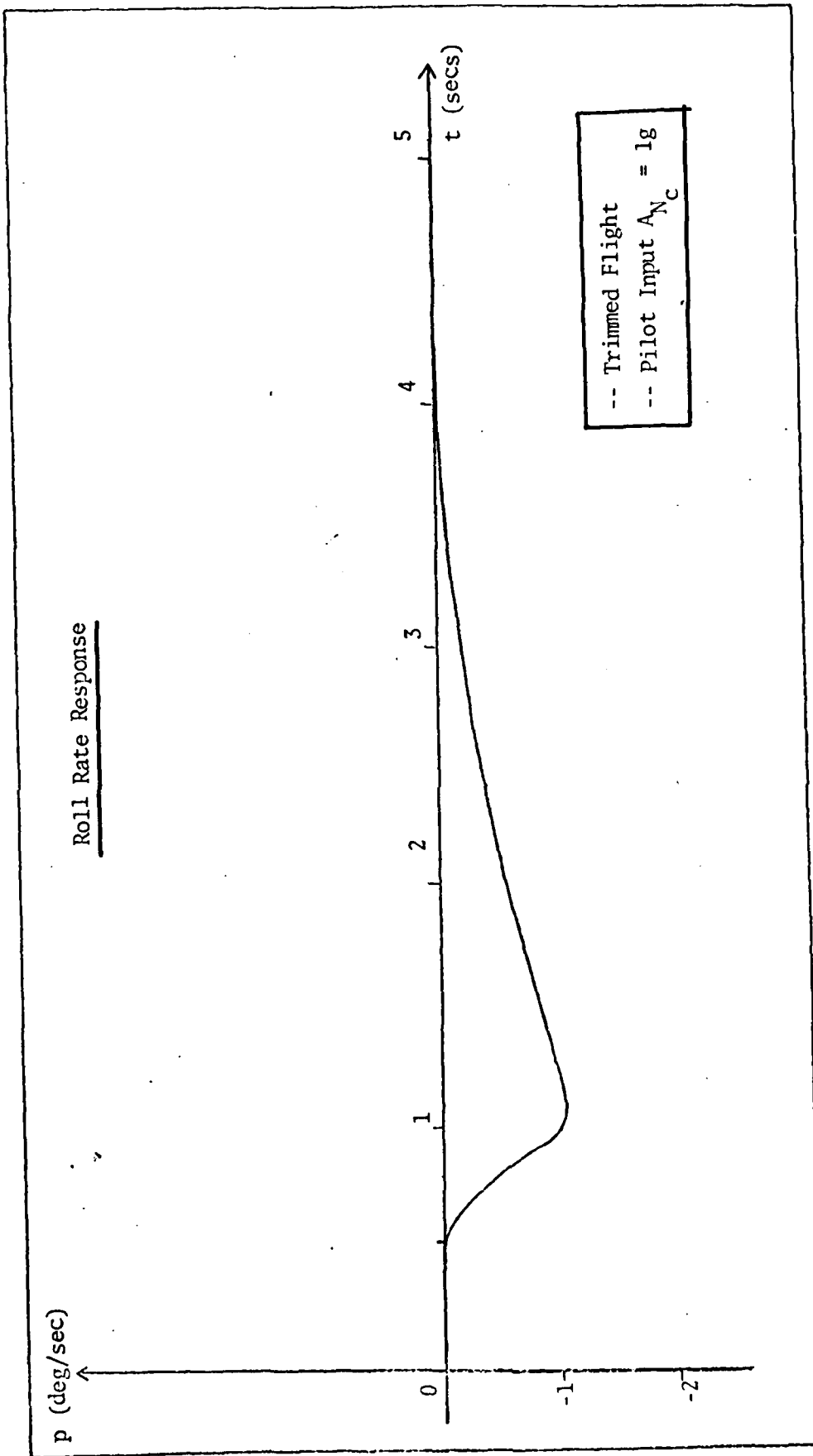


Figure 6.7 Right Elevator Failure at Zero Degrees; With Reconfiguration

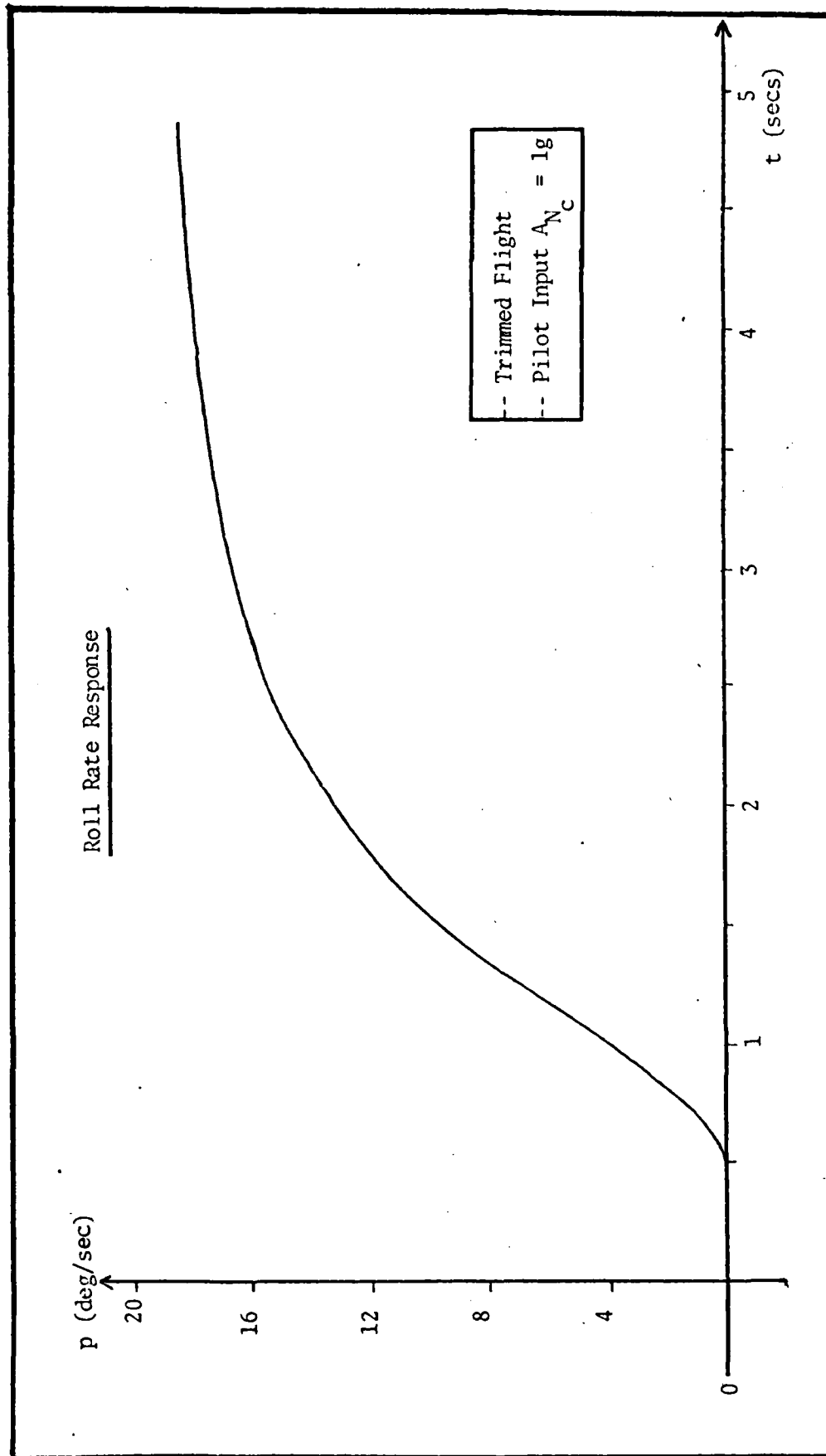


Figure 6.8 Right Aileron Failure at Zero Degrees; No Reconfiguration

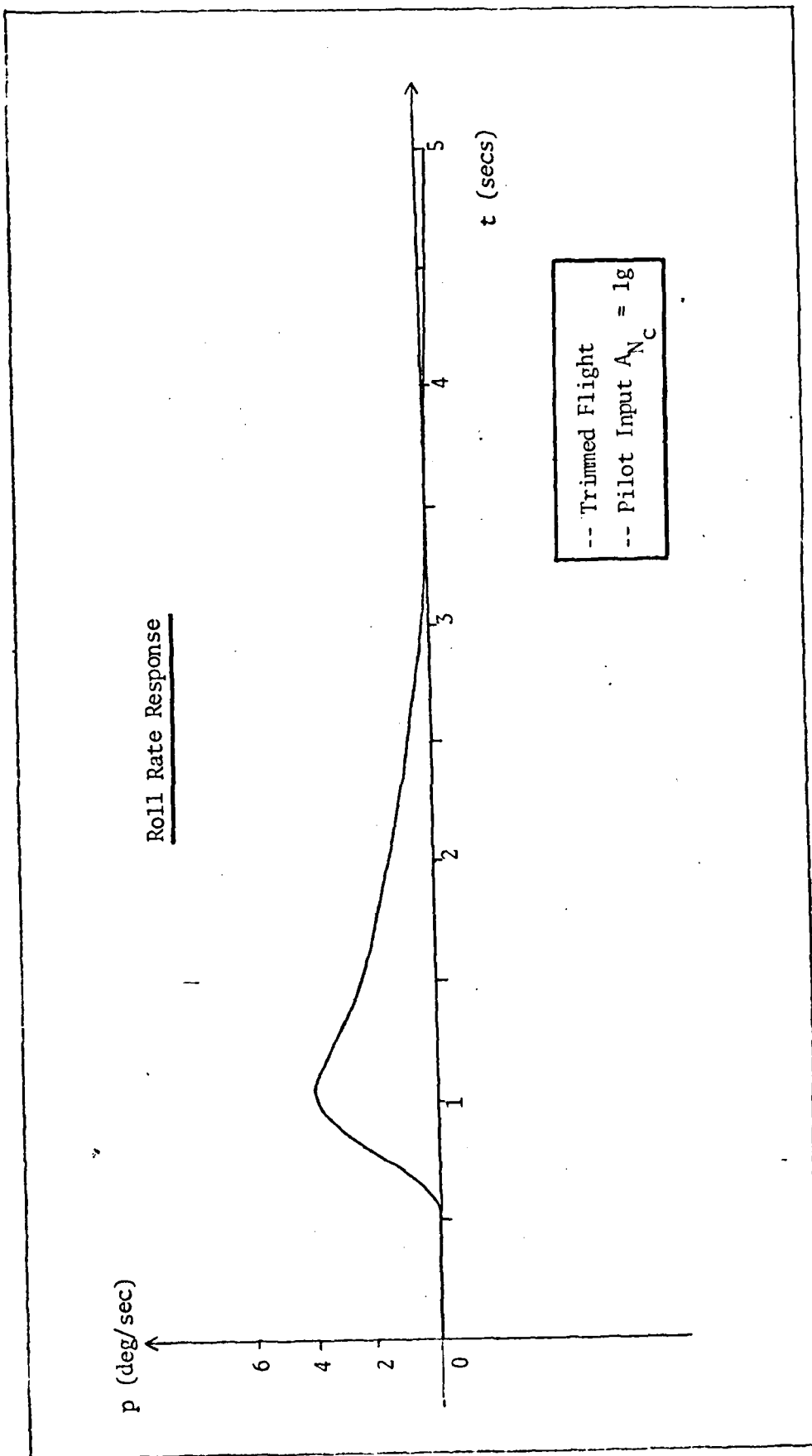


Figure 6.9 Right Aileron Failure at Zero Degrees; With Reconfiguration

Next, flight simulation was carried out with the same flight condition and inputs, but with reconfiguration of the flight control system. Various quantities exhibited significant improvement in response in this case. Particularly, the roll rate was found to be completely controlled. Time response of the roll rate is shown in Figure 6.7. In the first five seconds, roll rate was brought to zero with a negligible bank angle of  $-1.7^\circ$ . Similarly, the maximum excursion on the aileron and the left elevator were about  $6^\circ$  and  $4^\circ$ , respectively. All other quantities like  $q$  and  $r$  were also controlled. A comparison of  $A_N$  response (Figure 6.5) with the previous case shows improvement in response as well as steady state value.

Right Aileron Failure at Zero Degrees Deflection. A response of 1g pull-up in the case of right aileron failure without reconfiguration indicated unstable  $p$  and  $r$ . Both were faster than in the previous case and, again,  $p$  was the worst of the two. In the first five seconds,  $p$  reached a value of about  $18^\circ/\text{sec}$ , resulting in a bank angle of  $65^\circ$ . Similarly,  $r$  reached  $3.6 \text{ deg/sec}$  and a heading angle of about  $12^\circ$ . Roll rate response for this case is given in Figure 6.8.

Once again, the next step was simulation of the same failure flight with reconfiguration. The time response indicated desirable characteristics in the case of all moments  $p$ ,  $q$  and  $r$ . For instance, the roll rate, which was causing the greatest difficulty, had a response shown in Figure 6.9. In the first five seconds,  $p$  was brought to less than half a

degree per second. Maximum excursions on the elevator and ailerons in achieving this were  $12^\circ$  and  $10^\circ$ , respectively, both being less than maximum deflections of the control surfaces.

Right Elevator Failure at Maximum Deflection. Reference 5 indicated an upper limit on control augmentation elevator deflection of about  $5^\circ$ . This figure was used for maximum deflection failure simulation. The surface was simulated to fail during trimmed flight and aircraft response was studied for no commanded input. For the no reconfiguration case, roll rate was again found to be growing rapidly and causing control problems (Figure 6.10). For the reconfigurable case, the roll rate response is shown on the same plot (Figure 6.10). The response is much improved; in fact, definitely controlled. However, it shows a large steady state error. This is obviously caused by the right elevator which is failed and stuck at five degrees, and is seen by the flight control system as a constant disturbance. Based upon usual disturbance rejection techniques, the steady state response may be improved by enhancing the p-loop closure gain  $K_p$ . In general, the response shows a controlled roll rate as opposed to the rapidly growing response in the case of no reconfiguration. Maximum excursions on the left elevator and the ailerons are less than  $5^\circ$  and  $9^\circ$ , respectively.

Right Aileron Failure at Maximum Deflection. Once again, maximum deflection was assumed to be  $5^\circ$ . As pointed out earlier, this is an extreme case and poses a severe control

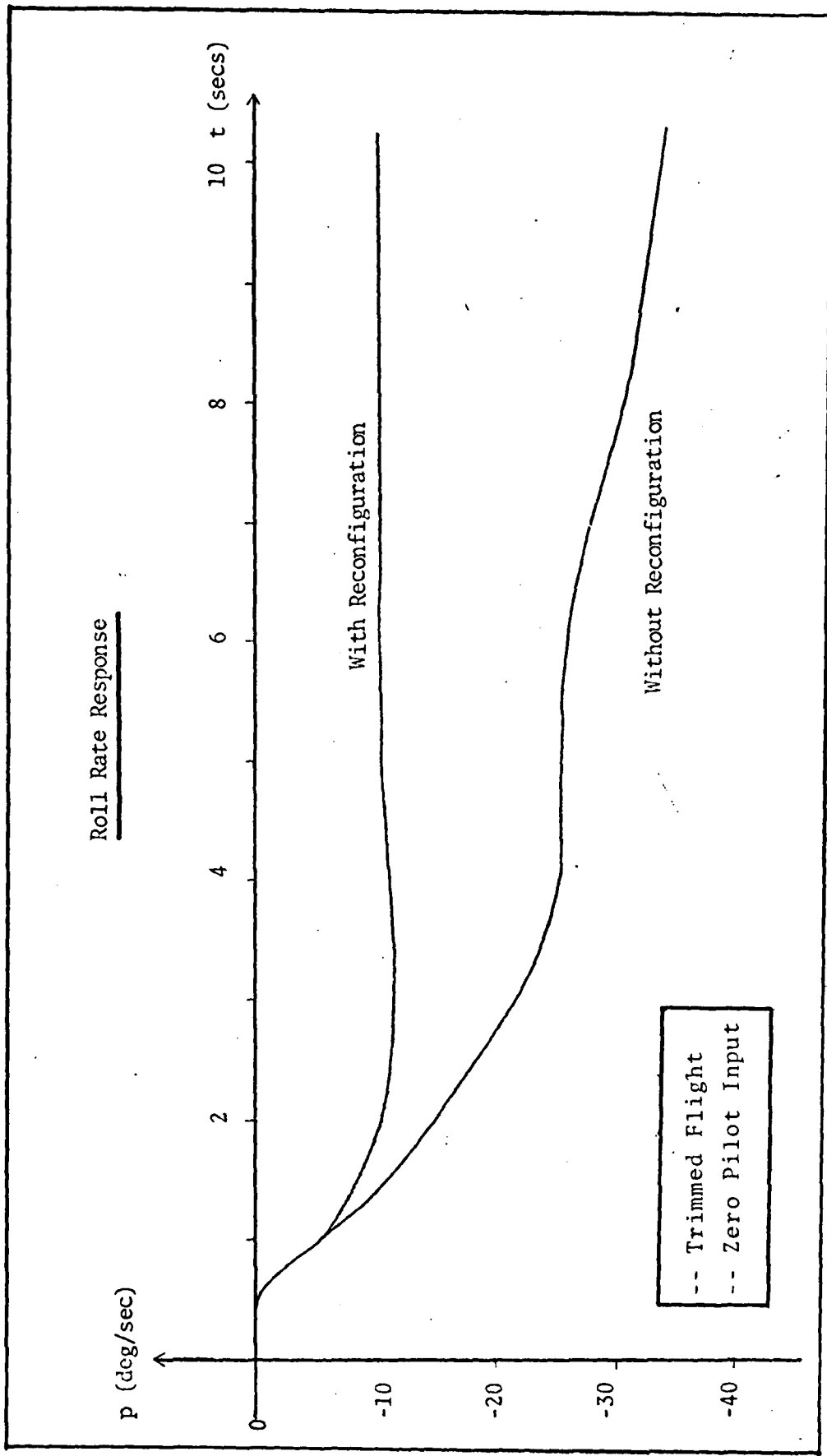


Figure 6.10. Right Elevator Failure at Maximum Deflection

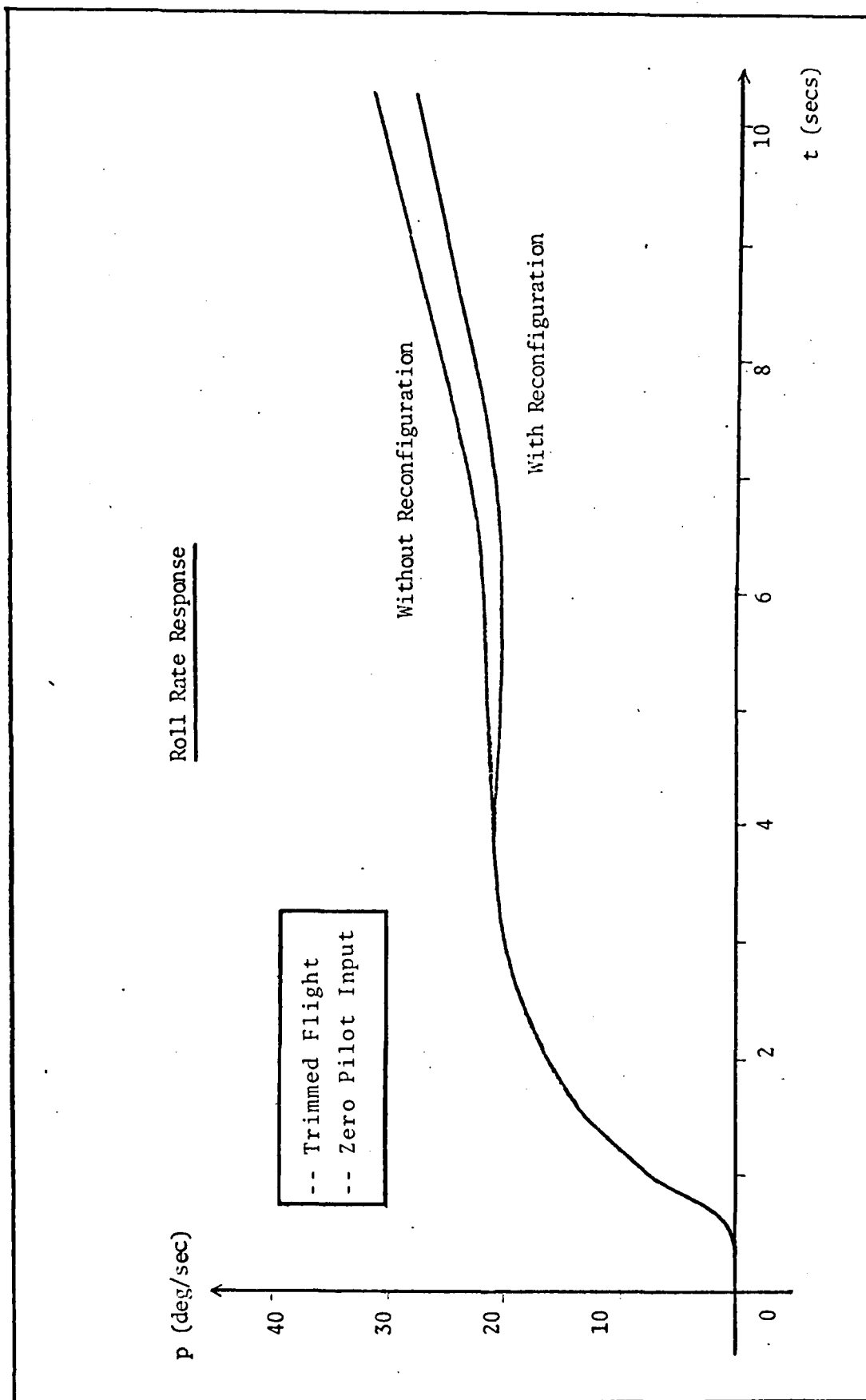


Figure 6.11 Right Aileron Failure at Maximum Deflection



problem. Figure 6.11 shows the roll rate response with and without reconfiguration. The time response indicated very little input to elevators and the left aileron. Maximum excursions on both these were found to be less than a degree. This indicates the need to enhance appropriate feedback loop gain to improve steady state response. Due to limitation on time, the author could not iterate on the process to achieve desired results. However, the trend of reconfiguration and the disturbance rejection analysis is indicative that it may be done without much complication.

To summarize, it may be said that the results show a definite improvement in aircraft response in case of specific failures considered when reconfiguration was implemented.

#### Determining Time Specifications for Failure Identification

In the real world, the sequence of events in the case of reconfiguration would be the occurrence of failure, its identification by some means, and then implementation of reconfiguration. The time delay between actual failure and implementation of reconfiguration could be critical. The intent in this paragraph is to develop specifications for this time delay beyond which reconfiguration would not be effective. In the earlier simulations, a constant time delay factor of 0.5 seconds was used. Now, in order to find the maximum permissible time delay, right elevator failure at zero degrees with 1g pilot input command is simulated for time delays ranging from 0.5 to 5 seconds.

Aircraft response indicated roll rate as the critical quantity. Results of these various simulations are summarized below in Table VI.

#### SUMMARY OF RESULTS FOR DELAY TIME SPECIFICATIONS

TABLE VI				
Time Delay (secs)	Maximum Excursions in first 5 secs			
	p (°/sec)	$\phi$ (deg)	$\delta_e$ (deg)	$\delta_a$ (deg)
0.5	1.0	1.6	5.4	8.4
1.0	3.3	5.4	7.4	11.6
1.5	5.15	9.3	6.4	10.0
2.0	6.2	12.8	6.2	10.5
2.5	7.0	16.6	6.9	11.9
* 5.0	8.0	26.0	8.5	13.3
* $\infty$ (no reconfiguration)	8.8	75.4	5.6	14.5

\* Maximum excursions in first 10 seconds

These results indicated that, although roll rate was controlled by the flight control system even for a delay time of five seconds, it took relatively longer time as the lag increased. Furthermore, bank angle was not neutralized and would require pilot's input for correction.

#### Sensitivity to Parameter Variations

Simulation tests of the reconfigurable flight control system thus far have been done for one particular flight condition which was specified in Chapter II. It is obvious

that such an assumption of nominal characteristics is purely theoretical since, in real life, the aircraft flies through varying flight conditions. The purpose of this paragraph is, therefore, to consider off-nominal behavior caused by variations in the system parameters from their assigned values.

This objective was accomplished by studying aircraft response while varying dynamic pressure that effectively implies variations in the B matrix of Eq (27). Simulations were carried out for variations of  $\bar{q}$  by 10, 20, 30 and as an extreme case, of 50 percent for a 1-g pull-up command for the case of right elevator failure at zero degrees with reconfiguration. Table VII summarizes the results for critical quantities.

SUMMARY OF RESULTS FOR SENSITIVITY ANALYSIS

TABLE VII						
Variation in $\bar{q}$	Maximum Excursions				$T_S$ for $A_N$ (secs)	$T_p$ (secs)
	p deg/sec	$\phi$ deg	$\delta_e$ deg	$\delta_a$ deg		
Actual	1.0	1.6	5.4	8.4	2 sec	0.65
10%	1.1	1.89	6.7	9.1	2 sec	0.75
20%	1.2	2.2	6.4	9.9	2 sec	0.85
30%	1.3	2.6	7.0	11.0	3.3 sec	1.80
50%	1.6	3.8	11.0	17.2	> 15 sec	1.55

These results indicate that the reconfigurable flight control system response varies almost linearly with variations in  $q$  of up to 30 percent. That is to say that, for a 30% variation in  $q$ , the maximum excursion on  $p$ ,  $\delta_e$  and  $\delta_a$  are all less than 30%. Thus, depending on the nature of accuracy required in the response, an upper limit on permissible variations may be established.

## VII. Conclusions and Recommendations

### Conclusions

A reconfigurable flight control system was developed using the concept of generic inputs and evaluated by employing six degree-of-freedom simulation. Results have indicated that reconfiguration by this method is practical and can achieve a marked improvement in combat aircraft survivability.

The Aircraft Model. The aircraft model developed in Chapter II and represented by Eq (27) is accurate up to four significant digits. The concept of independent individual surface control inputs has been meticulously incorporated in the system equations. The successful results of the reconfigurable flight control system using this model and concept of independent controls indicate the effectiveness of both. This aircraft model may, therefore, be used for further studies with confidence either in the area of reconfiguration or elsewhere.

Use of the Pseudo-Inverse. Application of the pseudo-inverse to reconfiguration (as demonstrated in this study), though new, is found to be effective. In this study, since all five inputs were independent, the control matrix B had a full rank and pseudo inverse technique was successfully employed to evaluate various transformation matrices in the design process. Its effectiveness may be noted from the desired B matrix that the transformation matrices reproduce.

Design with Generic Inputs. The concept of generic inputs has been found to be a powerful technique, especially for reconfiguration studies. It gives freedom of picking the desired control matrix to the designer which may be effectively used to achieve various purposes. An example is the advantage of getting direct lift from ailerons in a normal acceleration command as shown in Chapter IV.

Reconfigurable Flight Control System. The concept of reconfiguration by use of generic inputs and appropriate transformation matrices has been found to be a successful technique. The simulation results indicated significantly improved (or completely controlled) response in the case of single surface failure when reconfiguration was employed. Even though only the primary flight control systems were used to control the aircraft in the event of single surface failures, the maximum excursions on remaining control surfaces were found to be within the aircraft's limitations. The overall success of this scheme indicates its potential for future use in survivability enhancement.

Design in Analog Domain. It is found that using classical techniques of design in the continuous time domain has been an advantageous method for this problem since it permitted concentration of effort on reconfiguration. The design scheme developed, however, is in no way limited to analog domain and is directly transferrable to the digital domain.

### Specifications on Time Delay

A time delay of up to five seconds before implementation of this reconfigurable flight control system does not affect its performance except in the maximum excursions and steady state value of certain quantities, such as roll rate and control surface deflections.

### Sensitivity to Parameter Variations

Based on the results of Chapter VI, it is concluded that the reconfigurable flight control system response to parameter variations is good. It still provides the necessary control with surface failure, although the performance is degraded by approximately the same percentage as variation in the parameter.

## Recommendations

The successful results achieved in reconfiguration studies in this thesis encourage recommendations to pursue this research further. The areas that need further investigation could be:

1. Improvement in the present design to achieve better response in case of surface failure at maximum deflection. It may be achieved by enhancing appropriate feedback loop gains, such as a high gain roll rate loop.
2. Development of a surface failure and identification scheme which is obviously the first step in reconfiguration. This would determine which control surface is not following commanded inputs and may be accomplished by means of a Kalman Filter.
3. Development of a reconfiguration scheme for two or more surface failures based on the present design scheme. This will have to be done by incorporating additional inputs such as flaps and spoilers since (otherwise) the remaining three primary surfaces will not provide sufficient control in both longitudinal and lateral-directional axes.
4. Analysis of gain scheduling required for practical implementation of this design scheme. This will involve a detailed study of sensitivity to parameter variations and its consequences on feedback loop gains.



5. As a final recommendation, it is suggested that a scheme for implementation of this reconfigurable flight control system may be developed. This could be done, for instance, for a fly-by-wire flight control system by simply following the design scheme of this thesis.

## Bibliography

1. Boudreau, J.A. and Berman, H.L., Dispersed and Reconfigurable Digital Flight Control System, AFFDL-TR-79-3125, December 1979.
2. Potts, D.W., Direct Digital Design Method for Reconfigurable Multivariable Control Laws for the A-7D, Digitac II Aircraft, Master's Thesis, Air Force Institute of Technology, Wright-Patterson AFB OH, December 1980.
3. Roskam, Jan., Airplane Flight Dynamics and Automatic Flight Controls, Part I. Lawrence KS: Roskam Aviation and Engineering Corporation, 1979.
4. Jane's All The World's Aircraft 1970-71, McGraw Hill.
5. Bender, M.A., Wolf, Flight Test Evaluation of a Digital Flight Control System for the A-7D Aircraft Simulation Test Plan. Contract F33615-73-C-3098. Aeronautical Systems Division, Wright-Patterson AFB OH, 15 February 1974.
6. McDonnell Douglas Corporation, The USAF Stability and Control Digital Datcom, Vol I, User's Manual. AFFDL-TR-76-45, Air Force Flight Dynamics Laboratory, Wright-Patterson AFB OH, 1976.
7. Noble, Benjamin, Applied Linear Algebra, Prentice-Hall, 1969.
8. AF Flight Dynamics Laboratory, Background Information and User's Guide for MIL-F-8785B(ASG), "Military Specification - Flying Qualities of Piloted Airplanes." Technical Report AFFDL-TR-69-72, August 1969, Wright-Patterson AFB OH.
9. McRuer, D., Ashkenas, I., and Graham, D., Aircraft Dynamics and Automatic Control. Princeton University Press, 1973.
10. D'Azzo, J.J. and Houpis, C.H., Linear Control System Analysis and Design. McGraw Hill Book Company, 1981.
11. Strang, Gilbert, Linear Algebra and Its Applications, 2d Ed., Academic Press, 1980.
12. IMSL Library Edition 8, Routine DVERK, IMSL, Inc., Houston TX, 1980.

13. Larimer, S.J., TOTAL - An Interactive Computer Aided Design Program for Digital and Continuous Control System Analysis and Synthesis. Master's Thesis, Air Force Institute of Technology, Wright-Patterson AFB OH, March 1978.

## APPENDIX A

### Basic Flight Control System Design Using Classical Techniques

#### Longitudinal Flight Control System Design

System Equations. The decoupled longitudinal set of equations for the flight control system design is developed in Chapter IV and given by Eq (38). Assuming actuator dynamics to be represented by the transfer function

$$\frac{\delta_{\text{long}}}{\delta_{\text{long}_c}} = \frac{-20}{s + 20}$$

gives:  $\delta_{\text{long}} = -20 \delta_{\text{long}} - 20 \delta_{\text{long}_c}$

Incorporating  $\delta_{\text{long}}$  as a state variable in the above set yields

$$\begin{bmatrix} \dot{u} \\ \dot{\alpha} \\ \dot{q} \\ \dot{\theta} \\ \dot{\delta}_{\text{long}} \end{bmatrix} = \begin{bmatrix} -0.00083 & 5.48 & 0 & -32.17 & -32.86 \\ -0.00018 & -0.997 & 1.0 & 0 & -0.135 \\ 0.00038 & -8.27 & -0.709 & 0 & -15.91 \\ 0 & 0 & 1 & 0 & 0 \\ 0 & 0 & 0 & 0 & -20 \end{bmatrix} \begin{bmatrix} u \\ \alpha \\ q \\ \theta \\ \delta_{\text{long}} \end{bmatrix}$$

$$+ \begin{bmatrix} 0 \\ 0 \\ 0 \\ 0 \\ -20 \end{bmatrix} \begin{bmatrix} \delta_{\text{long}_c} \end{bmatrix}$$

(A-1)

### Inner Loop (Pitch Stability Augmentation System) Design

The pitch stability augmentation system is essentially feedback of pitch rate  $q$  to the longitudinal control as shown in Figure A.1. One of its purposes is to achieve

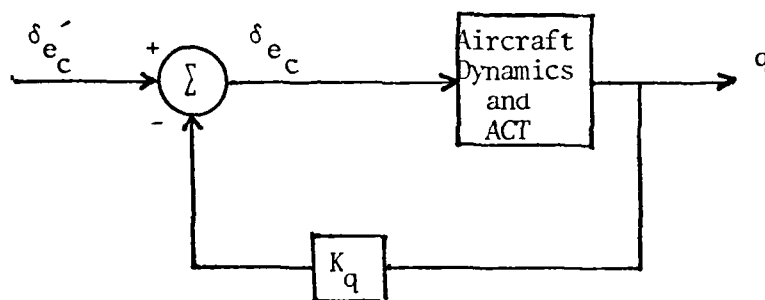


Figure A.1. Inner Loop Closure

enhanced short period damping. Reference 13 was used to design the inner loop gain parameter  $K_q$  to achieve desirable short period damping. Damping ratios ( $\zeta_{sp}$ ) of 0.6, 0.7, 0.8 and 0.95 were specified successively and the necessary  $K_q$  was found. For each case, the response was analyzed as shown:

$\zeta_{sp}$	$k_q$	$\omega_{sp}$
0.6	0.138	3.55 rad/sec
0.7	0.181	3.76 rad/sec
0.8	0.223	4.00 rad/sec
0.95	0.261	4.28 rad/sec

A moderately high  $\zeta_{sp}$  of 0.8 was selected initially, fixing  $k_q$  at 0.223.

Outer Loop ( $A_N$  Command System) Design. Figure A.2 depicts the outer loop closure initially used. For the design of this outer loop, the plant matrix is found from Eq (A.1) by noting that the input is

$$\begin{aligned}\delta_{e_c} &= \delta_{e_c'} - k_q q \\ &= \delta_{e_c'} - k_q [0 \ 0 \ 1 \ 0 \ 0] \underline{x}\end{aligned}$$

Closing the inner loop with this input produces the closed loop state equations. These may be simplified in the usual manner to obtain the standard format

$$\dot{\underline{x}} = A_{c_L} \underline{x} + B_{c_L} \delta_{e_c'}$$

Furthermore, an expression obtained for  $A_N$  from Reference 3 is:

$$A_N = -Z_u u - Z_\alpha \alpha - Z_q q - Z_{\delta_{long}} \delta_{long}$$

Substituting parameter values, and rewriting in state variable form yields

$$A_N = [ \begin{matrix} 0.113 & 632.6 & 0 & 0 & 85.45 \end{matrix} ] \underline{x}$$

This system of equations was analyzed using Reference 13 to design the outer loop gain  $k_A$ . An initial estimate for this gain was made by assuming  $k_A = \frac{1}{Z_\alpha M_{\delta_e}}$ . In the desing process, it was increased to a finally selected value of 0.0016.

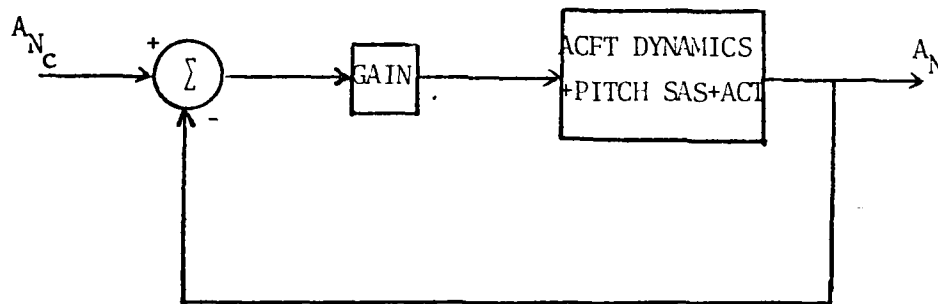


Figure A.2. Longitudinal Flight Control System;  
Initial Outer Loop Closure

This value gave a closed loop unit step frequency response shown in Figure A.3. In order to improve the steady state response of the pure gain controller and to eliminate the "droop" near the closed loop natural frequency, proportional plus integral control is introduced as shown in Figure 4-1. Now, two parameters are to be determined; namely, the feedback loop gain  $k_A$  and the compensator zero location "z". This zero is to be chosen so that its breakpoint "z" is greater than the phugoid natural frequency.  $k_A$  was therefore varied for  $z = .5, 1, 2$  and  $4$ , and again using Reference 13, time and frequency responses were studied. From the detailed study, the combination of gain  $k_A = .0016$  and compensator  $\frac{s+2}{s}$  was found to give the most desirable response in both frequency and time domain. This response is shown in Figure A.4 and A.5, respectively. A comparison of Figures A.4 and A.5 shows elimination of the "droop" in frequency response. A closed loop response analysis gave the following short period characteristics

$$\omega_{sp} = 5.54 \text{ rad/sec}$$

$$\zeta_{sp} = 0.33$$

To improve  $\zeta_{sp}$  further, the inner loop gain was increased. This time,  $k_q$  corresponding to  $\omega_{sp}$  of  $0.95$  was used. With this inner loop gain and the same compensator  $(0.0016)(\frac{s+2}{s})$ ,



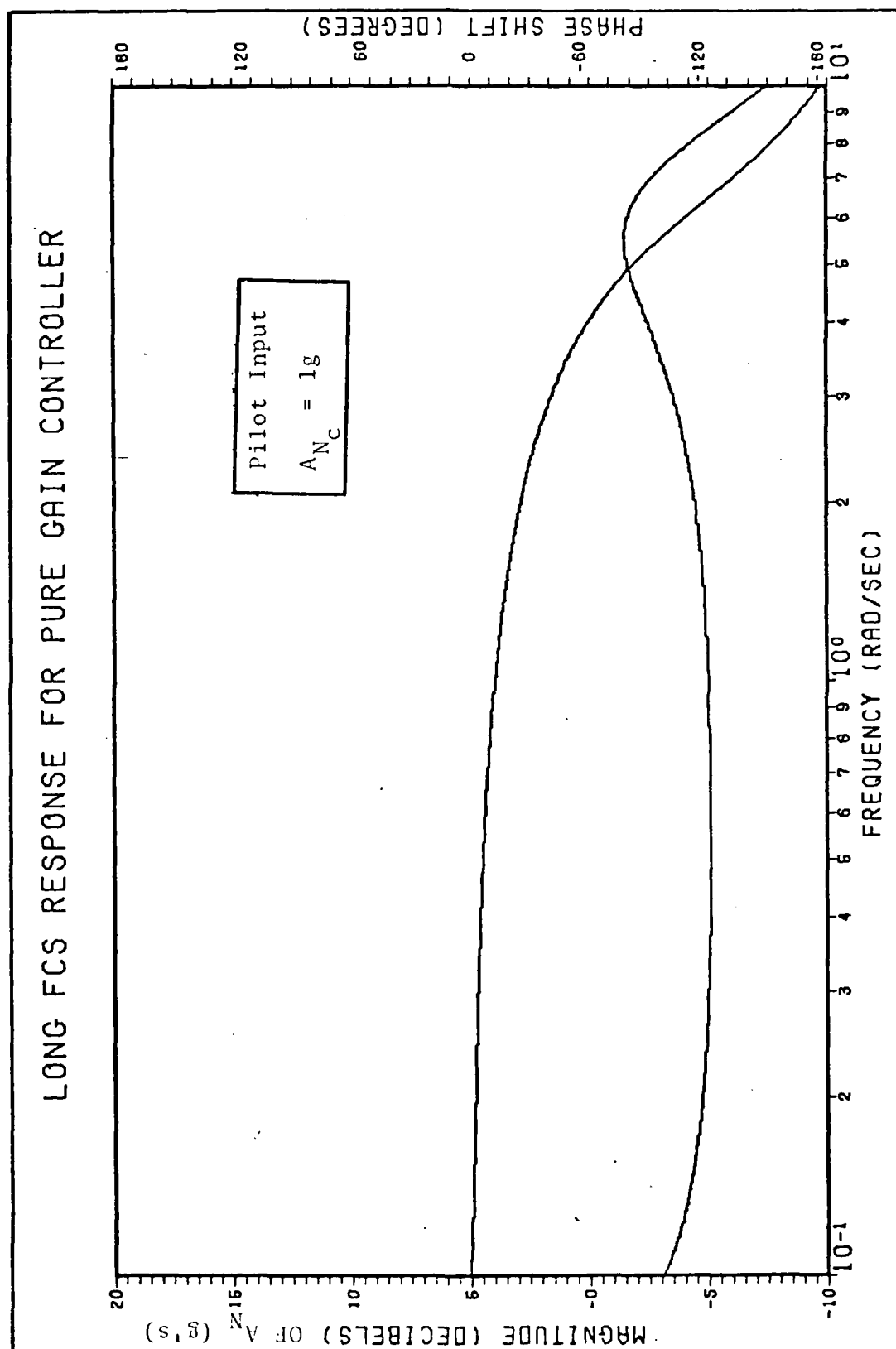
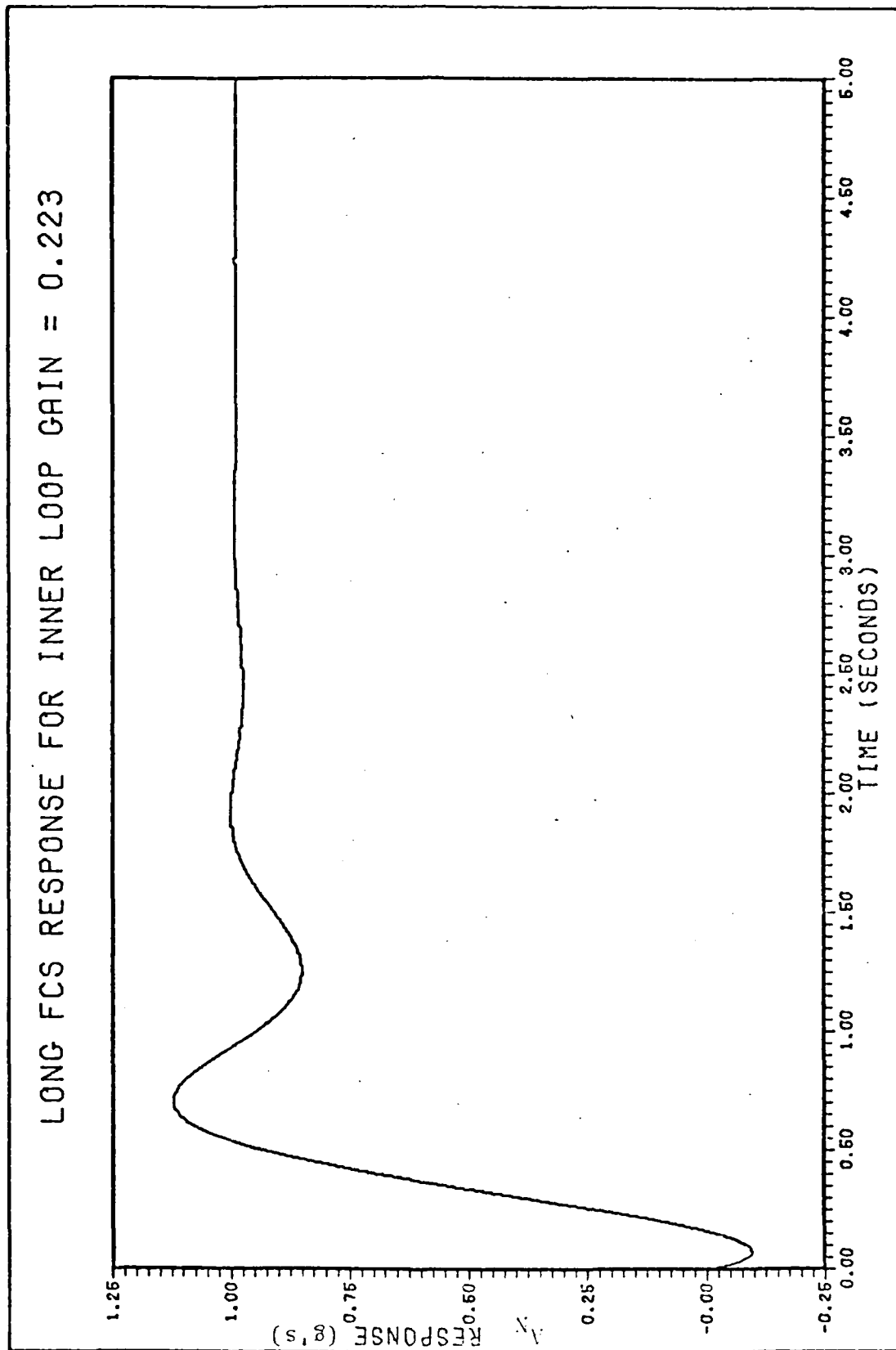
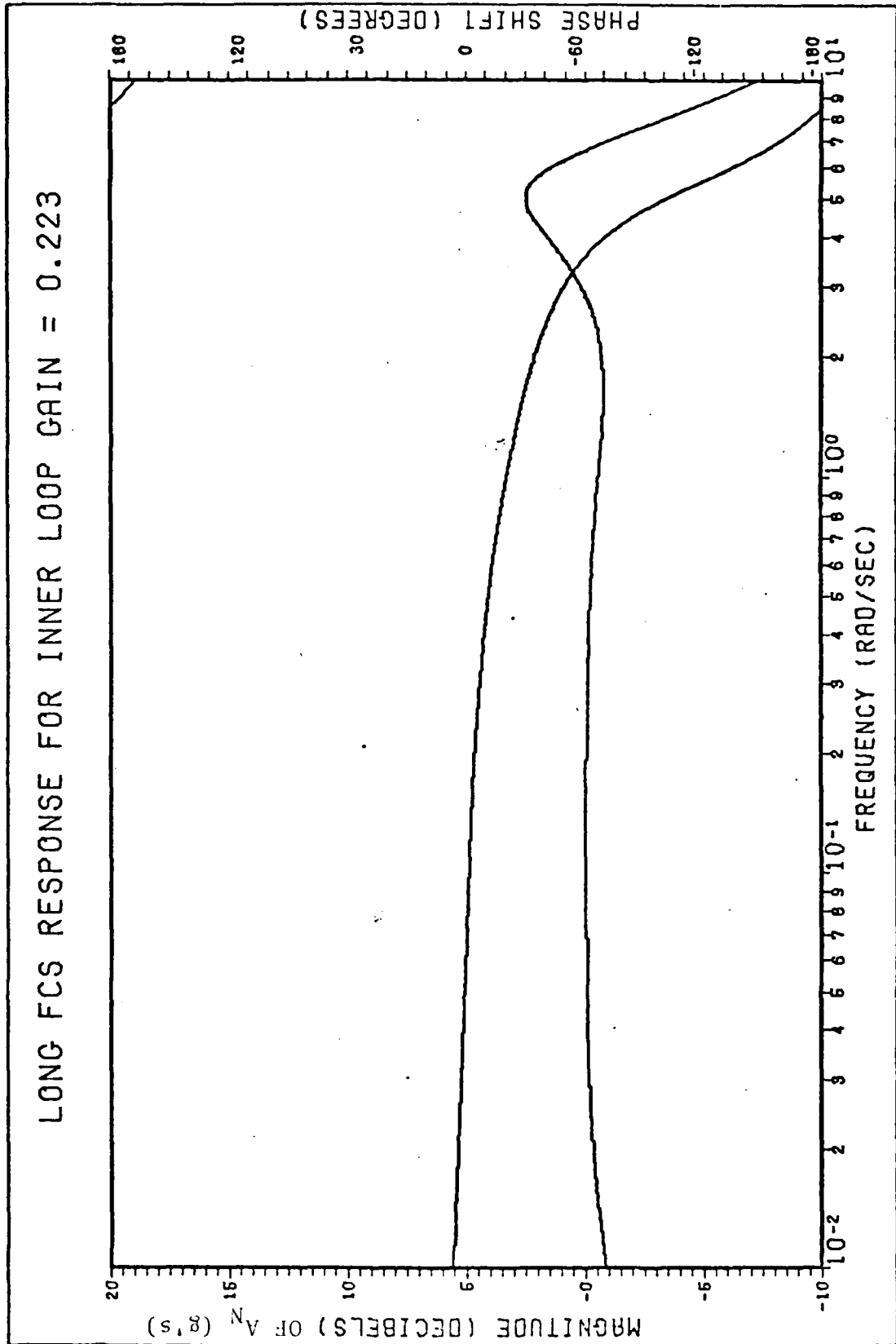


Figure A.3. Pure Gain Controller Frequency Response



A.4. Proportional + Integral Controller Time Response

LONG FCS RESPONSE FOR INNER LOOP GAIN = 0.223



A.5. Proportional + Integral Controller Frequency Response

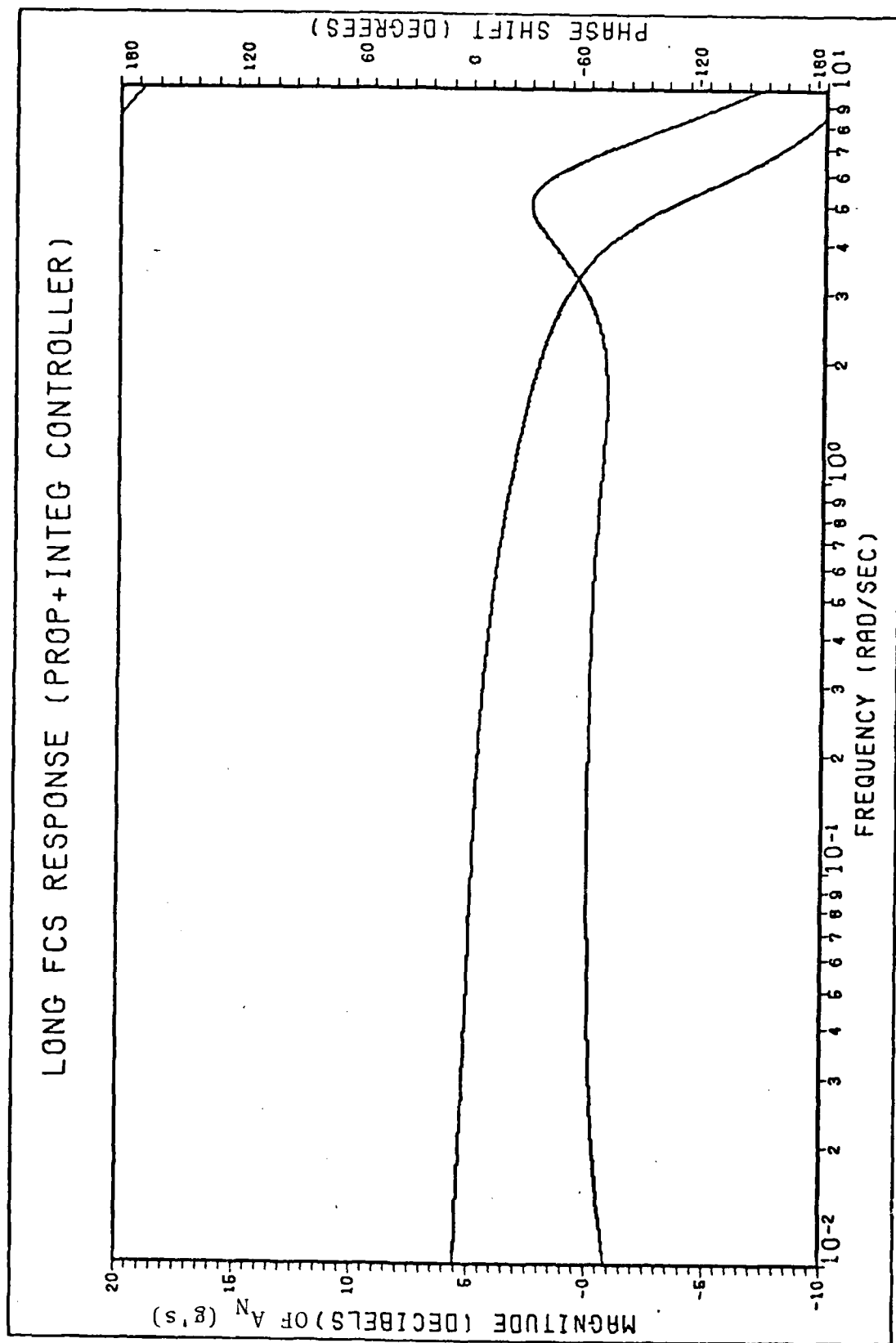


Figure A.6. Frequency Response of Longitudinal Flight Control System

the following response was achieved:

$$\omega_{sp} = 5.57 \text{ rad/sec}$$

$$\zeta_{sp} = 0.42$$

This being desirable and within specifications of Reference 8, values of the design parameters were selected as

$$k_q = .2612 \quad , \quad k_A = .0016 \quad \text{and} \quad z = 2.0 \quad .$$

Frequency response response of this double loop closure is shown in Figure A.6, while its time response is given in Figure 4.2.

#### Lateral-Directional Flight Control System Design

The lateral directional flight control system includes a yaw stability augmentation system with washout and a roll damping system. The design process for each of these is shown below.

Yaw Stability Augmentation System. The layout of yaw stability augmentation with washout circuit is as given in Figure 4.4. The two parameters to be determined in the design process are feedback loop gain  $k_r$  and washout pole location "a". The decoupled lateral directional equations

for the yaw stability augmentation system analysis are represented in state variable form by Eq (41). Assuming actuator dynamics to be represented by

$$\frac{\delta_r}{\delta_{r_c}} = \frac{-20}{s+20}$$

gives

$$\dot{\delta}_r = -20\delta_r - 20\delta_{r_c}$$

Including  $\delta_r$  as a state variable in Eq (41) yields

$$\begin{bmatrix} \dot{\beta} \\ \dot{p} \\ \dot{r} \\ \dot{\phi} \\ \dot{\delta}_r \end{bmatrix} = \begin{bmatrix} -0.162 & 0.00089 & -0.998 & 0.051 & 0.045 \\ 26.23 & -3.010 & 0.959 & 0 & 5.97 \\ 4.55 & 0.057 & -0.530 & 0 & -5.31 \\ 0 & 1 & 0 & 0 & 0 \\ 0 & 0 & 0 & 0 & -20 \end{bmatrix} \begin{bmatrix} \beta \\ p \\ r \\ \phi \\ \delta_r \end{bmatrix} + \begin{bmatrix} 0 \\ 0 \\ 0 \\ 0 \\ -20 \end{bmatrix} \begin{bmatrix} \delta_{r_c} \end{bmatrix} \quad (\text{A.2})$$

For the  $\frac{r}{\delta_r}$  transfer function  $c = [0 \ 0 \ 1 \ 0 \ 0]$ . Since the dutch roll natural frequency was found to be approximately 2 rad/sec, it was decided to place the washout pole as a first trial at -1.0.

Using Reference 13, the system was analyzed to find the gain for maximum dutch roll damping. Corresponding to a  $\delta_{dr}$  max of 0.45, a gain of  $k_r = 0.386$  was selected as the design value. This selected controller,  $.386 (\frac{s}{s+1})$ , gave a dutch roll response characterized by

$$\omega_{dr} = 1.41 \text{ rad/sec}$$

$$\zeta_{dr} = 0.454$$

which meets the criterion of Reference 8. Hence, these values were selected as design parameters.

#### Roll Damping (p-command) System Design

The general layout of the roll damper is shown in Figure 4-5. Since this forms the outer loop to the yaw damper closure, the closed loop system equations are obtained by noting from Figure 4-4 that the input is

$$\delta_{r_c} = \delta_{r'_c} - k_r r_{w_o}$$

Assuming  $\frac{\delta_a}{s} = \frac{20}{s+20}$ , taking yaw rate feedback as the inner loop closure, and including the relevant yaw rate variables in the state vector, the lateral-directional set of equations, Eq (A.2), may be written as

$$\begin{bmatrix} \dot{\beta} \\ \dot{p} \\ \dot{r} \\ \dot{\phi} \\ \dot{r}_{wo} \\ \dot{\delta}_r \\ \dot{\delta}_a \end{bmatrix} = \begin{bmatrix} -0.162 & 0.00089 & -0.998 & 0.051 & 0 & 0.045 & -0.0114 \\ -26.23 & -3.010 & 0.959 & 0 & 0 & 5.97 & 34.55 \\ 4.55 & 0.057 & -0.530 & 0 & 0 & -5.31 & 0.061 \\ 0 & 1 & 0 & 0 & 0 & 0 & 0 \\ 4.55 & .057 & -0.53 & 0 & -1 & -5.31 & 0.061 \\ 0 & 0 & 0 & 0 & 7.722 & -20 & 0 \\ 0 & 0 & 0 & 0 & 0 & 0 & -20 \end{bmatrix} \begin{bmatrix} \beta \\ p \\ r \\ \phi \\ r_{wo} \\ \delta_r \\ \delta_a \end{bmatrix}$$

$$+ \begin{bmatrix} 0 \\ 0 \\ 0 \\ 0 \\ 0 \\ 0 \\ 20 \end{bmatrix} \begin{bmatrix} \delta_{a_c} \end{bmatrix}$$

$$c = [0 \quad 1 \quad 0 \quad 0 \quad 0 \quad 0 \quad 0]$$

Analyzing this set of equations to determine  $k_p$  by using Reference 13 gives a value of  $k_p = 0.014$  that results in a desirable roll response.



For the selected values of  $k_r = 0.386$ ,  $k_p = 0.014$  and washout,  $\frac{S}{S+1}$ , the closed loop response is characterized by

$$\omega_{dr} = 1.436$$

$$\zeta_{dr} = 0.539$$

$$\text{Spiral Time Constant } T_S = 37.4 \text{ sec}$$

$$\text{Roll Time Constant } T_R = 0.294 \text{ sec}$$

which meets the criterion of Reference 8. Hence, these values were selected as design parameters.

## APPENDIX B

### Existing and Design Flight Control System Representation

#### Existing Flight Control System

Details of the existing flight control system of the A-7D have been obtained from Reference 5. These were simplified by deleting systems such as trim inputs and saturation limits, but maintaining all the significant characteristics of the flight control system. These simplified flight control systems for the pitch, roll and yaw axes are shown in Figures B.1, B.2, and B.3, respectively. For each one, the transfer function between input and output is developed in the form of a set of differential equations as follows:

Elevator Command. Referring to Figure B.1,

$$\dot{\delta}_{e_1} = \delta_{e_{\text{pilot}}} + 2.75 A_N + 0.167 \dot{q}$$

$$\dot{\delta}_{e_m} = (-0.5 k_{fs}) \delta_{e_m} + 0.5 \delta_{e_1}$$

$$\dot{\delta}_{e_2} = (-\delta_{e_2} + A_N + 0.3 \delta_{e_{\text{pilot}}})/0.55$$

$$\delta_{e_{\text{CAS}}} = (\text{Gain})(\delta_{e_2} + 0.25 q)$$

where Gain = 1.0 was used as recommended  
in Reference 5.

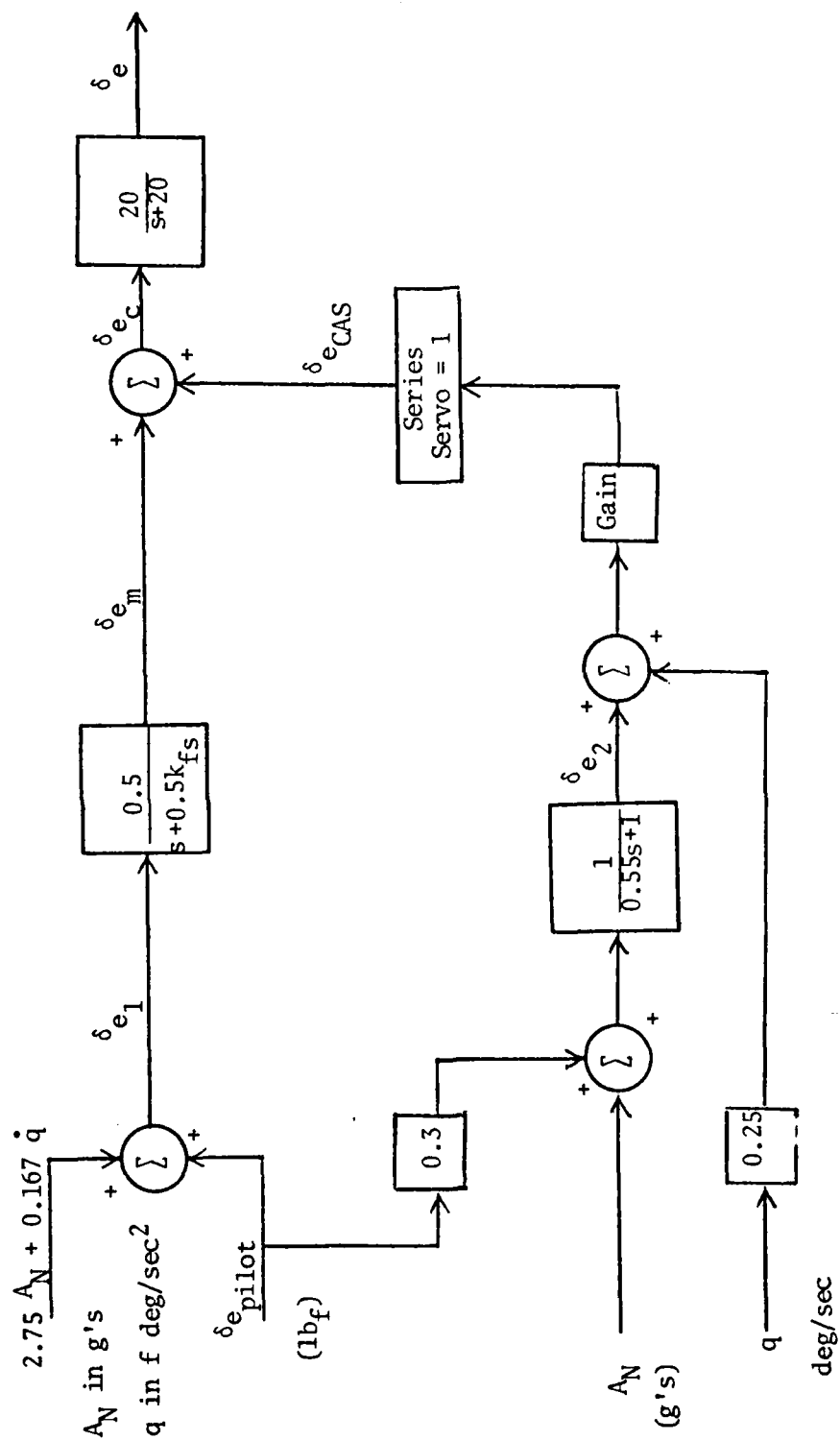


Figure B.1. A-7D Existing Pitch Axis Control (Simplified)

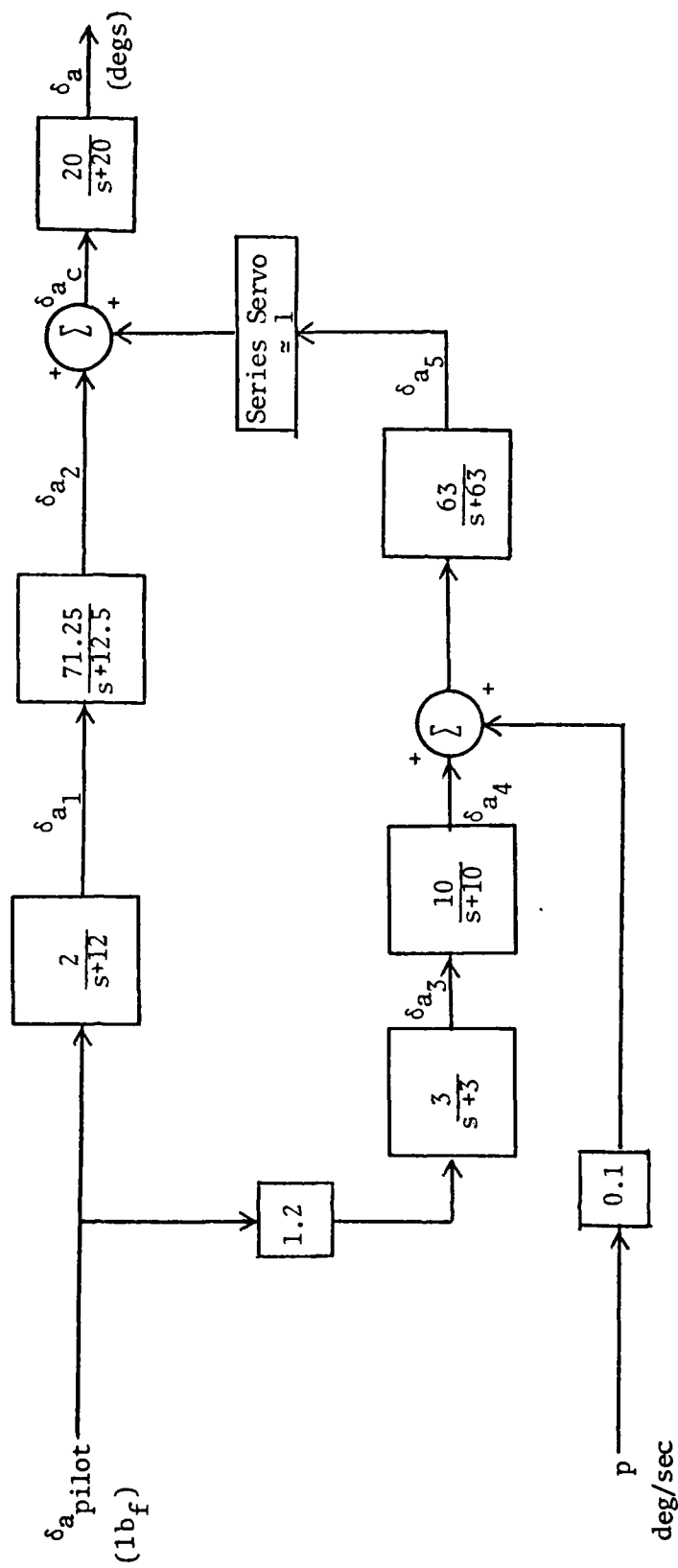


Figure B.2. A-7D Existing Roll Axis Control (Simplified)

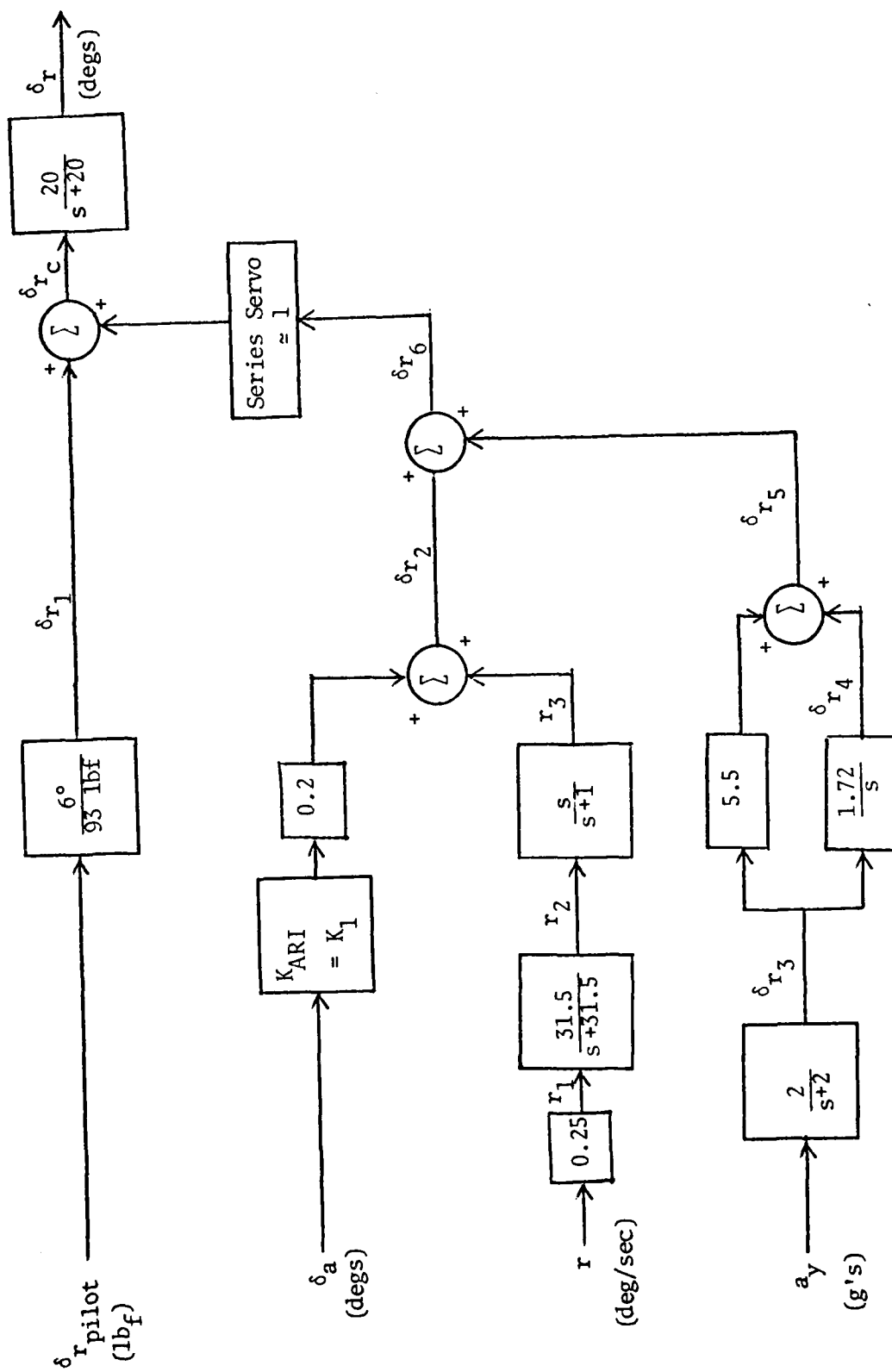


Figure B.3. A-7D Existing Yaw Axis Control (Simplified)

$$\delta_{e_c} = \delta_{e_m} + \delta_{e_{CAS}}$$

$$\delta_e = -20\delta_e + 20\delta_{e_c} \quad (B.1)$$

This set is coupled with Eq (56) to form the closed loop longitudinal flight control system. The value of  $k_{fs}$  is obtained from Reference 5, and can be described by the relationships

$$k_{fs} = \delta_{e_{pilot}}/32 \text{ for } \delta_{e_{pilot}} < 8 \text{ lbf}$$

$$k_{fs} = 0.25 + (\delta_{e_{pilot}} - 8)(0.344) \text{ for } \delta_{e_{pilot}} \geq 8 \text{ lbf}$$

Aileron Command. With reference to Figure B.2:

$$\delta_{a_1} = -12\delta_{a_1} + 2\delta_{a_{pilot}}$$

$$\delta_{a_2} = -12.5\delta_{a_2} + 71.25\delta_{a_1}$$

$$\delta_{a_3} = -3\delta_{a_3} + 3.6\delta_{a_{pilot}}$$

$$\delta_{a_4} = -10\delta_{a_4} + 10\delta_{a_3}$$

$$\dot{\delta}_{a_5} = -63\delta_{a_5} + 63\delta_{a_4} + 63(0.1)p$$

$$\dot{\delta}_{a_c} = \delta_{a_2} + \delta_{a_5}$$

$$\dot{\delta}_a = -20\delta_a + 20\delta_{a_c} \quad (B.2)$$

This set is coupled to Eqs (56) to form a closed loop roll axis flight control system.

Rudder Command. With reference to Figure B.3:

$$\delta_{r_1} = (6/93)\delta_{r_{pilot}}$$

$$\dot{r}_2 = -31.5r_2 + 31.5(0.25r)$$

$$\dot{r}_3 = -r_3 + \dot{r}_2$$

$$\begin{aligned} \delta_{r_2} &= r_3 + 0.2k_1\delta_a \quad \text{where } k_1 = 1.0 \text{ for } \delta_e \leq -4.5 \\ &= -1.0 \text{ for } \delta_e \geq 1.5 \\ &= -0.5 - \delta_e/3 \text{ for } -4.5 < \delta_e < 1.5 \end{aligned}$$

$$\delta_{r_3} = -2\delta_{r_3} + 2a_y \quad \text{where } a_y = (\bar{q}sC_y)/25338$$

$$\delta_{r_4} = 1.72\delta_{r_3}$$

$$\delta_{r_5} = \delta_{r_4} + 5.5\delta_{r_3}$$

$$\begin{aligned}
\delta_{r_6} &= \delta_{r_2} + \delta_{r_5} \\
\delta_{r_c} &= \delta_{r_1} + \delta_{r_6} \\
\dot{\delta}_r &= -20\delta_r + 20\delta_{r_c}
\end{aligned}
\tag{B.3}$$

When this set is coupled to Eqs (56), it forms the closed loop directional flight control system.

The comprehensive set of equations that represents aircraft dynamics including closed loop flight control system is, therefore, the set of 24 first order coupled differential equations as follows:

- 10 equations of aircraft motion (Eqs (56))
- 3 equations of longitudinal flight control system (Eqs (B.1))
- 6 equations of lateral flight control system (Eqs (B.2)), and
- 5 equations of directional flight control system (Eqs (B.3))

In addition, supporting algebraic expressions must be used.

#### Reconfigurable Flight Control System

Feedback control loop diagrams for the design longitudinal, lateral and directional flight control systems are shown in Figures B.4, B.5 and B.6, respectively. The set of equations representing these systems are developed for each case as follows:



Pitch Axis Control. With reference to Figure B.4:

$$E_1 = A_{N_C} - A_N$$

$$\dot{E}_I = E_1$$

$$E_2 = k_A E_1 + 2k_A E_I$$

$$\delta_{\text{long}_C} = E_2 - k_q q$$

$$\dot{\delta}_{\text{long}} = -20\delta_{\text{long}} - 20\delta_{\text{long}_C} \quad (\text{B.4})$$

This set, when coupled with Eqs (56), forms the design closed loop longitudinal flight control system.

Roll Axis Control. With reference to Figure B.5:

$$p_e = p_C - p$$

$$\delta_{\text{lat}_e} = k_p p_e$$

$$\delta_{\text{lat}} = -20\delta_{\text{lat}} + 20\delta_{\text{lat}_C} \quad (\text{B.5})$$

This set, when coupled with Eqs (56), forms the closed loop lateral flight control system.

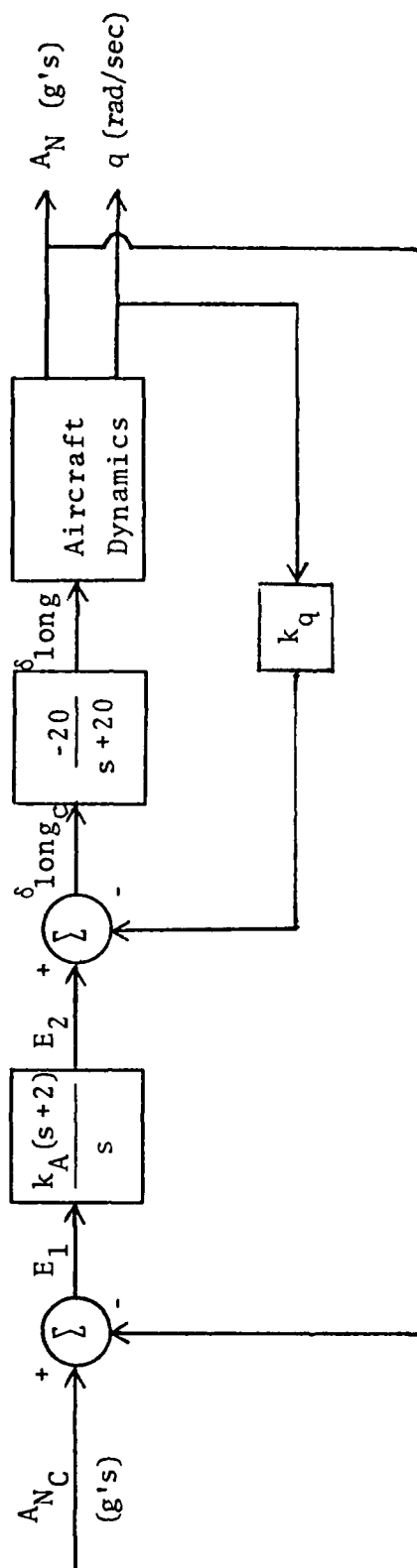


Figure B.4. Design Pitch Axis Control System

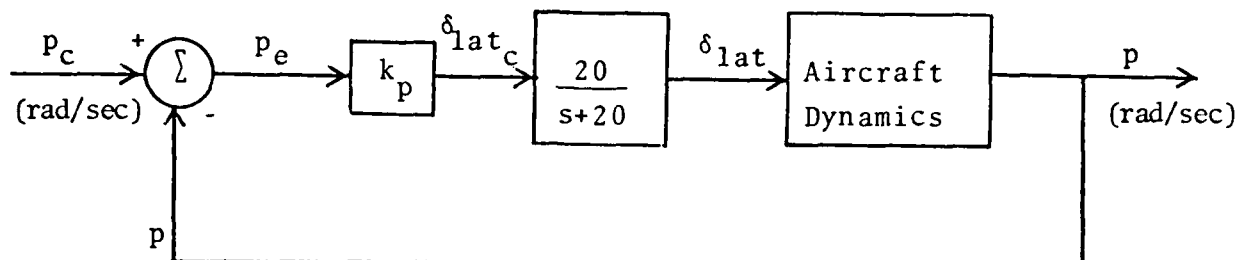


Figure B.5. Design Roll Axis Control System

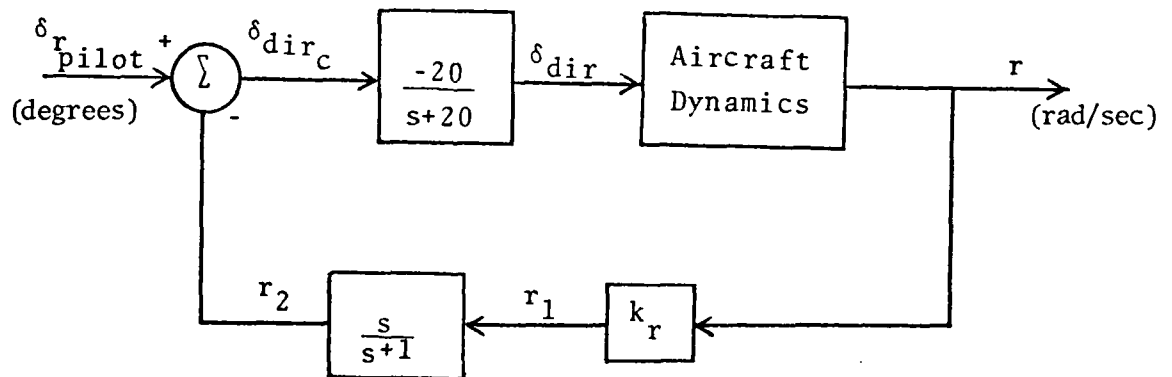


Figure B.6. Design Yaw Axis Control System

Yaw Axis Control. With reference to Figure B.6:

$$r_1 = k_r r$$

$$r_2 = r_1 - r_3 \quad (r_3 \text{ not shown in Figure})$$

$$\dot{r}_3 = r_2$$

$$\delta_{dir_c} = \delta_{r_{pilot}} - r_2$$

$$\delta_{dir} = -20\delta_{dir} - 20\delta_{dir_c} \quad (B.6)$$

This set, when coupled with Eqs (56), gives the closed loop directional flight control system.

The comprehensive set of equations that represents aircraft dynamics including closed loop reconfigurable flight control systems is the set of 15 coupled first order differential equations as follows:

- 10 equations of aircraft motion (Eqs (36))
- 2 equations of longitudinal flight control system (Eqs (B.4))
- 1 equation of lateral flight control system (Eq (B.5)), and
- 2 equations of directional flight control system (Eq B.6))

In addition, supporting algebraic relations must be used.

### Vita

Syed Javed Raza was born on 15 November 1948 in Karachi, Pakistan. He matriculated with distinction from Karachi in 1964, did F.Sc. with first division from Rawalpindi in 1966 and joined the PAF College of Aeronautical Engineering in 1967. He graduated with honors from the CAE in 1971 with a Bachelor of Aerospace Engineering degree, and was commissioned as a Flying Officer in the PAF. As an engineering officer, he was assigned to various duties in the PAF and the Ministry of Defence and did several appropriate professional courses. He was detailed for a Master's course in Aeronautical Engineering at the Air Force Institute of Technology in June 1980. He is a member of the Institute of Engineers Pakistan, the American Institute of Aeronautics and Astronautics, and of Tau Beta Pi.

Permanent Address: C/o Gulistan-e-Raza  
154-F Block II  
P.E.C.H. Society  
Karachi 2917  
PAKISTAN

UNCLASSIFIED

SECURITY CLASSIFICATION OF THIS PAGE (When Data Entered)

REPORT DOCUMENTATION PAGE		READ INSTRUCTIONS BEFORE COMPLETING FORM
1. REPORT NUMBER AFIT/GAE/AA/81D-23	2. GOVT ACCESSION NO. AD-1111112	3. RECIPIENT'S CATALOG NUMBER
4. TITLE (and Subtitle) USE OF THE PSEUDO-INVERSE FOR DESIGN OF A RECONFIGURABLE FLIGHT CONTROL SYSTEM		5. TYPE OF REPORT & PERIOD COVERED MS Thesis
7. AUTHOR(s) Syed Javed Raza Sqn. Ldr. PAF		6. PERFORMING ORG. REPORT NUMBER
9. PERFORMING ORGANIZATION NAME AND ADDRESS AF Institute of Technology (AFIT-EN) Wright-Patterson AFB OH 45433		8. CONTRACT OR GRANT NUMBER(s)
11. CONTROLLING OFFICE NAME AND ADDRESS		10. PROGRAM ELEMENT, PROJECT, TASK AREA & WORK UNIT NUMBERS
14. MONITORING AGENCY NAME & ADDRESS (if different from Controlling Office)		12. REPORT DATE December 1981
		13. NUMBER OF PAGES 153
		15. SECURITY CLASS. (of this report) UNCLASSIFIED
16. DISTRIBUTION STATEMENT (of this Report)  Approved for Public Release; Distribution Unlimited.		15a. DECLASSIFICATION DOWNGRADING SCHEDULE
17. DISTRIBUTION STATEMENT (of the abstract entered in Block 20, if different from Report)		
28 JAN 1982		
18. SUPPLEMENTARY NOTES  Approved for Public Release IAW AFR 190-17 <i>Frederick C. Lynch</i> FREDERICK C. LYNCH, Major, USAF Director of Public Affairs		
19. KEY WORDS (Continue on reverse side if necessary and identify by block number) Control Laws of the Flight Control System Reconfiguration Pseudo-Inverse Flight Control Surface Failure Design with Generic Inputs		
20. ABSTRACT (Continue on reverse side if necessary and identify by block number) Reconfiguration of the flight control system is achieved using generic inputs and transformation matrices for single primary control surface failure. Pseudo-inverse is used to evaluate appropriate transformation matrices. Design is tested against non-linear six degree-of-freedom model of the A-7D by simulating failure flights. System was found to provide desirable flying qualities upon reconfiguration.		

DD FORM 1 JAN 73 1473

EDITION OF 1 NOV 65 IS OBSOLETE

UNCLASSIFIED

SECURITY CLASSIFICATION OF THIS PAGE (When Data Entered)

END

DATE  
FILMED

3-82

DTIC